EFFECT OF PECTINMETHYLESTERASE ON THE FLOW BEHAVIOR OF FRESH VALENCIA ORANGE PULP

by

XUAN LI

(Under the Direction of José I. Reyes De Corcuera)

ABSTRACT

Orange pulp has a complex flow behavior displaying slippage at very low shear rates (0.6-0.9 s^{-1}), in addition to changing rapidly with storage time. That change was attributed to pectinmethylesterase (PME) activity in unpasteurized orange pulp but had not been characterized. Flow behavior of orange pulp was fitted to power law at shear rates smaller than those where slippage occurred. Shear stress-controlled rotational rheology tests were conducted on fresh orange pulp stored for 0 to 48 h at 4 °C. Flow behavior index (n) was 0.32, independent of storage time ($p>0.05$). Consistency coefficient (K) increased 65.5% after 48 h storage (119.7 to 198.1 $Pa \cdot s^n$). Pressure drop was determined in a pilot scale flow system as a function of flow rate for ~650 $g \cdot L^{-1}$ orange pulp stored for 0 to 72 h at 22 °C. Pressure drop increased non-linearly with storage time and was inclined to level off after 36 h due to the completion of deesterification of pectin. At 0.8 GPM (5.05×10^{-5} $m^3 \cdot s^{-1}$), the pressure drop due to major friction increased 51.1% (607.2 to 917.4 kPa) as storage time increased from 0 to 72 h and the power requirement increased from 30.3 to 45.9 W.

INDEX WORDS: Pectinmethylesterase; Flow behavior; Valencia orange pulp; Storage time;

EFFECT OF PECTINMETHYLESTERASE ON THE FLOW BEHAVIOR OF FRESH VALENCIA ORANGE PULP

by

XUAN LI

BS, Fujian University Of Traditional Chinese Medicine, China, 2012

A Thesis Submitted to the Graduate Faculty of The University of Georgia in Partial Fulfillment of the Requirements for the Degree

MASTER OF SCIENCE

ATHENS, GEORGIA

2015

EFFECT OF PECTINMETHYLESTERASE ON THE FLOW BEHAVIOR OF FRESH VALENCIA ORANGE PULP

by

XUAN LI

Major Professor: José I. Reyes De Corcuera

Committee: William L. Kerr
Louise Wicker

Electronic Version Approved:

Suzanne Barbour
Dean of the Graduate School
The University of Georgia
December 2015

DEDICATION

I would like to dedicate this work to my family. I greatly respect and appreciate for their unconditionally love and support.

ACKNOWLEDGEMENTS

First of all, I would like to thank Dr. Reyes for his guidance, support and trust throughout these two years. Thank Dr. Reyes for introducing this interesting project that I really loved. He is not only a good academic advisor, but also a good life mentor. He taught me to live with things I am afraid of, and learn to conquer problems independently. Without his help, I would not have been able to learn, to challenge myself and to grow to be a person I am today.

I would like to thank my committee members Dr. Kerr and Dr. Wicker for their guidance and help with any problems I encountered in my work. Also, thank them for their kindly providing me instruments and materials to help me finish my work.

Thank all my lab mates Dr. Garcia, Ali Halalipour, Daoyuan Yang, Victoria Ramirez, Martina Irene, Kwanena Afari, and Tristin Leigh for their help and encouragement. My graduate school experience would not have been full of fun without these guys.

Finally, I would like to thank my family who are always supportive in my academic career. Thank my friends in China for encouraging me all the time when I got anxious about my research.

TABLE OF CONTENTS

Page

LIST OF TABLES

Page

LIST OF FIGURES

Page

CHAPTER 1

LITERATURE REVIEW

Introduction

Citrus utilized production was 9.4 million tons for 2013-2014 year, down 15% from 2012 and the value of citrus crop was up 7% from the previous season, at 3.4 billion dollars (USDA, 2014). Pulp is an important by-product of the orange juice industry. Citrus pulp is an important by-product of citrus juice production (Payne, 2011). During pulp recovery, pulpy juice from the juice extractor passes through a first finisher where some defects like large seeds, peel, and rag fragments are removed. The pulpy juice then passes to conical cyclone separator or 'hydrocyclone' where embryonic seeds and defects denser than juice and pulp collect against the wall and are discharged through a valve located at the bottom of the cyclone. The discharged pulpy juice stream then passes through to a second finisher for recovery of pulp with concentration to ~500 $g \cdot L^{-1}$, which is considered as low concentrated pulp or 'low density' pulp. The next step involves low concentrated pulp pasteurization at near 90 °C for 1-2 min for microbe kill and enzyme inactivation, followed by chilling treatment to 2-5 °C. Chilled pulp then passes through a final finisher where pulp is concentrated to over 900 $g \cdot L^{-1}$, packaged into containers, and stored frozen (Braddock, 1999). Storing orange pulp frozen requires to extra energy and results in increased transportation costs. Pulp concentration or 'dryness' expressed in grams per liter refers to an empirical method commonly used in the citrus industry. In citrus processing industry, pulp concentration is usually determined by a modified quick fiber test. The quick fiber test apparatus is shown in Figure 1.1. During the test, approximately 500 mL citrus

pulp is first weighed and loaded into a 20-mesh screen of the quick fiber apparatus. After about 2-min mechanical shaking, the total weight of screen and pulp is recorded. The weight of pulp after shaking is calculated as the total weight minus the weight of screen. The pulp concentration is then calculated as (Munoz, 2012)

$$\text{Pulp concentration} = \frac{\text{weight of pulp after shaking (g)}}{\text{volume of juicy pulp (L)}} \tag{1-1}$$

The citrus processing industry would like to concentrate and pasteurize the orange pulp at high concentration, typically referred as 'high density pulp' (>900 $g \cdot L^{-1}$) to be able to fill, store and ship the product aseptically, which would reduce refrigerated storage and shipping costs. However, pumping high density pulp in conventional pasteurizers results in a large pressure drop. This in turn requires a large positive displacement pump that also consumes more power that when pumping low density pulp, thus, resulting in increased pumping costs (Payne, 2011). Also, when pumping very viscous fluids in pipes, the flow regime is laminar. Therefore, in the absence of turbulence heat is transferred mainly by conduction instead of convection, and radial temperature gradients result in non-uniform thermal treatment conditions (Munoz, 2012). Currently, small diameter pipes are used to favor rapid heat transfer but produce a large pressure drop (Payne, 2011). High concentration orange pulp pasteurizers have been designed and are currently in use in the citrus industry. However, to our knowledge, rigorous optimization has not been possible due to the lack of published rheological and thermal properties of pulp and to the quantification of the effects of PME on citrus pulp rheology.

The objective of this chapter was to provide background information on pectin, pectinase especially PME activity and their impact on the rheology of fruit pulps and concentrates. This chapter also provides background information on slippage and effect of slippage on the rheological properties of orange pulp.

Pectin

In fruits and vegetables, pectic substances, also called pectins, are complex polysaccharides that are mainly present in the middle lamella and primary cell wall of parenchyma cells (Kar and Arslan, 1999; Van Buggenhout et al., 2009). Pectin contributes to the firmness and structure of plant tissue as a part of the primary cell wall and the main middle lamella component involved in intercellular adhesion (Thakur et al., 1997). Pectin is widely used as gelling, thickening and stabilizing agent applied to the production of jam, jelly, juice, confectionary products, and bakery fillings (Corredig and Wicker, 2001; Rolin and Vries, 1990; Willats et al., 2006).

Homogalacturonan (HG), rhamnogalacturonan I (RG I) and rhamnogalacturonan II (RG II) are three major pectic polysaccharide structures that constitute pectin. Homogalacturonan is referred to as the 'smooth' region, which represents the backbone chain of pectin, containing α-1, 4 linked residues of D-galacturonic acid that can be methylated at the O-6 position (Yadav et al., 2009). The zone with abundant rhamnose is called the 'hairy' region, as there are neutral oligosaccharides side chains carried by sugar (Kim, 2004).

The degree of esterification (DE) is defined as the moles of methoxyl groups per 100 moles of galacturonic acid residues. Traditionally, pectins are categorized in terms of the degree of methyl esterification (DE) as high-ester (DE > 50%) pectin and low-ester (DE < 50%) pectin (Rinaudo, 1996; Voragen et al., 1995). Both DE and the degree of acetylation (DA) are associated with the functional properties of pectin. Increased DE results in more rapid gel formation for high-ester pectin but the rate of gel formation decreases as DE increase for the low-ester pectin (Löfgren et al., 2002). Pectin gel is formed when portion of homogalacturonan domains associate at junction zones. In high-ester pectin, the junction zones are formed by

hydrogen bridges and hydrophobic force between methoxyl groups while junction zones are formed by calcium cross-linking between free carboxyl groups in low-ester pectin (Willats et al., 2006).

The gelling ability of pectin depends on its solubility and viscosity (Rao, 1993). Based on solubility, there are two different types of pectins: water-soluble or free pectin and the water-insoluble pectin. Solubility in water depends on pectin's degree of polymerization and distribution of methoxyl groups. Although solution pH, temperature and the concentration of the solute present have a marked effect on solubility, pectin's solubility generally increases with decreasing molecular weight (Thakur et al., 1997). The water-insoluble pectin decreases and water-soluble pectin increases then decreases as the fruits become over-ripen (Seymour et al., 2012). In fresh squeezed 'Valencia' orange juice with soluble solid content 10.8 °Brix, the pectin content was 0.14% (Hernandez et al., 1995). It was also reported that washed orange pulp dried in forced-air oven at 80 °C for 12 h (9% moisture content) contained 35.45% pectin, with 2.07% was water-soluble pectin (Larrea et al., 2005). The viscosity of pectin is affected by concentration of the polymer solution, molecular weight and shape, and ionic strength. The higher the molecular weight of the pectin in solution, the higher its viscosity (Thibault and Rombouts, 1986).

Previous study indicated that gelling ability and rheological properties of pectin are also influenced by the length of its side branches and acetylation (Matthew et al., 1990). Side chains with length required to cause significant amount of additional interchain entanglement conferred larger viscosity at low shear rate compared to linear polymers with same molecular weight. However, branches not long enough to cause entanglement was observed with lower viscosity compared to linear polymers (Schmelter et al., 2002).

Pectinases

Pectinases are enzymes involved in pectin degradation. In the fruit juice industry, pectinases play an important role in clarification (Rodriguez-Nogales et al., 2008), extraction, and viscosity reduction (MariaTeresa Pretel, 1997). Pectinases are widely distributed in higher plants and microorganism. Plant's cell wall extension and tissue soften during maturation and storage are related to pectinases (Jayani et al., 2005). About 25% of the global food enzyme sales are microbial pectinases. *Aspergillus niger* is one of the most common fungal species to produce pectinase in industry (Naidu and Panda, 1998). Based on mode of reaction and preferred substrate, pectinases are mainly classified into three categories: esterases, depolymerases and lyases. Pectin lyase (PL) degrades pectin polymers by β elimination resulting in the formation of 4, 5-unsaturated oligogalacturonides without disturbing ester groups (Yadav et al., 2009). Depolymerases such as polygalacturonase (PG) depolymerize pectin by hydrolyzing glycosidic bonds that link to galacturonic acid residues. By cleaving the backbone of pectin, polygalacturonase and pectin lyase cause a reduction of pectin viscosity. Pectinmethylesterase (PME) is the third type of pectinase that is discussed in greater detail in the next section because the main focus of this research was to investigate the effect of pectinmethylesterase on the rheology of orange pulp.

Pectinmethylesterase (PME)

Pectinmethylesterase catalyzes demethylesterification of pectin to form polygalacturonic acid. In citrus, pectinmethylesterase (PME) is mostly attached to the cell wall and the detectable amount of PME after extraction varies (Corredig et al., 2000). For example, when extracted with 1 M NaCl without pH adjustment, thermostable pectinesterase (pectinesterase remains active at temperature greater 70 °C) extracted from 'Marsh' grapefruit pulp retained 98% of total activity;

when extracted with 1 M NaCl, 0.25 M Tris-Cl at pH 8.0, only 17% PE activity was retained (Wicker, 1992). In the presence of cations, gelation occurs when sufficient galacturonic acid groups link together via divalent cations such as calcium to form pectate gel. During citrus juice extraction, because of its solubility in the juice a fraction of PME detaches from the cell wall and, along with the fraction that remains attached to the cell wall of pulp vesicles, PME reacts with pectin resulting in cloud precipitation, which is unattractive to the consumer. In concentrated citrus juice, gel formation occurs in the presence of active PME when sufficient amount of demethylated pectins accumulate. Gel formation entraps water by forming a three-dimensional network. Formation of such gels result in increased apparent viscosity of the concentrate which translates into high pumping costs and the need for blending of the product during bulk storage (Baker and Cameron, 1999).

In general, three different types of PME action patterns are considered: (1) a single-chain mechanism, where all contiguous methyl esters from a single HG chain are removed by PMEs before dissociating from substrate; (2) a multiple-chain mechanism, where enzyme-substrate complex dissociates after each reaction, resulting in only one galacturonic acid residue; (3) a multiple-attack mechanism, where PMEs catalyze a limited number of methyl esters before releasing enzyme-pectin complexes. The action mode of PME isozymes in orange were considered as multi-chain or multi-attack mechanism (Kim, 2004).

PME isozymes

Multiple isozymes of PME are present in fruit and vegetable tissues. Though they catalyze same reaction, PME isozymes differ in isoelectric pH (pI), molar mass, degree of glycosylation, thermal stability and catalytic properties (Bosch, 2005; Cameron et al., 1998; Jolie et al., 2010). Pectinmethylesterase is very sensitive to ionic environment, the optimum pH for

different PMEs varies depending on their wide pI ranges. Most plant and bacterial PMEs have optimal pH ranging from neutral to alkaline while most fungal PMEs have acidic to neutral optimal pH (Pelloux et al., 2007).

Based on thermostability, different isozymes of PMEs are isolated and described in previous literatures. Pectinmethylesterases resisting inactivation at temperatures greater than 70 °C are considered thermalstable PME (TS-PME). Thermostable citrus PME retain activity when heat treatment is inadequate and cause juice clarification. Thermolabile PMEs (TL-PME) also clarified citrus juices (Cameron et al., 1998; Wicker et al., 2002)

Cameron et al. (1998) studied different PME isozymes in Valencia orange peel using a combination of anion exchange and affinity chromatography. Four different PME isozymes were discovered. Only one of these four was TS-PME (PME 3). The other three PMEs catalyzed destabilization of orange juice cloud within 10 days at 30 °C. Citrus juice was destabilized rapidly at 4 °C by PMEs 1 and 3 but relatively slower by PME 2. Isozyme PME 4 did not affect juice destabilization at either 30 °C or 4 °C.

Two isozymes of PME have been discovered in tomato plants: the type 1 isozyme was synthesized only in fruit issues while the type 2 isozyme expressed not only in fruit but generally in vegetative tissues. These two types of isozymes can be distinguished biochemically that cations were not required for type 1 isozyme whereas necessary for type 2 isozyme (Joel Gaffe, 1994).

In another research, six forms of PMEs from valencia juice sac-derived tissue culture cells were obtained (Cameron et al., 1994). One of these isoforms (PME 3b) was the thermally stable form which retained 29% activity after being incubated at 95 °C for 30 s. Two other forms

retained activity after treatments at 80-90 °C. The most active form, comprised 93.6% of total activity at 30 °C was completely inactivated after being incubated at 80 °C for 2 min.

Four different kinds of PMEs have been purified and characterized from sweet cherry in previous research (Alonso et al., 1996). Two kinds of these PMEs present thermolabile properties that gradually loss activity as temperature increase. The other two PME isozymes in sweet cherry were more thermostable forms remaining 100% activity at 60-70 °C after 1 min heat treatment.

Cameron and Grohmaa (1995) particially purified four different kinds of PME from red grapefruit finisher pulp by chromatography on Heparin-Sepharose CL-6B. One thermostable form retained 66.7% activity after incubating in 80 °C water bath for 2 min and about 45.2% activity after incubating in 95 °C for 1 min.

PME reaction in the presence of cations

Cation affects both gelation and PME activity. Mineral content in juices varies depending on growing region, cultivar, production practice etc. Once solubilized, PME reacts with pectin forming inactive enzyme-substrate complexes. At low level, cations displace PMEs from pectin substrate, increasing apparent activity of PMEs thus increasing potential of clarification of citrus juice (Wicker et al., 2002).

According to their mode of interaction with pectin, pectic enzymes can be classified into two categories: side chain modifying enzyme and backbone modifying enzyme. In general, side chain modifying enzymes catalyze different reactions of sugar with neutral oligosaccharides in side chain of pectin while backbone modifying enzymes catalyze reaction in homogalacturonan backbone chain. When calcium was absent, pectin solutions incubated with side chain modifying enzymes (galactase, arabinase, endoglucanase or xylanase) were more likely to give viscous

solution rather than gel. Schmelter et al. (2002) demonstrated that in all treatments, apple pectin solutions reacted with side chain modifying enzymes resulting in the decrease of viscosity. Moreover, the viscosity was independent of shear rate in this case, at shear tress about 0.1 to 0.5 $Pa \cdot s^{-1}$ when shear rate ranged from 5 to 500 s^{-1}. While incubated with backbone modifying enzymes like PME in the absence of calcium, the zero-shear viscosity of apple pectin solution increased remarkably, about 4 or 7-fold and the viscosity became strongly shear rate-dependent. The increase of the zero-shear viscosity was even larger in the case of citrus pectin, about 14-fold increase.

Two basic types of reactions are usually considered resulting in gelation in citrus concentrates or cloud loss in single-strength citrus juices. One common form refers to the reversion of acid or base catalyzed esterification of carboxyl groups of the galacturonic acid components of pectins. Gel formation occurs when there are sufficient galacturonic acids groups, which link together via divalent cations to form pectates. Another type of deesterification results from the pectinase enzymes like PME that was mentioned before. Pectinmethylesterase naturally attached to orange pulp was most likely the cause for the large change in the rheological properties of unpasteurized pulp. Gel formation or increased viscosity of the liquid phase made rheological determination of fresh citrus pulp more challenging on account of their complicated structural matrix of small solids surrounded by liquids (Payne, 2011).

Rheological models for citrus pulp and other Non-Newtonian fluid foods

The interaction of PME and pectin contributes to the rheological properties variation of unpasteurized orange pulp. The variation changes with time. The rheological properties of orange pulp are essential and need to be characterized to optimize processing equipment in the citrus industry. Some of the most commonly used flow models that describe shear stress versus

shear rate were listed in Table 1.1 by Rao (2010). However, none of these equations was able to describe flow behavior at those shear rates where slippage occurs. Furthermore, other effects like temperature and concentration also affect rheology of orange pulp, which induce to the rheological characterization more challenging. In previous research, Payne (2011) pointed out that at very low shear rates (below 4 s^{-1}) the relationship between shear rate and shear stress of orange pulp was best described by power law model after evaluating power law, Herschel-Bulkley and Casson models.

Most rheological models describe the relationship between shear stress and shear rate. However, from a practical perspective, in the equipment design, apparent viscosity is frequently used. For example, it is necessary to characterize the apparent viscosity of fruit juices when concentrating to calculate the rate of heat transfer and energy consumption in such operations.

An apparent viscosity mathematical model to describe the combined effect of concentration, temperature and shear rate on the apparent viscosity for tahin/pekmes (seasame paste and grape juice concentrate) blends have been investigated for engineering applications in pasteurization system. The apparent viscosity model was described as

$$\eta_a = K_1 \exp\left(\frac{E_a}{RT} + d_1 C\right)\dot{\gamma}^{n-1} \tag{1-2}$$

Where K_1 is the proportionality constant related to consistency coefficient, d_1 and R are constants, E_a is the activation energy, $\dot{\gamma}$ is the shear rate, n is the average flow behavior index. C and T are centration and temperature (Arslan et al., 2005).

Most shear-thinning biopolymers and hydrocolloid dispersions at sufficiently high concentration exhibit three similar stages of viscous status when sheared over a wide shear rate range: (1) at low shear rates, dispersions show constant zero-shear viscosity (η_0) as initial shear rate tends to zero, (2) at shear-thinning range, the viscosity of the solution decreases in

accordance with the power law relationship, (3) η_∞ is the apparent viscosity reaching to a constant value at high shear rate (Rao, 2014).

The apparent viscosity (η_a) versus shear rate ($\dot{\gamma}$) plots can be described by Cross (1-3) and Carreau (1-4) models.

$$\eta_a=\eta_\infty+\frac{(\eta_0-\eta_\infty)}{1+(\alpha_c\dot{\gamma})^m} \quad (1\text{-}3)$$

$$\eta_a=\eta_\infty+\frac{(\eta_0-\eta_\infty)}{[1+(\lambda_c\dot{\gamma})^2]^N} \quad (1\text{-}4)$$

Where α_c and λ_c are time constants in accordance with the relaxation times of the polymer in solution, m and N are dimensionless exponents. η_∞ is usually neglected due to its magnitude in food polymer dispersions with practical interest concentrations are usually very low. The relationship between viscosity and shear rate of aqueous dispersions of high methoxyl pectins and locust bean gum (Silva et al., 1992), konjac flour gum (Jacon et al., 1993), mesquite gum solution and other gums (Yoo et al., 1995) were described well by the Cross and Carreau models.

Falguera and Ibarz (2010) developed a new model regarding a new expression that related apparent viscosity to shear rate of concentrated orange juice:

$$\eta_a=\eta_\infty+(\eta_0-\eta_\infty)\cdot\dot{\gamma}^{-k} \quad (1\text{-}5)$$

Where γ is the shear rate and K is the consistency coefficient.

Wall slip

Unlike most fruit pastes and concentrates, orange pulp and some food emulsions like peanut butter and mayonnaise display slippage. At shear rate ranges greater than ~4 s^{-1}, slippage plays an important role in determining the energy loss due to friction thus optimizing processing equipment in orange pulp pasteurization system.

The wall slip phenomenon of molten polymers had been reviewed and compiled by Hatzikiriakos (2012). According to his review, there were two slip regions in the flow of polymers. In the first slip region, slippage was caused by a few chains of polymers detaching from the wall. The first region was usually observed macroscopically at a relatively small magnitude of the critical wall shear stress (Hatzikiriakos, 1995). In the second slip region, a transition from a weak to a strong slip took place at a critical wall shear stress value. The mechanism of slip in the second region was a sudden disentanglement of the polymer chains in the bulk from those polymers chains in a monolayer adhered at the wall (Allal and Vergnes, 2007).

In suspensions, slippage is caused by different velocities between a thin layer of fluid and the bulk material that do not interact or weakly interacts with the wall. When sufficient shear rate is provided, the liquid phase in the bulk material tends to separate from the bulk and move toward the wall, resulting in a thin layer of fluid near the wall. The formation of this liquid-rich thin layer made any bulk flow easier to move due to a lubrication effect (Chen et al., 2009). Previous researchers measured the particle concentration in the thin layer near the wall with thickness between 0.3 and 1.4 μm with a technique based upon attenuated total reflection-Fourier-transform infrared (ATR/FTIR) spectroscopy. They observed significantly decrease of the particle concentration near the wall suspension, which was consistent with the statement that there existed a thin layer of fluid with lower viscosity compared to that in bulk material flow (Kok et al., 2002). The wall slip in concentrated suspension is considered as “apparent slip” (Lam et al., 2007). The wall slip of orange pulp flow in our research is considered as “apparent slip” because orange pulp can be considered as particles suspended in juice. This apparent slip is different from the mechanism of slip of polymer melts, for polymer melts are single phase

viscous liquids that the velocity discontinuity exists between the polymer and the wall, and is denoted as “true slip” (Jana et al., 1995).

Slippage influences the apparent measurement of rheological properties of fluids. The effect of slippage on the rheological properties of fluids is usually determined by capillary or rotational rheometry.

Determination of slippage by capillary rheometry

Capillary viscometer or rheometer works either through gravitational force, hydrostatic force or pressurized gas/piston movement. The mechanism of capillary rheometry is to measure the pressure drop and/or flow rate of a flowing fluid through a known length of pipe of known diameter over a period of time to calculate the apparent viscosity (Payne, 2011).

Lam et al. (2007) investigated the effect of particle concentration of a mixture of polymer ethylene vinyl acetate (EVA) polymer and non-colloidal spherical powder (glass microspheres) on wall slip behavior in a capillary rheometer. For suspensions with different particle concentration, the slip velocity V_s increased as the particle concentration increased at the same temperature. Slip velocity is a function of wall shear stress and it is accounted for the added flow rate due to the wall slip compared to flow rate without slippage (Chakrabandhu and Singh, 2005). They inferred it as a result of the hydrodynamic interaction between the dispersed particles and the solid wall. At the same particle concentration, as the flow rate increased, the pressure drop difference between experimental data and predicted pressure drop without slippage increased, which illustrated that slippage had an effect on flow behavior of fluid.

Determination of slippage by rotational rheometry

Rotational viscometer or rheometer is commonly used to establish the relationship between shear stress and shear rate thus, to measure viscosity for Newtonian fluids, or apparent

viscosity for Non-Newtonian fluids. The principle of operation is based on the viscous drag caused by the speed of the rotating body in contact with the liquid (Payne, 2011).

The effect of the solid content, temperature on slip velocity and slip layer thickness of hydroxyl-terminated polybutadiene (HTPB) mixed with different sizes of aluminum powder and glass beads was characterized using parallel disk rotational rheometer by Soltani and Yilmazer (1998). They found the slip velocity increased linearly with the shear stress. At constant shear stress, the slip velocity increased as the temperature increased. For slip layer thickness, as the glass bead particle size increased, the layer thickness increased proportionally at constant concentration.

The effect of wall slip on the yield stress of cement paste was determined using a rotational rheometer with smooth-walled concentric cylinder and vane geometries (Figure 1.2). The data obtained using a vane geometry presented slip occurring as a sudden decrease in shear stress after 180 s. The flow curve obtained using a cylinder geometry showed slippage at 50 s, presented as an instantaneous decrease in stress. The decrease in stress was caused by development of a solvent-rich layer due to the displacement of the cement particles away from the smooth walls of the cylinder. This solvent-rich layer produces a lubricating effect and make flow easier. Then, the stress developed again due to the resistance to flow of cement paste (Figure 1.3). The influence of rotational speed on yield stress using vane geometry was investigated. A minimal yield stress happened at rotational speeds near 0.01 $rad \cdot s^{-1}$ with vane geometry. As the concentration of cement paste increased, the yield stress increased. For the same concentration cement paste, at low rotational speeds, the development of stress in the sample was low and the duration of time to observe slippage was very long, about 450 s at 0.005

rad/s at water to cement ratio 0.3. On the contrary, at high rotational speeds, the duration of time to observe slippage was very short, approximately 1-3 s at 1 rad·s^{-1} (Saak et al., 2001).

Walls et al. (2003) investigated yield stress and wall slip phenomena for colloidal gels consisting of hydrophobic silica, polyether, and lithium salts with serrated, smooth, hydrophilic and hydrophobic surfaces using a rheometric dynamic stress rheometer. The solvating medium with higher viscosity appeared to lower the occurrence of wall slip. The formation of slip layer was affected by testing geometries with hydrophobic and hydrophilic surface chemistries. The hydrophilic surface had minimal effect on slip whereas the hydrophobic surface decreased slip behavior.

Modeling of slippage

Below is a summary of slippage models that might be applied to citrus pulp. Various models have been developed to describe slippage. The most common model was the Mooney's method (Mooney, 1931). Mooney's method has been extensively used to characterize the wall-slip velocity and the rheological behavior of various materials like polymers or suspensions. Mooney's explicit formulas for slip and fluidity were built on three assumptions: (1) the thickness of the slip layer involved is small compared to the dimensions of the pipe (2) the flow should always be laminar, fully developed, incompressible and isothermal, (3) all surfaces contacted with the moving fluid should be alike in order to ensure that slip depend only upon shear stress (Crawford et al., 2005; Mooney, 1931).

In Mooney's method, the shear stress at a point in the capillary is given by

$$\sigma=\frac{\pi r^2 P}{2\pi r}=\frac{rP}{2r} \tag{1-6}$$

Where *r* is the distance from the center axis of capillary to the point; P is the pressure gradient equals to pressure drop at two points of capillary divided by pipe length ($\frac{P_1-P_2}{L}$).

So the wall shear stress would be calculated as

$$s=\frac{aP}{2} \tag{1-7}$$

Where a is the radius of the capillary tube.

Then, the velocity at any point can be described as

$$v=\frac{aP}{2}\beta+\int_r^a \frac{rP}{2}\phi dr=\frac{P}{2}(a\beta+\int_r^a \phi r dr) \tag{1-8}$$

Where β is the slip coefficient and ϕ is velocity at the shear stress σ.

Then the efflux *E* is

$$E=\int_0^a 2\pi r v dr=\frac{\pi a^3 P\beta}{2}+\pi P\int_r^a(\int_r^a \phi r dr)rdr \tag{1-9}$$

Equation 1-9 can be simplified as

$$E=\frac{\pi P}{2}(a^3\beta+\int_0^a \phi r^3 dr) \tag{1-10}$$

Combine with equation 1-6, we can now change the variable from *r* to σ

$$\frac{E}{\pi a^3}=\frac{s\beta}{a}+\frac{1}{s^3}\int_0^s \phi\sigma^3\, d\sigma \tag{1-11}$$

$$\frac{\partial(\frac{E}{\pi a^3})}{\partial(\frac{1}{a})}=s\beta=v_a \tag{1-12}$$

Ramamurthy successful used Mooney's model to illustrate that during the extrusion of polyethylene melts, wall slip occurred above a critical shear stress level (Ramamurthy, 1986). He concluded that linear low-density polyethylene's (LLDPE) critical shear stress level was approximately 0.14 MPa. Vinogradov and Ivanova (1968) investigated flow behaviors of various rubbers and concluded that under certain conditions, a power law dependence of slip velocity on shear stress was found. Other researchers used Mooney's method to investigate the slippage of High-density polyethylene (HDPE) on a sliding plate rheometer obtained power law relationship

between shear stress and slip velocity as well (Hatzikiriakos and Dealy, 1991). But the Mooney's method was not always successful and it sometimes gave researchers unreasonable results. For example, in Mourniac's investigation about styrene-butadiene rubber (SBR) flow, he obtained Mooney plots with negative intercept on shear rate axis and the correlation was poor (Mourniac et al., 1992). Other researchers also obtained unexplainable results using Mooney's method (Halliday and Smith, 1995).

Several modifications have been applied to Mooney's method. The Rabinowitsch correction was used to correct Mooney's method for non-Newtonian fluid behavior and Jastrzebski characterized the entrance effects and wall effects for the flow of concentrated suspension (Jastrzebski, 1967). Crawford improved previous slip models for silicone gums and rubbers application. He proposed the new model to be used in computational fluid dynamics (CFD) simulations.

According to Crawford et al. (2005) and Chen et al. (2009), the proposed new slip analysis is that the wall slip velocity, v_s is a function of wall shear stress, τ_w, and capillary radius, R at a given stress level:

$$v_s = \frac{\zeta \tau_w}{R^d} \tag{1-13}$$

Where ζ is the slip coefficient. When d=0, the new slip analysis is equal to the Mooney method (Mooney, 1931). In equation 1-13 "d" is an empirical parameter as adjusted to minimize the overall error between the data points and the best-fit lines on $\frac{4Q}{\pi R^3}$ versus $\frac{1}{R^{1+d}}$ in equation (1-18).

The total volumetric flow rate in a flow system Q can be derived by:

$$Q = Q_s + Q_b = 2\pi \int_0^R (v_s + v_b) r dr = \frac{\pi R^2 \zeta \tau_w}{R^d} + 2\pi \int_0^R v_b r dr \tag{1-14}$$

Where Q_b and Q_s are the volumetric flow rate of the bulk materials and the flow rate caused by slip effect; r is the radius from the center line (Figure 1.4).

$$Q_s = \pi R^2 v_s = \frac{\pi R^2 \zeta \tau_w}{R^d} \tag{1-15}$$

$$Q_b = 2\pi \int_0^R v_b r dr = \frac{\pi R^3}{\tau_w{}^3} \int_0^{\tau_w} \tau^2 f(\tau) d\tau \tag{1-16}$$

In the above equation, it is always assumed that the bulk material is homogenous, and the relationship between shear stress τ and shear rate γ can be described by $y = f(\tau)$.

The apparent wall shear rate γ_{aw} can be expressed as

$$\gamma_{aw} = \frac{4Q}{\pi R^3} = \frac{4\zeta\tau_w}{R^{1+d}} + \frac{4}{\tau_w{}^3} \int_0^{\tau_w} \tau^2 f(\tau) d\tau \tag{1-17}$$

The second term on the right hand is independent of the pipe radius at constant shear stress. So, the derivative of the apparent wall shear rate can be described as:

$$\frac{\partial(\frac{4Q}{\pi R^3})}{\partial(\frac{1}{R^{1+d}})} | \tau_w = 4\zeta\tau_w \tag{1-18}$$

The second term on the right side of eqution 1-17 becomes zero at constant shear stress. Therefore, plots of $\frac{4Q}{\pi R^3}$ versus $\frac{1}{R^{1+d}}$ at a constant shear stress generates the gradient of $4\zeta\tau_w$. Then, the slip velocity can be expressed as

$$4v_s = \frac{4\zeta\tau_w}{R^d} \tag{1-19}$$

The value of d can be found by an iteration method that minimizes the overall error between the data points and the best-fit lines on plots of $\frac{4Q}{\pi R^3}$ versus $\frac{1}{R^{1+d}}$. In the investigation, an average deviation of less than 5% between the data points and the fit lines on the modified Mooney plots. The true wall shear rate of the bulk material at constant shear stress would be derived by:

$$\gamma_{tw}=\left(\frac{Q-Q_s}{\pi R^3}\right)\left\{3+\frac{d\ln\left[\frac{Q-Q_s}{\pi R^3}\right]}{d\ln\tau_w}\right\} \quad (1\text{-}20)$$

Where γ_{tw} is the true wall shear stress.

Based on power law, the true rheological plots for non-newtonian fluids with wall slip can be described as:

$$\tau_w=K\gamma_{tw}^{\ n} \quad (1\text{-}21)$$

Where K is the consistency coefficient and *n* is the flow behavior index.

Temperature and concentration effects on the flow behavior of fluid

Besides the effect on rheological properties caused by interaction of PME and pectin in orange pulp and the effect of slippage at shear rate greater than 4 s^{-1}, temperature is another important factor affecting flow behavior of fluid. Effect of temperature and concentration on the flow behavior of pasteurized orange pulp has been characterized by Payne (2011) and Munoz (2012). In the food industry, different temperature gradients are usually chosen according to different processing conditions and demands, from freezing to 135 °C in ultra-high temperature pasteurization (Payne, 2011). An Arrhenius-type equation is often used to quantify the effect of temperature in the consistency of a fluid.

$$\mu=Ae^{E_a/RT} \quad (1\text{-}22)$$

$$K=Ae^{E_a/RT} \quad (1\text{-}23)$$

Where A is constant; E_a is activation energy of flow; R is the ideal gas constant; and T is the absolute temperature. At the highest activation energy and concentration, the viscosity of fluid was most affected by temperature (Belibağli and Dalgic, 2007). This Arrhenius-type equation describes the effect of temperature on the consistency coefficient of Non-Newtonian fluids (1-23).

Solute concentration is also a very important factor determining flow behavior. Effect of concentration on the flow behavior of concentrated milk was evaluated by Vélez-Ruiz and Barbosa-Cánovas (1998), which could be empirically described as equation below:

$$n = A_n \exp(b_n X) \tag{1-24}$$

$$K = A_K \exp(b_K X) \tag{1-25}$$

Where A and b are empirical constant and X is the concentration.

The combined effect of temperature and concentration can be written as:

$$K = A\exp(E_a/RT)BX \tag{1-26}$$

$$\ln K = \beta_0 + \beta_1\left(\frac{1}{T}\right) + \beta_2 X \tag{1-27}$$

Where $\beta_0, \beta_1, \beta_2$ are empirical parameters.

Rheological properties of some processed liquid foods and semisolid foods

Rheological properties of some processed fluids and semisolid foods were discussed by Rao (2010). The rheological properties of orange juice and frozen concentrated orange juice (FCOJ) were investigated. The rheological properties of FCOJ depend on the soluble solids content, pulp content, size and shape of the particles and temperature. For Pera orange juice with 5.7% pulp, the K value increased from 0.89-23.58 $Pa{\cdot}s^n$ as °Brix increased from 50.8-65.3 at 10 °C, and the apparent viscosity of Pera orange juice increased from 0.29-3.38 Pa·s (Vitali and Rao, 1984). The effect of pulp content and temperature on consistency coefficient for orange juice was also determined by Vitali and Rao (1984). The consistency coefficient increased from 5-11 $Pa{\cdot}s^n$ as the pulp content increased from 0-11% at 20 °C. For tomato juice, at pH 4.3, no significant difference in consistency coefficient (K) and flow behavior index (n) of tomato juice with solid contents below 16% was observed at shear rate range 500 to 800 s^{-1}. When solid content was more than 20%, a significant decrease in K (18.7-6.1 $Pa{\cdot}s^n$) was noticed with

increasing temperature (32.2 to 82.2 °C), while n remained almost constant (0.38-0.54). More extensive magnitudes of flow parameters of processed fluid and semisolid foods were summarized in Table 1.2.

Previous work

Rheological properties determination of pasteurized citrus pulp from 503 to 795 $g \cdot L^{-1}$, at temperature from 4 to 80 ° C were recently done (Payne, 2011). Payne observed that slippage occurred at shear rates above 2 and 4 s^{-1} and was more pronounced at low temperature and high concentration. Payne used power law to fit shear stress versus shear rate plots at shear rates smaller than 2 to 4 s^{-1}. The flow behavior index (n) ranged from 0.18 to 0.42, which was independent on temperature and concentration. The consistency coefficient (K) increased as temperature decreased or concentration increased, ranging from 33.0 to 233.6 $Pa \cdot s^n$. All the K and n values are summarized in Table 1.3. Slippage coefficient (β_c) and pressure drop (ΔP) for the pulp at different temperatures and concentrations in a flow system were also determined. Generally, as the measured flow rate increased, pressure drop increased, as well as slippage coefficient. Pressure drop increased as the temperature decreased or concentration increased.

Based on this research, Muñoz in 2012 determined the thermal properties and heat transfer characteristics for high concentration orange pulp. In first part of his study, moisture content, density and thermal properties were determined for pulp with concentrations ranging from 500 to 800 $g \cdot L^{-1}$. Moisture content was similar for all pulp concentrations, from 82.1% to 82.7%. Since in general, the thermal properties of high moisture foods are a function of moisture content, there was no significant difference between obtained specific heat capacity, thermal diffusivity and thermal conductivity for pulp with different concentrations. For orange pulp with concentration ranging from 500 to 800 $g \cdot L^{-1}$, heat transfer coefficient had positive linear

correlation with velocity. The local heat transfer coefficient increased as the concentration of pulp decreased. The overall heat transfer coefficients obtained in heating section for different concentrations and velocities did not change a lot compared to local heat transfer coefficients. They were similar at pulp concentrations 700 and 800 $g \cdot L^{-1}$.

Though a lot of work has been done that covered the most important factors for measuring flow behavior of orange pulp, we became aware of another factor that needed to be considered: Pectinmethylesterase (PME). In Payne's research, she found that PME had an effect on the rheological properties of fresh orange pulp (Figure 1.5). But she did not characterize the effect. Instead, she pasteurized pulpy juice before recovering pulp to eliminate that effect. In citrus processing industry, rheological properties of pulp with active PMEs are practical to provide information for flow system optimization.

Pulp recovered from juice is not always pasteurized immediately after extraction. It may be refrigerated for some time before processing or accumulated until sufficient amount is available to pasteurize. As time passes, apparent viscosity of orange pulp increases due to PME activity. As a consequence, the power required to pump pulp increases. However, the effect of PME on the rheological properties of orange pulp has not been characterized. This information is necessary to optimize pulp pasteurization equipment and processing conditions. The overall objective of this and previous studies by our research team is to reduce capital and operating pumping costs while ensuring the uniform pasteurization of orange pulp. To achieve this overall objective it is necessary to develop a mathematical model that accounts for slippage and the effects of temperature, flow rate, pulp concentration, and PME activity.

The specific objective of this thesis was to determine the effect of PME on the flow behavior of fresh Valencia orange pulp and, thus, on the power required to pump pulp in a flow

system. This information is necessary to predict pump power requirement as a function of storage time.

The reported information about the rheological properties of unpasteurized orange pulp with different storage time is expected to assist citrus processors in better handling of pulp before pasteurization.

Gaps of knowledge

The following gaps of knowledge that need to be filled to optimize handling and pasteurization of orange pulp have been identified:

- Effect of pectinmethylesterase on the flow behavior of fresh 'Valencia' orange pulp and the pump power requirements in a flow system.
- Slip model to predict slip velocity and other flow parameters in the flow system for orange pulp pasteurization.

Research Studies

The experimental portion of this thesis consisted of two studies. Study #1 focused on the characterization of rheological properties of fresh citrus pulp at selected concentration across a range of storage times at 4 °C. Study #2 was to determine the pressure drop at different flow rates and storage time in pilot-scale flow system thus characterizing pump power required for pumping pulp after different storage time.

Table 1.1 Some flow behavior models to describe shear stress (σ) versus shear rate (γ) modified from Rao (2010).

$\sigma=\eta\dot{\gamma}$	Newtonian model
$\sigma=\frac{\dot{\gamma}}{[\frac{1}{\eta_0}+K_E(\sigma)^{\left(\frac{1}{n_E}\right)-1}}$	Ellis model for low-shear rate data include η_0
$\sigma=\eta_\infty\dot{\gamma}+K_s\dot{\gamma}^{n_s}$	Sisko model for high-shear rate data include η_∞
$\eta_a=\eta_\infty+\frac{\eta_0-\eta_\infty}{1+(\alpha_c\dot{\gamma})^m}$	Cross model for data over wide range of shear rates
$\eta_a=\eta_\infty+\frac{\eta_0-\eta_\infty}{[1+(\lambda_c\dot{\gamma})^2]^N}$	Carreau model for data over a wide range of shear rates
$\sigma=K\dot{\gamma}^n$	Power law model used extensively in handling application
$\sigma-\sigma_0=\eta'\dot{\gamma}$	Bingham model
$\sigma-\sigma_{0H}=K_k\dot{\gamma}^{n_H}$	Herschel-Bulkley model
$\sigma^{0.5}=K_{0c}+K_c(\dot{\gamma})^{0.5}$	Casson model used especially in treating data on chocolates

Table 1.2 Flow behaviors of some fruit and vegetable products modified from Rao (2010).

Product	Conc. (% Solids)	Method	Temp (°C)	Shear rate (1/s)	K ($Pa \cdot s^n$)	n	Yield stress (Pa)
Tomato juice (pH 4.3)	5.80	Cone cylinder	32.2	500-800	0.22	0.59	
			48.9		0.27	0.54	
			65.6		0.37	0.47	
Tomato juice (pH 4.3)	12.80	Cone cylinder	32.3	500-800	2.1	0.43	
			48.9		1.18	0.43	
			65.6		2.28	0.34	
			82.2		2.12	0.35	
Tomato juice (pH 4.3)	16.00	Cone cylinder	32.3	500-800	3.16	0.45	
			48.9		2.27	0.45	
			65.6		3.18	0.40	
			82.2		3.27	0.38	
Tomato juice (pH 4.3)	25.00	Cone cylinder	32.3	500-800	12.9	0.41	
			48.9		10.5	0.42	
			65.6		8.0	0.43	
			82.2		6.1	0.44	
Tomato concentrate	35.74	Parallel plate carimed	25.0	4-576	297.0	0.38	
	24.16				65.7	0.27	
	17.86				26.1	0.26	
	11.78				6.0	0.33	
	35.74	Back extrusion	25.0	4-576	249.0	0.29	
	24.16				58.5	0.21	
	17.86				24.3	0.23	
	11.78				5.82	0.27	
Apple sauce	11.00	Brookfield RTV	30.0	5-50	11.6	0.34	
	11.00		82.0		9.0	0.34	11.6
Pear puree	14.60	Tube viscometer	27.0	100-2000	5.3	0.38	
Pear puree	16.00	Tube viscometer	30.0	100-2000	5.6	0.35	
Apricot puree	16.00	Brookfield RTV	30.0	5-50	6.8	0.30	
Apricot puree	13.8	Tube viscometer	27.0	5-50	7.2	0.41	
Guava puree	7.2 °Brix	Tube viscometer	24	100-10000	0.26	0.68	
Guava puree	7.4 °Brix	Tube viscometer	25.0	100-10000	0.28	0.68	
Guava concentrate	12.3°Brix		24.0		1.60	0.55	

Guava concentrate	15.9°Brix		24.0		5.00	0.32
Guava concentrate	22.7°Brix		24.0		41.00	1.65
Orange juice concentrate Hamlin early	42.5 °Brix	Haake RV 12 concentrate cylinder		0-500	0.41	0.59
Orange juice concentrate Hamlin late	41.4 °Brix	Haake RV 12 concentrate cylinder	25.0	0-500	0.19	0.735
Orange juice concentrate Hamlin late	41.4 °Brix		15.0	0-500	0.81	0.56
Orange juice concentrate Hamlin late	41.4 °Brix		0.0	0-500	0.18	0.62
Valencia orange juice, 21.2% pulp	65.3 °Brix		-18.3		109.9	0.55
Valencia orange juice, 21.2% pulp	65.3 °Brix		-14.2		59.7	0.61
Valencia orange juice, 21.2% pulp	65.3 °Brix		-9.7		40.6	0.6
Valencia orange juice, 21.2% pulp	65.3 °Brix		-5.1		24.5	0.63
Valencia orange juice, 21.2% pulp	65.3 °Brix		-0.4		18.5	0.62
Valencia orange juice, 21.2% pulp	65.3 °Brix		10.2		8.3	0.65
Valencia orange juice, 21.2% pulp	65.3 °Brix		19.7		6.1	0.61
Valencia orange juice, 21.2% pulp	65.3 °Brix		29.6		2.5	0.68
Mango pulp juice	16.0 °Brix	Concentrate cylinder	25.0		10.0	0.32
Mango pulp juice	17.0 °Brix	Rheotest 2 Rotational RVT Brookfield	25.0		27.8	0.33

Table 1.3 Average (n=3) power law parameters, activation energies for different temperatures and concentration of pasteurized orange pulp (Payne, 2011).

Temperature (K)	503 g/L		597 g/L		643 g/L		795 g/L	
	K	n	K	n	K	n	K	n
277	0.42	70.0	0.41	123.5	0.36	137.2	0.39	233.6
293	0.32	50.5	0.29	91.3	0.40	109.7	0.33	180.1
311	0.37	50.9	0.34	83.6	0.30	88.9	0.30	146.7
331	0.37	43.0	0.25	61.5	0.29	78.3	0.23	115.1
353	0.18	33.0	0.22	59.9	0.22	74.9	0.21	112.6
E_a (kJ/mol)	7.1		9.7		8.2		10.2	


Figure 1.1 Quick fiber test apparatus (Courtesy of Juan Fernando Munoz).

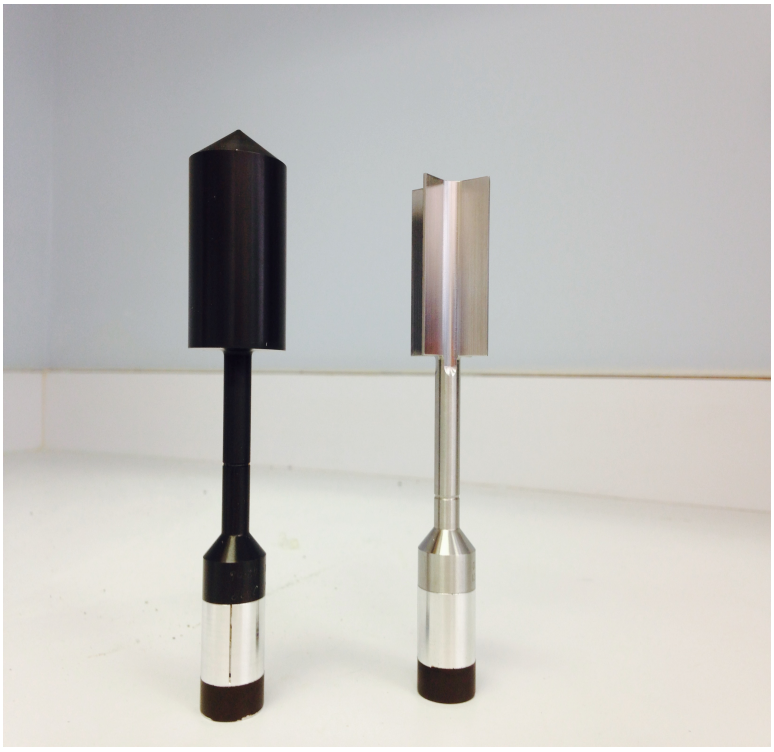
Figure 1.2 concentric cylinder (a) and vane (b) geometry.

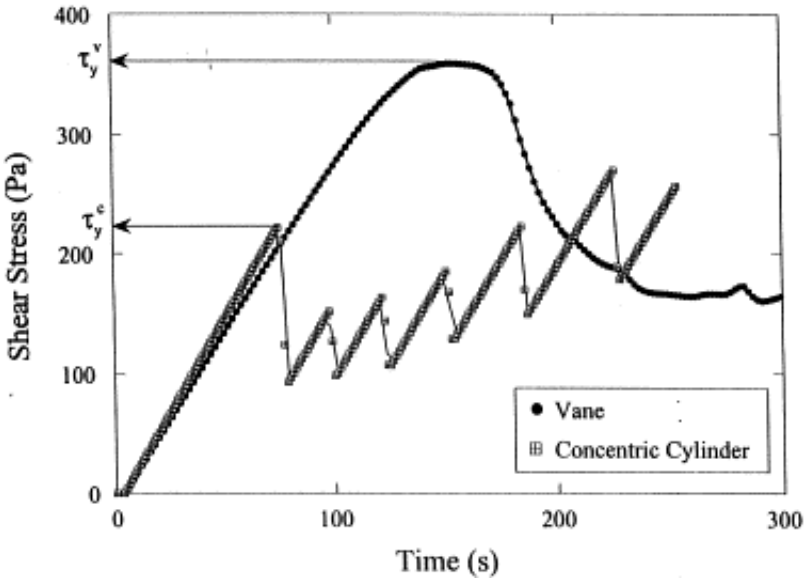

Figure 1.3 Representative stress growth curves for concentric cylinders and vane at rotational speed = 0.01 rad/s (Saak et al., 2001).

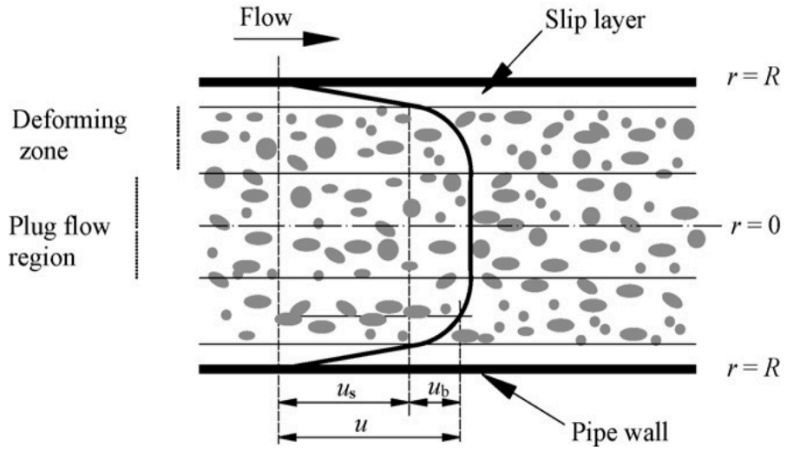

Figure 1.4 schematic of slip flow of water slurry in pipelines (Chen et al., 2009).

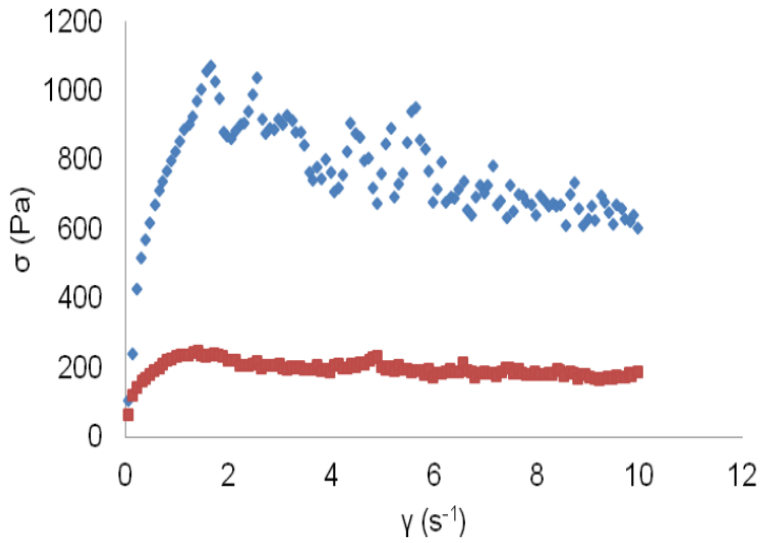

Figure 1.5 Effect of pasteurization on shear stress at selected shear rates at 4 °C for 795.1 g • L^{-1} orange pulp. (◆) Unpasteurized and (■) Pasteurized (Payne, 2011).

CHAPTER 2

RHEOLOGICAL CHARACTERIZATION OF FRESH UNPASTEURIZE VALENCIA ORANGE PULP

Introduction

The rheology of orange pulp is critical to handling as an ingredient added back to orange juice or for the formulation of other beverages. Fresh orange pulp has a complex flow behavior, displaying slippage in addition to changing with storage time. In a recent study, Payne (2011) found that pectinmethylesterase (PME) increased shear stress of orange pulp at any shear rate after storing pulp for several hours prior to making rheological measurements. However, Payne did not characterize the effect of PME on pulp rheology for different storage times. Instead, she pasteurized the pulpy juice immediately after extraction and before recovering the pulp to ensure reproducible rheological measurements. However, in the orange juice industry, depending on the processor, the time between pulp recovery and pasteurization as well as the storage conditions before pasteurization vary. Pectinmethylesterase affects rheology of orange pulp by demethlyesterifying pectin, which results in and increase in consistency or apparent viscosity, most likely due to the formation of pectate gels in the presence of calcium cations. That increase in apparent viscosity results in increasing pressure drop in pulp pasteurizers. Slippage occurs at shear rates above 0.6-0.9 s^{-1} producing a liquid-rich thin layer near the wall and makes bulk material flow easier in the pipe due to the lubrication effect (Chen et al., 2009). This lubrication effect also has an effect on pressure drop and pump power requirement in pulp pasteurizers.

The objective of this study was to characterize the effect of PME on the flow behavior of unpasteurized Valencia orange pulp stored for 0 to 48 h at 4 °C.

Materials and Methods

Materials

Fresh Valencia sweet oranges were purchased from a local grocery store (Athens, GA). A Cuisinart pulp control citrus juicer CCJ-500 (East Windsor, NJ) was used to extract fresh orange pulp. An Isotemp 6200 H11 water bath from Fisher Scientific (Waltham, MA) was used to heat-inactivate fresh orange pulp PME after storage for 0 to 48 h at 4 °C by heating at 90 °C for 2 min. Test tubes 16 × 150 mm from Fisher Scientific (Cat. No. 14-961-31) were used to hold separated orange pulp samples for heat treatment. Rheological determinations of pulp were conducted using an AR 2000 Discovery Hybrid rheometer (Figure 2.1) interfaced to a PC using 'TRIOS' computer program from TA instruments (New Castle, DE). A vane geometry (Bob diameter: 28 mm and Bob length: 48 mm) was used to reduce slippage effect of orange pulp against the cup (cup diameter: 37 mm). Orion Versastar advanced electrochemistry pH meter (Suwanee, GA) was used to measure orange pulp's pH during titration thus determining the PME activity of orange pulp. Moisture content of orange pulp was determined using a HR 73 Halogen Moisture Analyzer from Mettler Toledo (Columbus, OH). Soluble solids content (SSC) of orange pulp was determined using an Extech RF 12 Portable Brix Refractometer (0-18%) from MSC Industrial Supply Co. (Melville, NY). Pectin from citrus peel purchased from Sigma-Aldrich (St. Louis, MO) and 1 N standardized NaOH solution purchased from Fisher Scientific (Pittsburgh, PA) were used for PME activity test. Particle size distribution of orange pulp samples was measured using LS 13 320 Laser Diffraction Particle Size Analyzer from Beckman Coulter (Brea, CA).

Methods

Pulp preparation

To ensure random selection of samples, one orange pulp sample were extracted from five to seven oranges from different bags purchased at the local grocery store. The oranges were cut in halves and raw orange pulp was extracted using the citrus juicer. The citrus juicer was set at high level of pulp collection at regular speed. Then, the raw pulp was transferred from the pulp holder in the citrus juicer onto two layers cheesecloth laid on a plastic container that was placed on ice. Cooling the pulp helped to reduce PME activity while collecting enough pulp for the experiment. Seeds, rag and peel particles were removed using a spoon. Although pulp concentration was not determined, particular care was taken to manually obtain uniform consistency. After removal, pulp was collected into a 250 mL beaker. Finally, the beaker was covered with a parafilm and stored at 4 °C. Approximately 60 g of pulp was prepared for each storage time sample. Experiments were run in triplicate.

PME activity determination (PEU test)

Pectinmethylesterase activity is defined as the rate of production of H^+ per unit of time that result from the PME-catalyzed deesterification of pectin methoxyl groups under defined conditions. PME activity was determined using modified method from Kimball (2012). A 1% pectin solution and 0.05 N NaOH solution were prepared in water. The pectin solution was heated to 32 °C in the water bath before performing the assay. Approximately 0.2 g of freshly extracted orange pulp was accurately weighed and mixed with 40 mL of 1% pectin solution in a 100 mL beaker. The 100 mL beaker was immersed in a 250 mL beaker containing 30 °C water. The temperature of the water was controlled with a hot plate. A type K thermocouple connected to digital transducer and indicator model HH127 TC data logger from Omega (Stamford, CT)

and the pH probe were immersed in the pulp and pectin dispersion and stirred continuously to ensure temperature was constant and uniform, as well as to monitor pH as a function of time. A 1.0 N NaOH standardized solution was added to the pulp and pectin mixture until the pH reached 7.6 to 7.8. The pH was recorded and immediately after, 0.1 mL of a 0.05N NaOH solution was added. The time needed for the pH to return to the initially recorded value was recorded. Pectinmethylesterase activity was then calculated in terms of milliequivalents of OH^- that react with H^+ per unit of time and per weight of sample:

$$\text{PEU(unit/mL)} = \frac{(0.05\ \text{N NaOH})(0.1\ \text{mL})}{[\text{pulp sample weight(mL)}][\text{time(min)}]} \qquad (2\text{-}1)$$

The experimental set up is shown in Figure 2.2.

PME inactivation

Orange pulp samples were stored at 4 °C for 0, 2, 4, 8, 12, 16, 20, 24, or 48 h. After storage, about 70 g pulp was equally separated into 10 test tubes to accelerate heat transfer in oil bath. Test tubes were placed on ice to reduce PME activity. Orange pulp in test tubes was heat treated at 95 °C in a silicone 108 oil bath for 2 min to inactivate PME. According to published research (Lee et al., 2003), the D value of thermo stable PME inactivation for Valencia orange pulp heated at 90 °C was 33 s. The z value of thermo stable PME inactivation for Valencia orange pulp was 6.5 °C. After the heat treatment, because of the separation of juice and pulp, samples were collected onto two layers cheesecloth on ice again once heat treatment completed to drain juice and cool down. Finally, chilled and drained pulp samples were collected into 250 mL beakers. The beakers were covered with parafilm. Approximately 0.5 g of the chilled and drained orange pulp sample was used to measure moisture content and soluble solid content right before rheological measurements. Particle size was measured after experiment and calcium content was measured after experiment by soil, plant and water laboratory.

Rheological properties determination

Shear stress controlled rotational rheology tests were conducted using the AR 2000 Hybrid Discovery rheometer. Approximately 50 mL orange pulp were placed in the temperature-controlled jacketed cup. Vane geometry was selected because it minimized slippage between the geometry surface and the sample. Two shear rate ranges were selected: 0-80 s^{-1}, 0-5 s^{-1}. These two shear rate ranges were selected on account of the observation from previous work done by Payne (2011) that slippage occurred at about shear rate 5 s^{-1}. Therefore in our research, the shear rate range 0-80 s^{-1} was selected to determine where did slippage occur and the shear rate range 0-5 s^{-1} was selected to observe and analyze slippage. Temperature was set to 20 °C and duration of each test was 15 min. For shear rate range 0-80 s^{-1}, the shear stress points were collected each 0.1 s^{-1} per second. For shear rate range 0-5 s^{-1}, the shear stress points were collected each 0.01 s^{-1} per second. Rheological determinations were carried out in a completely randomized design.

Determination of particle size and calcium content of orange pulp

Particle size affects the rheological properties of orange pulp. In order to characterize the effect of PME on the rheology of orange pulp, the factor of particle size should be blocked. Particle sizes of four randomly picked orange pulp samples were measured using LS 13 320 laser diffraction particle size analyzer. Sample volume was approximately 7 mL. The optical model for the measurement was Fraunhofer.rf780d. Each measurement was run for 1 min.

Determination of calcium content

Calcium content affects the rheological properties of orange pulp. In order to characterize the effect of PME on the rheology of orange pulp, the factor of calcium content should be blocked as well. The calcium content determination of three randomly picked orange pulp

samples were conducted by soil, plant and water laboratory using ICP-OES at 2400 College Station Road, Athens GA 30602.

Calculation and Data analysis

As previously reported (Payne, 2011), pulp displays slippage at low shear rates as indicated by a sudden decrease in shear stress after an increase as shown in Figure 2.3 for pulp stored for 20 h at 4 °C . The flow behavior index (n) and the consistency coefficient (K) were calculated using the linear regression of the logarithmic form of the power law model (Equation 2-2) at very low shear rates (< 0.6 s^{-1}), smaller than those when slippage occurred.

$$\ln\sigma = \ln K + n\ln\gamma \qquad (2\text{-}2)$$

Linear regression, including the calculation of standard errors for slopes and intercepts was done using Microsoft Excel Mac 2011 version. Other data statistical analysis was done with Minitab 17 (State College, PA). Standard deviations of the three replications, 95% confidence intervals, one-way ANOVA analysis (p-values), and Tukey pairwise comparisons were analyzed to evaluate whether there were significant differences of K and n values for orange pulp stored for the selected storage times.

Results and Discussion

Determination of PME activity

Pectinmethylesterase activity determined for five pulp samples from five different orange batches are listed in Table 2.1. The PME activity of orange pulp was 0.011 ± 0.001 PEU/mL. In previous research, Lee et al. (2005) determined PME activity of unpasteurized orange juice (80% Hamlin, 19% pineapple and 1% others) using Kimball's method (Kimball, 2012). They concluded the PME activity of orange juice with pulp content 11.1% and soluble solids 11.4 °Brix was 5.59×10^{-3} PEU/mL. However, in our research, the PME activity (0.01 ±

0.001PEU/mL) was much higher compared to the orange juice in Lee's research. It was expected to found larger PME activity in orange pulp compared to orange juice because a large portion of PME is bound to orange pulp. PME activity in orange juice was a result of detachment of PME from pulp during extraction. During storage at 4 °C for 15 days, PME activity of the orange juice decreased from 5.59×10^{-3} to about 2.30×10^{-3} PEU/mL for the first 8 days, and then remained stable for the next 7 days.

Shear stress determination of orange pulp with selected shear rate ranges

Shear rate range 0-80 s^{-1}

According to previous research (Payne, 2011), pasteurized orange pulp displayed slippage at shear rates around 2 to 4 s^{-1}. In order to determine the shear rates at those where slippage occurred for unpasteurized orange pulp, rheological properties of orange pulp at selected shear rate range 0-80 s^{-1} for fresh unpasteurized orange pulp stored for 0-48 h at 4 °C were measured and are shown in Figure 2.4. At shear rates smaller than 2 to 5 s^{-1}, as the shear rate increased, the shear stress increased for all the flow curves. Sudden decreases of shear stress were observed at shear rates 2 to 5 s^{-1} for all the pulp samples were indicative of slippage.

The relationship between peak shear stress for shear rate range 0-80 $s^{-1}$and storage time are shown in Figure 2.5. For the pulp sample stored for 0 h, the peak shear stress was 130.7 ± 20.6 Pa before slippage occurred at 5.1 s^{-1}. For the pulp sample stored for 2 h, the shear stress increased to 120.4 ± 2.3 Pa as shear rate increased to 2.7 s^{-1}. For 4 h and 8 h stored samples, the peak shear stresses were 122.1 ± 19.5 and 111.6 ± 11.2 Pa at shear rate 3.0 s^{-1} and 3.3 s^{-1}, respectively. According to Tukey's test, peak shear stress of samples stored for 0, 2, 4, 8, 12 h did not have significant difference. For samples stored for 16, 20 or 24 h, significantly increase in peak shear stresses values ($p<0.05$) before slippage occurring compared to 0 h were observed,

they were 154.4 ± 18.3, 145.8 ± 3.15 and 141.2 ± 24.0 Pa at shear rates 4.6, 4.3, 2.4 s^{-1}, respectively. For the sample stored for 48 h, the highest peak shear stress (196.0 ± 20.9 Pa) before slippage occurring was obtained at shear rate 4.3 s^{-1}, followed by a sharp decrease in shear stress as shear rate increased. According to Tukey's test, the peak shear stress of orange pulp sample stored for 48 h was significantly different from the other pulp samples. There was no clear trend in the shear rate at which we found the peak shear stress as a function of storage time. All peak shear stresses and shear rates when those peak stresses were obtained at shear rate range 0-80 s^{-1} are listed in Table 2.2.

Shear rate range 0-5 s^{-1}

In order to observe and determine the shear rate of slippage occurrence more precisely, the shear stresses at a narrower shear rate range 0-5 s^{-1} for orange pulp stored for 0 to 48 h at 4 °C were also determined. The relationship between peak shear stress for shear rate range 0-5 s^{-1} and storage time was shown in Figure 2.6. In Figure 2.6, for orange pulp sample stored for 0, 2, 4, 8 and 12 h, the peak shear stress was similar and ranged from 104.6 ± 13.6 to 109.6 ± 29.0 Pa. For pulp samples stored for 16, 20 and 24 h, peak shear stress increased about 27.7% to 36.90% compared to pulp stored for 0 h. According to Tukey's test, peak shear stress of the pulp sample stored for 48 h was significantly different from the pulp sample stored for 0 h, increased 62.1%. All peak shear stresses and shear rates where those peak stresses were obtained at shear rate range 0-5 s^{-1} are listed in Table 2.2.

The relationship between shear stress and selected shear rate range 0-5 s^{-1} for orange pulp stored for 0-48 h are shown in Figure 2.7. Slippage displayed at shear rates 0.6-0.9 s^{-1}. Shear stresses increased as shear rate increased at shear rate before 0.6 s^{-1} for all the flow curves. The shear rate where slippage occurred at shear rate range 0-5 s^{-1} flow curve measurement was 0.6-

0.9 s^{-1}, which was much smaller compared to the shear rate where slippage occurred at 0-80 s^{-1} flow curve measurement. This is explained by the radian of rotation that caused the slippage. A certain amount of radian of rotation is necessary for the occurrence of slippage. According to Trio program that connected rheometer to the computer, shear rate (s^{-1}) can be converted to rad per second (rad s^{-1}) by

$$\text{Shear rate } (s^{-1}) = 28.98 \times \text{rad } s^{-1}$$

The radian can be calculated as

$$\text{Radian} = \text{rad } s^{-1} \times \text{step time (s)} \quad (2\text{-}4)$$

For example, radian of rotation for orange pulp stored for 48 h at 4 °C was calculated for both shear rate ranges: 0-80 s^{-1}, 0-5 s^{-1}. The relationship between step time and radian then was plotted and shown in Figure 2.8. According to Figure 2.4 and 2.7, slippage of orange pulp stored for 48 h occurred at about 2.44 s^{-1} and 0.61 s^{-1} at shear rate range 0-80 s^{-1} and 0-5 s^{-1}. According to equation 2-3 and 2-4, slippage occurred when the radian turned to about 2.31 rad (π/1.37) at step time 109.5 s (shear rate 0.61 s^{-1}) for shear rate range 0-5 s^{-1} and 2.29 (π/1.37) at step time 27.53 s (shear rate 2.44 s^{-1}) for shear rate range 0-80 s^{-1}. That was the same radian for both shear rate ranges.

Shear rate range 0-1000 s^{-1}

In order to observe flow behavior of the orange pulp at shear rates after slippage occurred, flow behavior of the orange pulp stored for 48 h was measured at shear rate range 0-1000 s^{-1}. The flow curve is shown in Figure 2.9. The flow behavior became unpredictable at shear rates after where slippage occurred. The rheological properties of orange pulp measured by rotational rheometer after slippage occurred were unreliable. As shear rate became faster, the orange pulp sample gradually detached from the cup wall and moved toward the vane geometry. When

sufficient shear rate was provided, the pulp adhered to the vane geometry and moved along with vane. Loss of contact with cup wall induced to invalid friction factor. Also, slippage is a function of shear stress at the wall. Without contact with wall, slippage disappeared.

Determination of flow behavior index (n) and consistency coefficient (K)

In order to evaluate if flow curves of fresh orange pulp fitted to power law model, the flow curves before slippage occurred were chosen, transformed to logarithm and shown in Figure 2.10. For example, Figure 2.11 showed the plot of the logarithm of the shear stress versus the logarithm of the shear rate for orange pulp stored for 20 h at 4 °C. In Figure 2.11, three sections can be observed. Section 3 was the area after slippage occurred, as unpredictable flow behavior presented in this area. Sections 1 and 2 were both before slippage occurred sections. Linear regression of section 1 and 2 were analyzed. The correlation coefficient of sections 1 and 2 were 0.93 and 0.98, respectively, which indicates the flow behavior of orange pulp fitted to power law before slippage occurred. All R-square values of section 1 and 2 for all flow curves are listed in Table 2.3. Flow behavior index (n) was calculated as the slope of logarithm of the power law and consistency coefficient (K) was calculated as the exponential of the intercept of logarithmic power law model. K and n value were both calculated for Section 1 and Section 2. Microsoft Excel was used to calculate these power law parameters.

In Figure 2.10, two linear portions of logarithm of the flow curves before slippage occurred were identified. Flow behavior index (n) and consistency coefficient (K) were calculated for both sections. Averages of K and n values were calculated and listed in Table 2.3. The n-values for section 1 ranged from 0.99-1.27, which meant the orange pulp in section 1 was either Newtonian or shear thickening fluid. There was no significant difference for n-value between samples stored for different storage times ($p>0.05$) in this section (Figure 2.12). The

K-values of section 1 also showed no significant difference between samples stored for different storage times ($p>0.05$) (Figure 2.13). Since the shear rate in section 1 was very low, the consistency coefficient remained constant and the flow behavior index was close to 1, which is not reasonable in view of the evident change in the consistency of the pulp over time, our interpretation was that the shear rate range in section 1 was beyond the sensitivity of the rheometer, thus it should be neglected.

In section 2, n-value ranged from 0.29 to 0.35, showing no significant difference for pulp stored for different storage times ($p>0.05$) (Figure 2.14). When compared to an earlier research report for high concentrated pulp (Payne, 2011), both studies confirmed that flow behavior indexes were less than 1, which meant that the orange pulp behaved as pseudo-plastic fluid. The K-value ranged from 119.7 to 198.1 $Pa{\cdot}s^n$, increased significantly with storage time ($p<0.05$) in section 2 (Figure 2.15). For orange pulp sample stored for 0, 2, 4, 8 and 12 h, the K-value ranged from 120.0 to 124.6 $Pa{\cdot}s^n$. K-values did not have significant difference between orange pulp samples stored for 0, 2, 4, 8, 12 h based on Tukey's test. Pulp samples stored for 16, 20, 24 h were observed with higher K-values, ranged from 155.9 to 160.1 $Pa{\cdot}s^n$, increased 30.0% to 33.5% compared to pulp sample stored for 0 h. The sample stored for 48 h was observed with highest K-value (198.1 $Pa{\cdot}s^n$) of all the samples, increased 65.5% compared to samples stored for 0 h. According to Tukey's test, the K-value of pulp sample stored for 48 h was significantly different from pulp stored for 0 h. Explanations for the increase of K-value might be micro-gels, localized gelation or calcium pectate chains. As a gel or calcium pectate chain formed, the consistency coefficient and apparent viscosity increased due to the increased resistance to gels or calcium pectate chains to flow relative to the fresh pulp. In addition, the gels or chains reduced the rearrangement of particles when the fluid was sheared. Increased K-value meant increased

apparent viscosity, which induced to higher pressure drop in pasteurization system. One practical implication of this result was that pasteurizing orange pulp as soon as possible helped reducing pressure drop and pump power requirement.

Literature regarding flow behavior of orange pulp is very scarce, especially unpasteurized orange pulp with active pectinmethylesterase. The effect of pectinmethylesterase on rheological properties of orange concentrate of 42 °Brix with low pulp content were determined by Gomez et al. (2011). Orange concentrate of 42 °Brix was treated at 60 °C for 10 s and then stored for 0-6 months at 3 °C. Orange concentrate of 42 °Brix was prepared by adding juice back to 62 °Brix orange concentrate. After heat treatment, the PME activity of the concentrate decreased 55.5% compared to the fresh juice. The K-value of the orange concentrate increased during the first month, from 0.04 to 0.14 $Pa{\cdot}s^n$, then remained stable over four months and again increased during sixth month. The K-value increased about 375% during 6 months. The increase in K-value can be attributed to the small gel lump formation in orange juice during storage. The K-value of the heat-treated orange juice concentrate of 42 °Brix was 0.01 to 0.19 $Pa{\cdot}s^n$, much lower than the fresh orange pulp in this research (120.0-198.7 $Pa{\cdot}s^n$). One explanation might be that orange pulp possesses a much larger portion of PME compared to orange juice because the main source of PME in orange is orange pulp as it naturally attaches to orange pulp. Larger amount of PME in orange pulp induced to higher PME activity. Furthermore, the amount of pectin substrate in orange pulp was greater than in orange juice. In this case, more gel formation occurred in orange pulp, resulting in larger K-value. The pasteurization process can be another reason for lower K-value of the heated-treated orange juice concentrate. PME activity after heat treatment was only 55% of the initial activity, which induced to less active reaction with pectin and lower K-value. The n-value of the orange concentrate decreased during first month ranging from 0.79

to 0.55, which indicated an increase in pseudoplasticity of the system. For the next five months, the n-value stayed without changes.

The effect of PME on rheological behavior of carrot pectin extracted from carrot root cell wall with different solvents was studied by Mierczyńska et al. (2015). PME and pectin were both extracted from the carrot root cell wall. They concluded that PME activity remained at a constant level during the storage. They also concluded that carrot pectin extracted with water, the K-value increased during the first month of storage, from 0.0013 to 0.7376 $Pa \cdot s^n$, and then decreased to 0.1085 $Pa \cdot s^n$ during the fifth month of storage. Water soluble pectin fraction was comprised of polymers weakly linked to cell wall by non-covalent bonds. Therefore, the K-value increased during the first month decreased during the following months because pectin in water can be easily unbound and precipitate. For carrot pectin extracted with chelate, the K-value remained stable for the first four months, at about 0.0012 $Pa \cdot s^n$, and then increased to 0.3342 $Pa \cdot s^n$ during fifth month of storage. The pectins are cross-linked with ionic bonds in chelate soluble pectin solution. For carrot pectin extracted with diluted alkali, the K-value increased from 0.0259 to 0.9008 $Pa \cdot s^n$ during five months. The diluted alkali soluble pectins are connected to the cell wall by covalent ester bonds. For the flow behavior index, only carrot pectin extracted with diluted alkali showed consistent dilatant properties ($n>1$) during the five months storage. Both water soluble pectin and chelate soluble pectin showed first dilatant properties ($n>1$) and then pseudoplastic properties ($n<1$).

Determination of moisture content, soluble solid content, particle size and calcium content

Moisture and soluble solid content (SSC) are two important factors that might affect the flow behavior of orange pulp. Therefore, in order to ensure the change in flow behavior was caused by PME reaction, moisture and soluble solid content should be characterized and clarified

to have no significant difference for orange pulp samples stored for different storage times. The moisture content of orange pulp was 83.51 ± 0.73%. The SSC of orange pulp sample was 11.8 ± 0.4 °Brix. There were no significant difference in both moisture and soluble solid content for orange pulp samples stored for different storage times ($p>0.05$). Detailed determinations of moisture content and SSC of orange pulp samples were shown in Figures 2.16.

Particle size was also an important factor that might affect the flow behavior of orange pulp. So particle size should also be blocked to make sure all the changes in flow behavior were caused by PME as well. Particle sizes of four randomly picked orange pulp samples were shown in Figure 2.17. All the curves had similar particle size distribution, which meant that the factor of particle size was blocked. There was no significant difference of particle size for orange pulp stored for selected storage times. For each orange pulp sample, most of the pulp particles were more than 2000 μm. Particle size more than 2000 μm was undetectable using LS 13 320 Laser Diffraction Particle Size Analyzer, that explained why the curves in Figure 2.16 were not normally distributed.

Calcium content was another important factor that should be blocked because PME activity can be affected by calcium content. The result of calcium content of three randomly picked orange pulp samples were shown in Table 2.4. The calcium contents of all the samples were 328, 351 and 549 ppm. According to previous research, calcium content had an effect on the PME activity. Since PME activity of all the pulp samples was similar, the effect can be neglected. Also, the correlation between PME activity and PME effect on pectin was unreported. In order to characterize PME's effect on the rheology of orange pulp, the correlation should be characterized. One part of future work for this research is to determine the correlation between PME activity and PME effect.

Summary

Orange pulp behaved as pseudo plastic fluid and can be modeled with power law at very low shear rates, before slippage occurs. Flow behavior index (n) was independent of storage time. Conversely, the consistency coefficient (K) was greatly affected by storage time when shear rates were smaller than 0.6 s^{-1}. The flow behavior of orange pulp at shear rates after slippage occurred became unpredictable and was not useful. As storage time increased, K-value increased. K-value increased by 65.5% for the pulp sample stored for 48 h at 4 °C compared to fresh pulp without storage. The K-value was correlated to pressure drop of orange pulp in pasteurization system. However, K-value was not a good indicator of the predicted pressure drop increase due to the different energy loss caused by slippage. With these data alone, it was not enough to design and optimize pasteurization system because both n and K-value were calculated from power law at very low shear rates, before slippage occurred. Only friction factor without slippage, which meant at very low shear rates, can be calculated.

However, in citrus processing industry, the practical shear rates that correlated to the flow rates in flow system were much higher than those before slippage occurred. So, the rheological determination using rotational rheometer did not apply to friction factor prediction in industrial conditions. Friction factor was correlated to the work calculation in flow system thus pump power requirement. In order to characterize pump power requirement and optimize flow system, the flow behavior of orange pulp in pipe system should be characterized.

Table 2.1 PME activity of five randomly picked orange pulp samples from five different batches in study 1.

Sample	PME's activity (PEU/mL)
1	0.012±0.002
2	0.012±0.002
3	0.014±0.002
4	0.010±0.002
5	0.009±0.002

Table 2.2 Peak shear stress and corresponding shear rate with standard deviations after selected storage time, for measurements carried out at shear rate range 0-80 s^{-1} and 0-5 s^{-1}.

Storage time (h)	0-80 s^{-1} Shear rate (s^{-1})	0-80 s^{-1} Peak shear stress (Pa)	0-5 s^{-1} Shear rate (s^{-1})	0-5 s^{-1} Peak shear stress (Pa)
0	5.09±2.32	130.7±20.6	0.84±0.42	106.5±9.4
2	2.74±0.31	120.4±2.3	0.65±0.10	104.6±13.6
4	3.01±0.59	122.1±19.5	0.74±0.13	109.3±18.9
8	3.30±0.87	111.6±11.2	0.67±0.02	105.9±11.0
12	4.11±0.21	122.1±37.5	0.84±0.10	109.6±42.6
16	4.63±2.46	154.4±18.3	0.74±0.11	145.8±21.0
20	4.34±1.13	145.8±3.1	0.67±0.05	136.0±29.0
24	2.35±0.39	141.2±24.0	0.90±0.14	142.4±25.6
48	4.28±1.44	196.0±20.9	0.75±0.07	172.6±19.6

Table 2.3 Average (n=3) power law parameters with standard deviations for fresh orange pulp stored with different storage hours (Section 1 and Section 2).

Storage time	Section 1			Section 2		
(h)	n_1	K_1 (Pa·s^n)	R_1^2	n_2	K_2 (Pa·s^n)	R_2^2
0	1.20±0.07	1825.7±225.2	0.98	0.31±0.04	120.0±29.8	1.00
2	1.23±0.02	1886.2±105.9	0.98	0.32±0.03	119.7±13.0	0.99
4	1.06±0.22	1428.6±728.0	0.98	0.31±0.04	124.6±21.4	0.99
8	1.28±0.15	2575.7±1414.6	0.99	0.32±0.02	123.7±14.8	1.00
12	1.15±0.04	1635.4±337.6	0.99	0.29±0.03	124.4±43.4	0.99
16	1.22±0.15	2682.1±1678.2	0.96	0.33±0.00	157.4±13.6	0.99
20	1.21±0.02	2146.7±294.5	0.99	0.35±0.01	155.9±22.3	0.99
24	1.23±0.07	2898.2±1076.2	0.98	0.30±0.01	160.1±14.5	0.99
48	0.99±0.14	1637.2±585.5	0.99	0.33±0.03	198.1±26.1	1.00

Table 2.4 Calcium content for three randomly picked orange pulp samples.

Mineral	Sample 1	Sample 2	Sample 3
		Parts per million (ppm)	
Calcium (Ca)	328	351	549.2

Figure 2.1 AR 2000 Hybrid Discovery Rheometer.

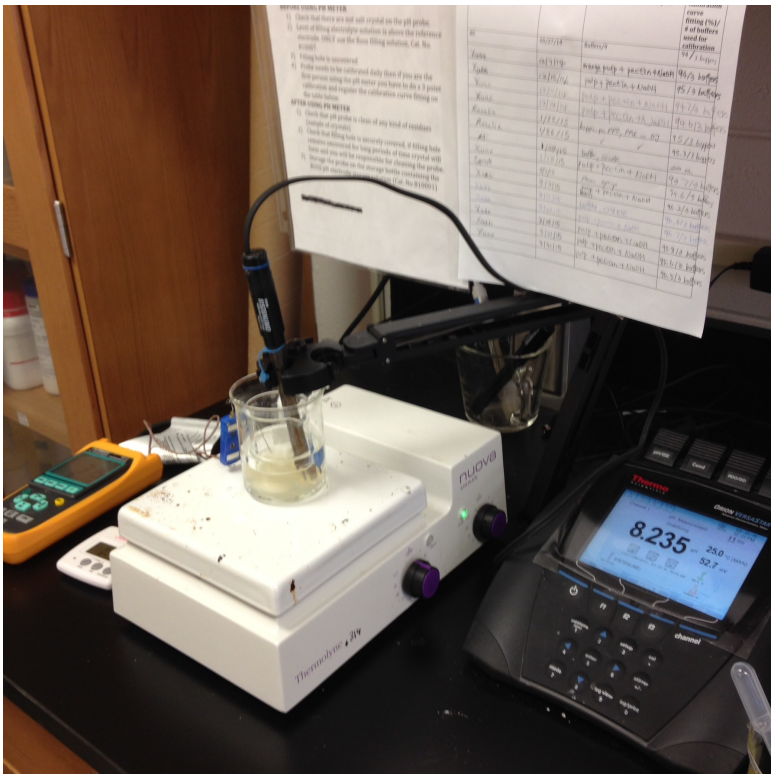

Figure 2.2 Experimental set up for PEU's test.

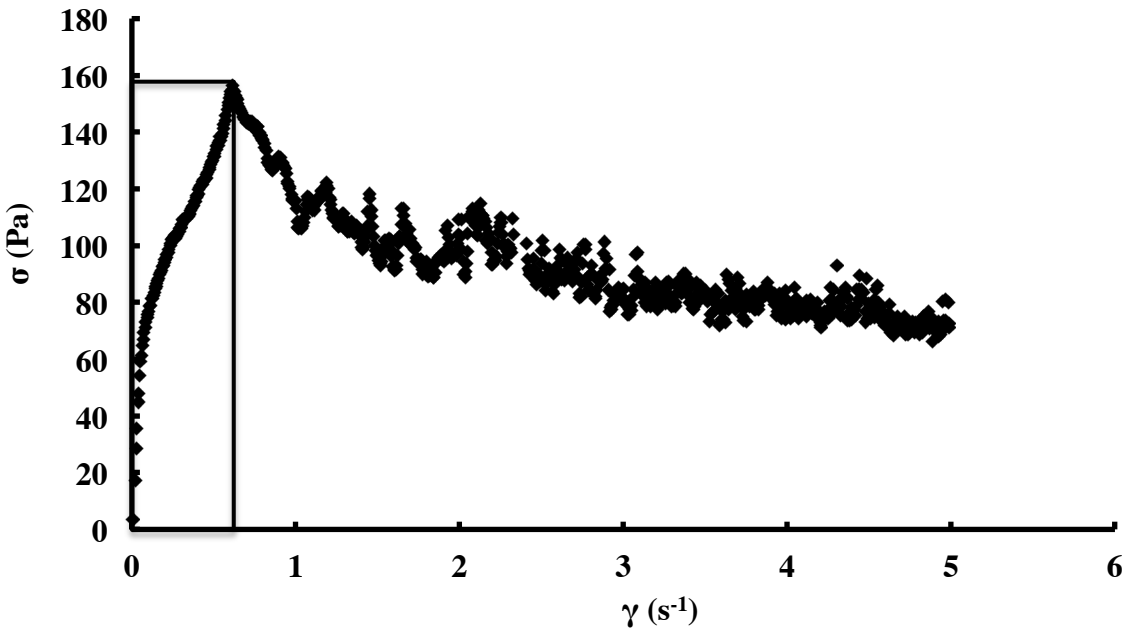

Figure 2.3 Shear stress-controlled rotational rheology of fresh 'Valencia' orange pulp stored for 20 h at 4 °C using a vane geometry.

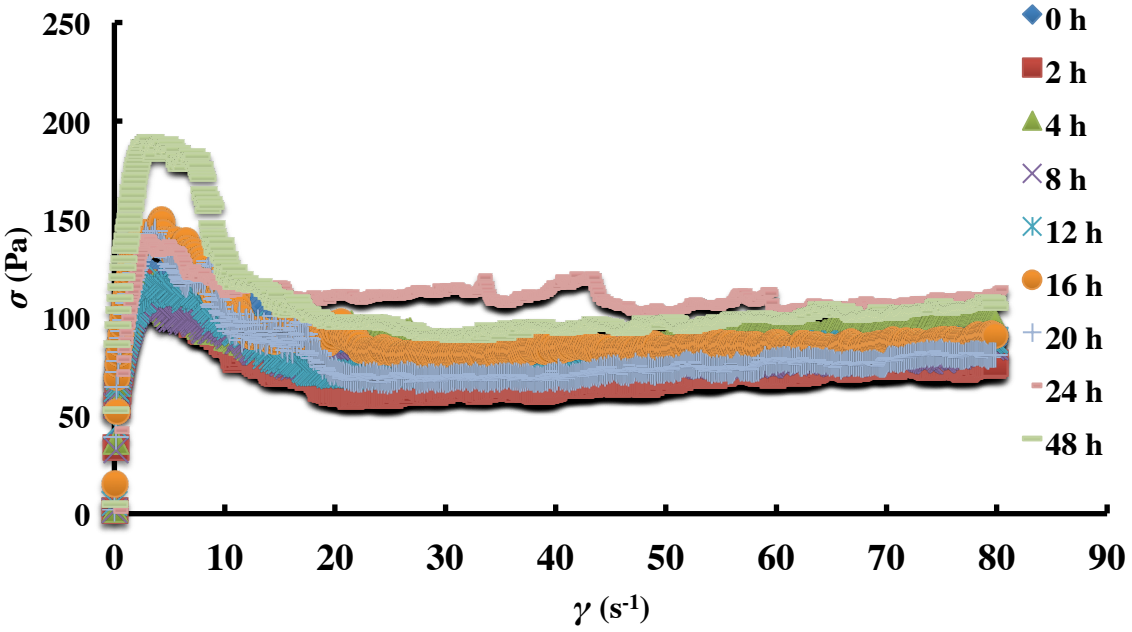

Figure 2.4 Flow curves of fresh Valencia orange pulp stored for 0-48 h at 4 °C at shear rate range 0-80 s^{-1} (n=3).

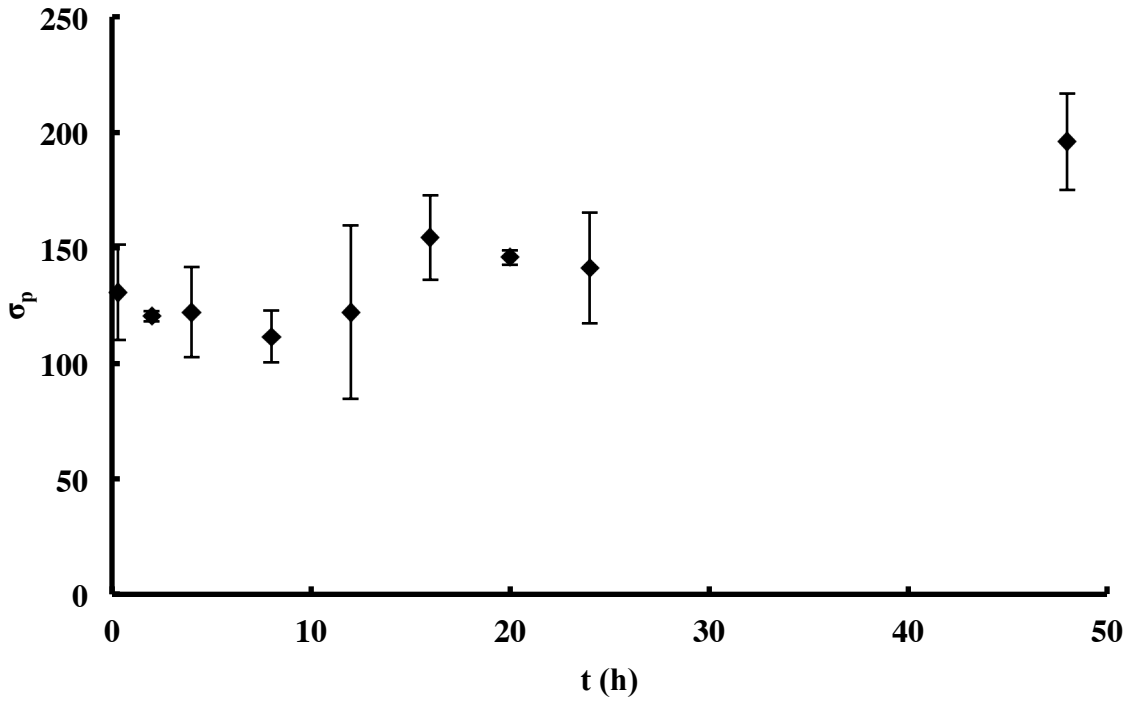

Figure 2.5 Peak shear stress (σ_p) of orange pulp stored for 0-48 h at 4 °C at shear rate range 0-80 s^{-1} (n=3).

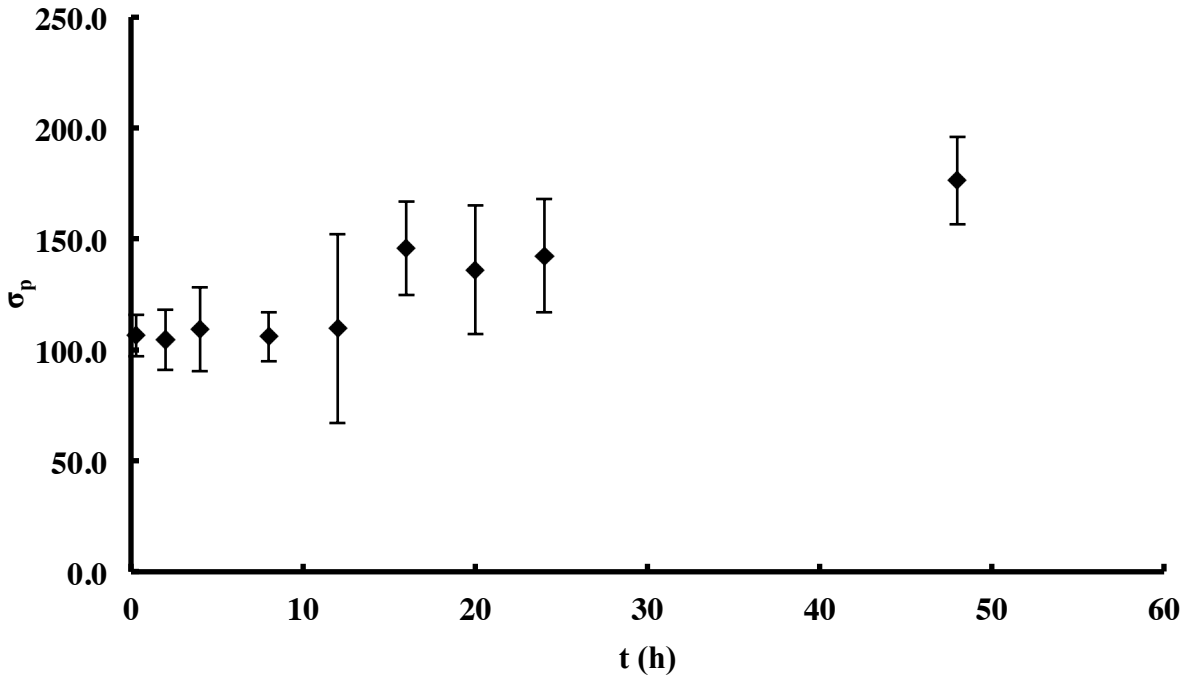

Figure 2.6 Peak shear stress (σ_p) of orange pulp stored for 0-48 h at 4 °C at shear rate range 0-5 s^{-1} (n=3).

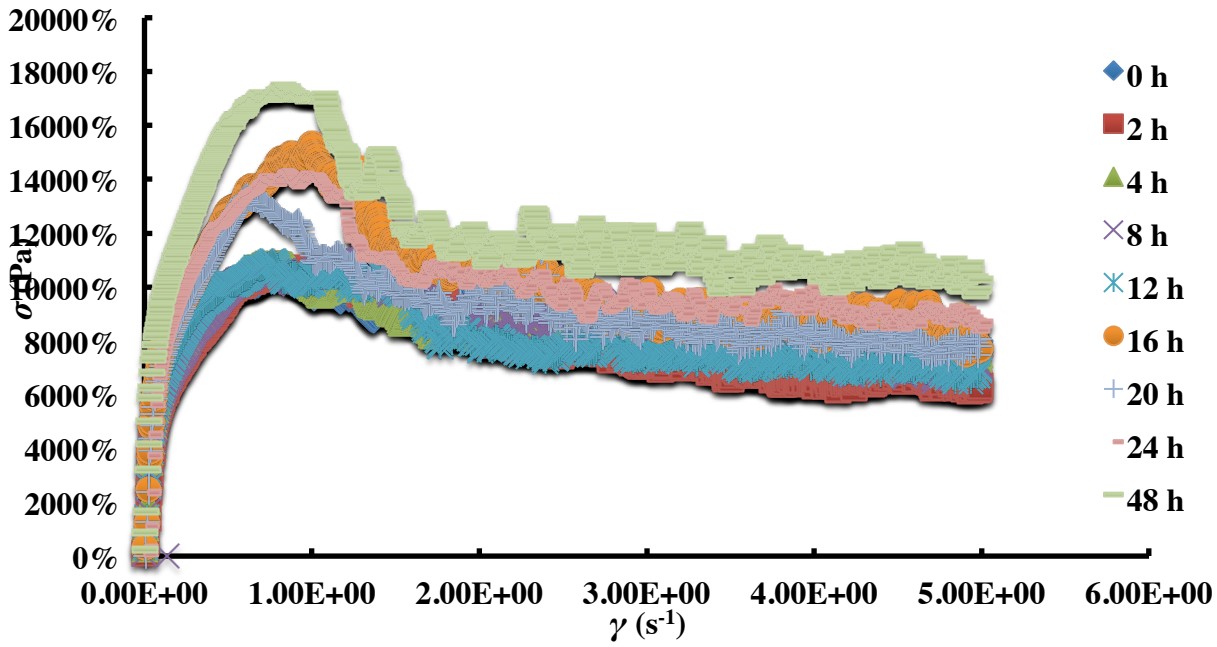

Figure 2.7 Flow curves of fresh Valencia orange pulp stored for 0-48 h at 4 °C at shear rate range 0-5 s^{-1} (n=3).

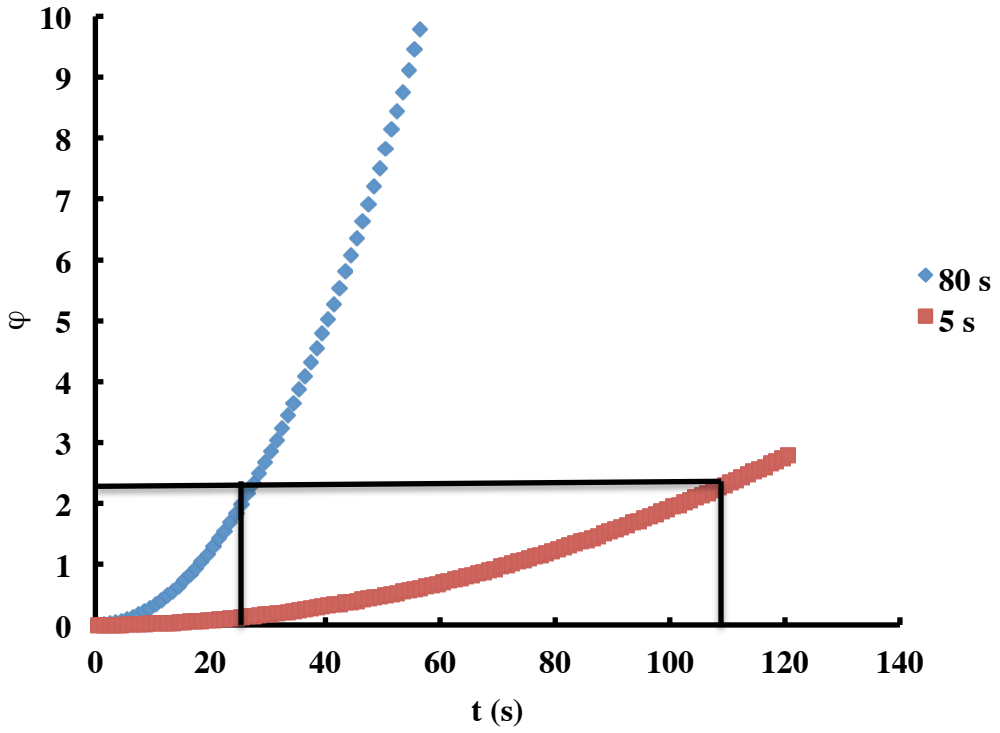

Figure 2.8 The effect of step time on the radian of rotation.

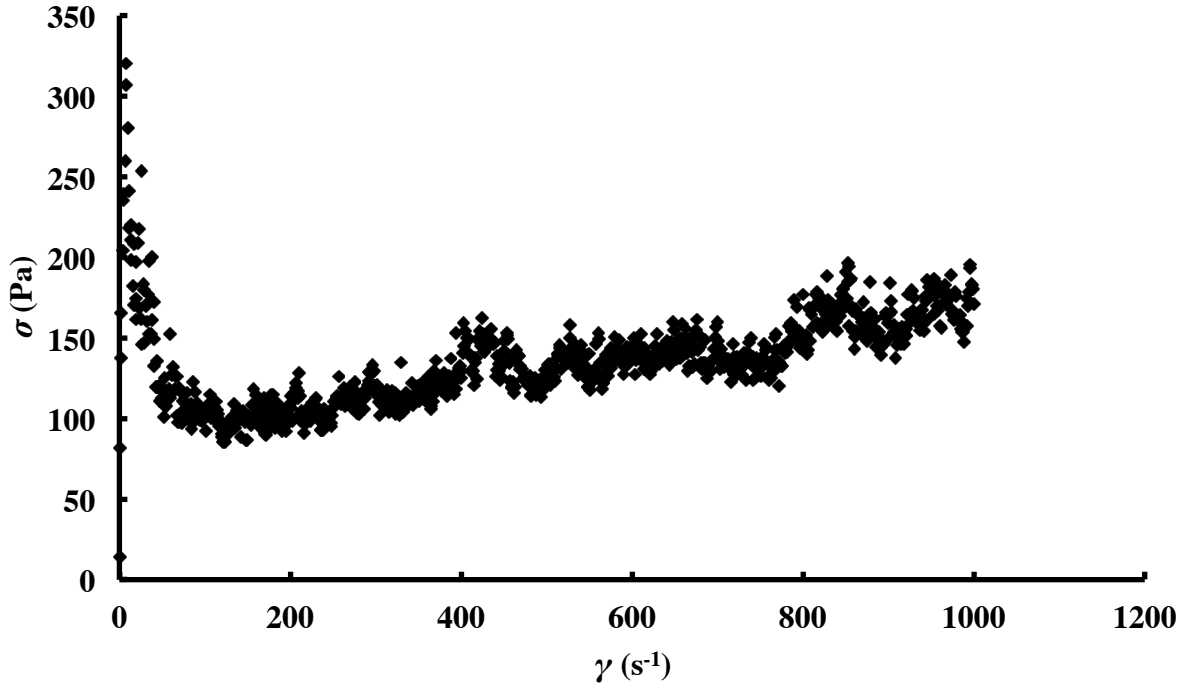

Figure 2.9 Flow curve of orange pulp stored for 48 h at 4 °C at shear rate range 0-1000 s^{-1}.

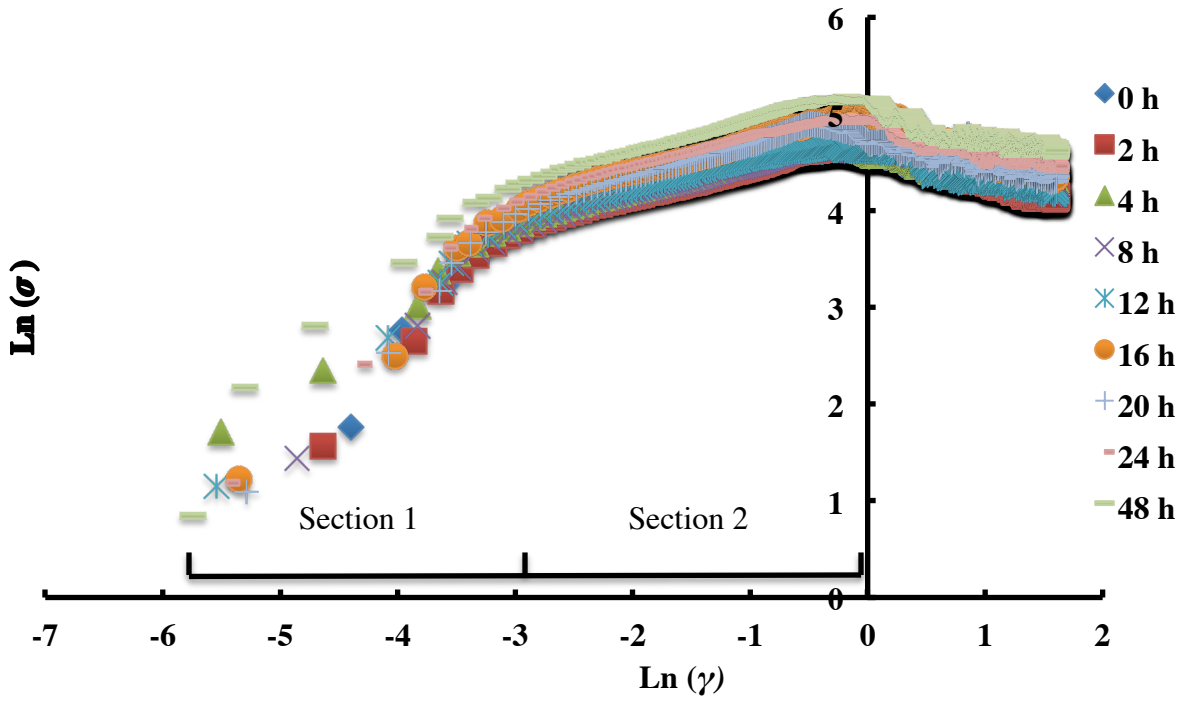

Figure 2.10 Logarithmic flow curves of fresh Valencia orange pulp stored for 0-48 h at 4 °C at shear rate 0-5 s^{-1} (n=3).

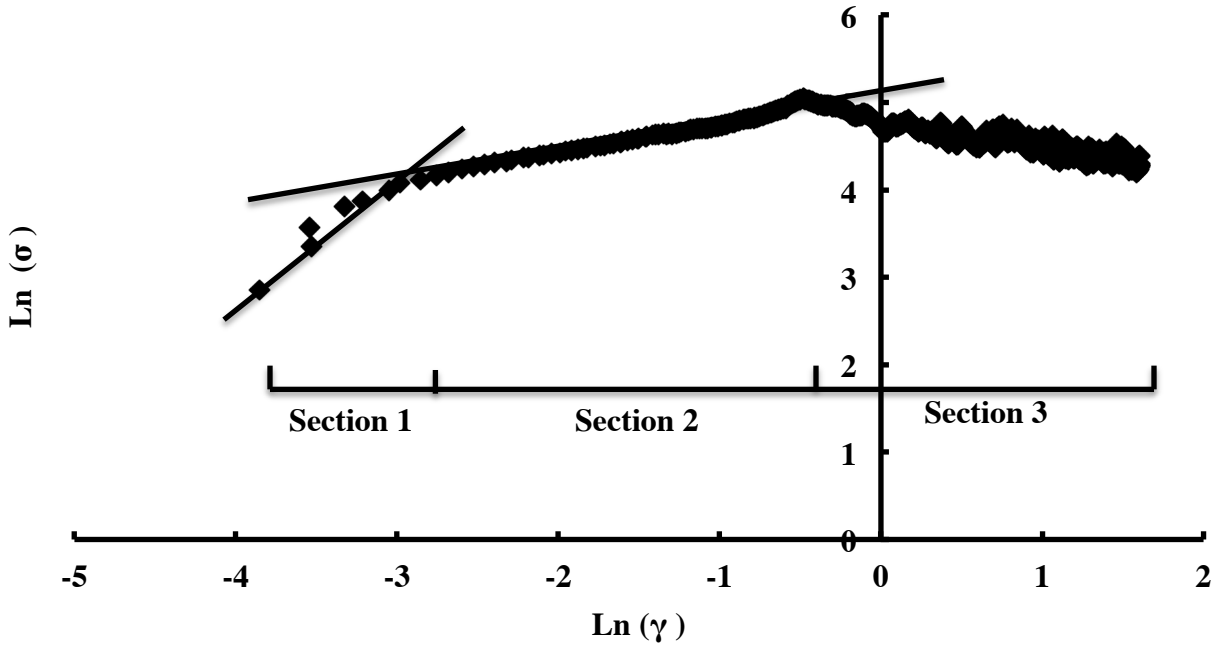

Figure 2.11 Logarithmic plot of the shear stress-controlled rotational rheology of orange pulp stored for 20 h at 4 °C using a vane geometry.

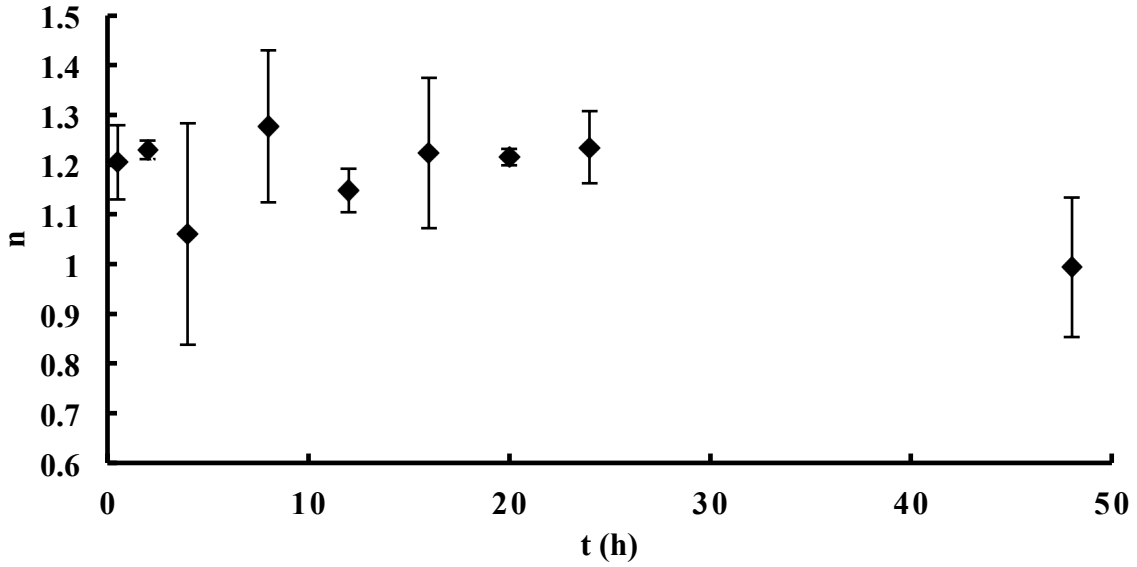

Figure 2.12 The effect of storage time on Flow behavior index for section 1 (n=3). Error bars represented standard deviations for the n values in section 1.

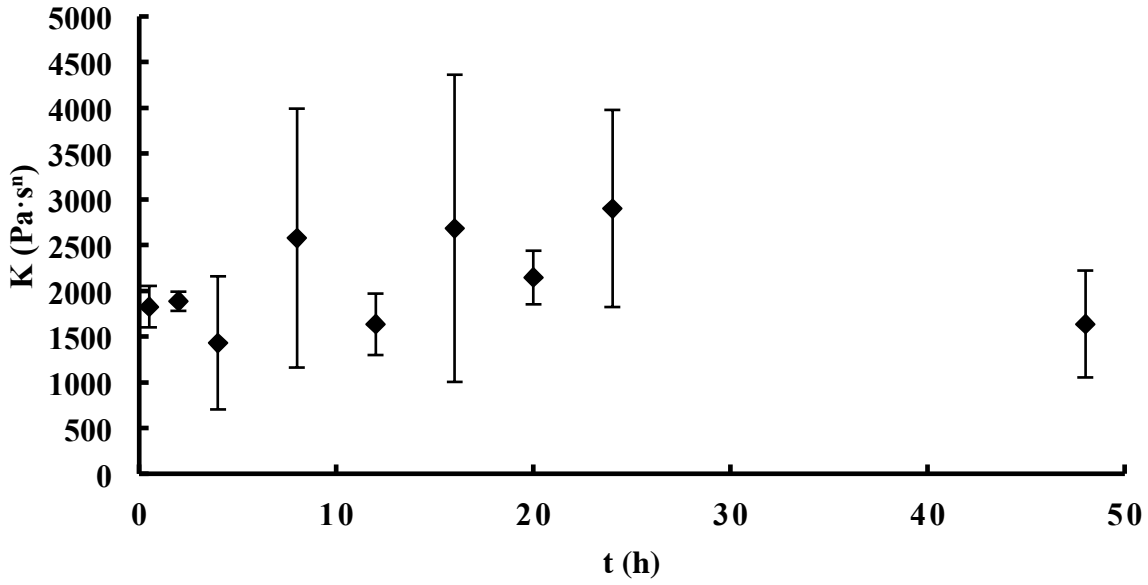

Figure 2.13 The effect of storage time on Consistency coefficient for section 1 (n=3). Error bars represented standard deviations for the K values in section 1.

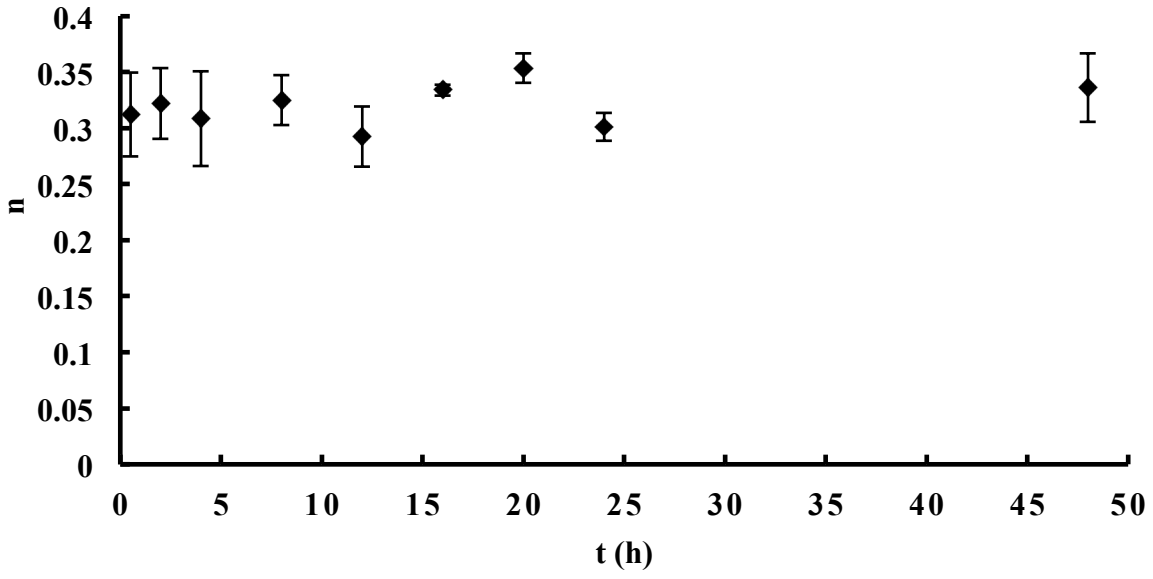

Figure 2.14 The effect of storage time on Flow behavior index for section 2 (n=3). Error bar represented standard deviations for the n values for section 2.

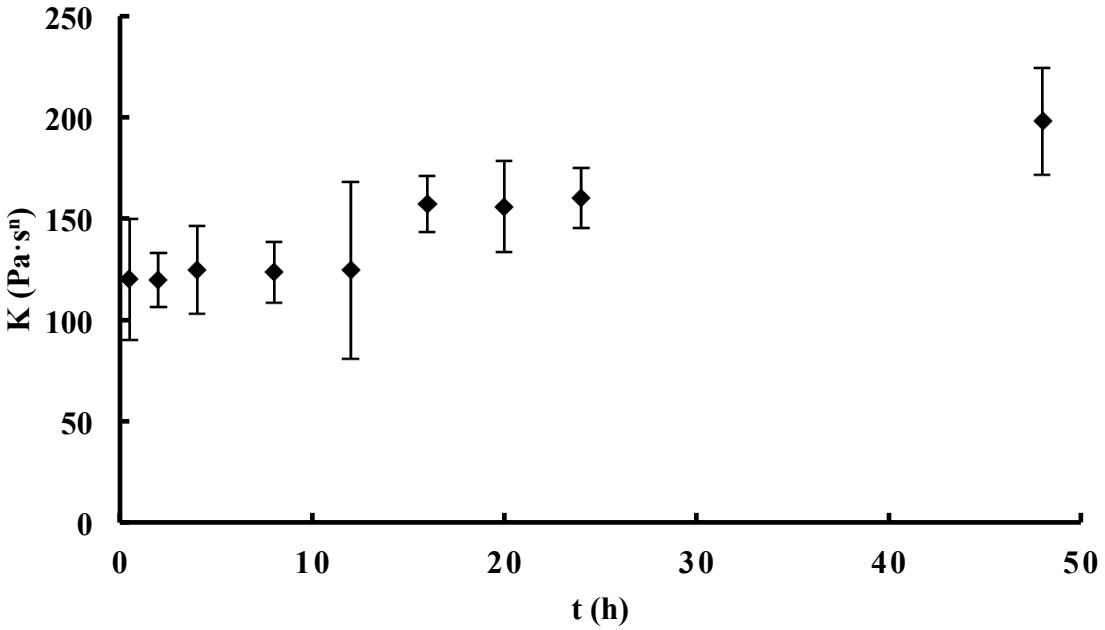

Figure 2.15 The effect of storage time on Consistency coefficient for section 2 (n=3). Error bars represented standard deviations for the K values in section 2.

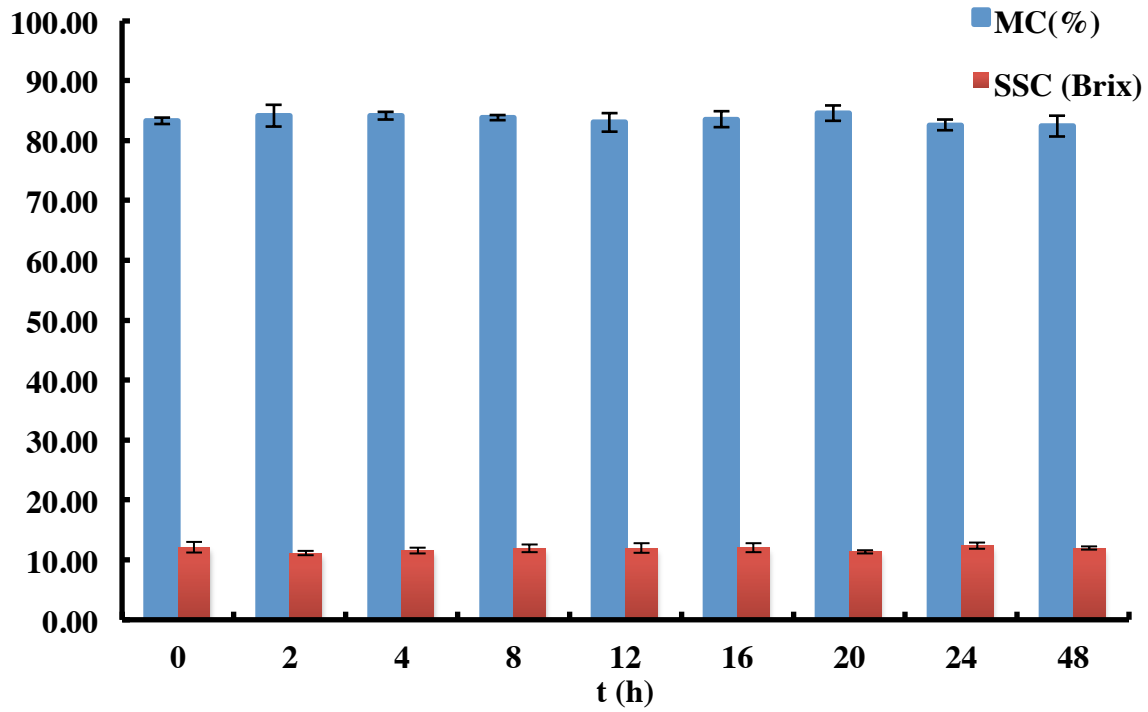

Figure 2.16 Moisture content and soluble solid content of all the orange pulp samples (n=3). Error bars represented standard deviations for all the moisture content and soluble solid content values.

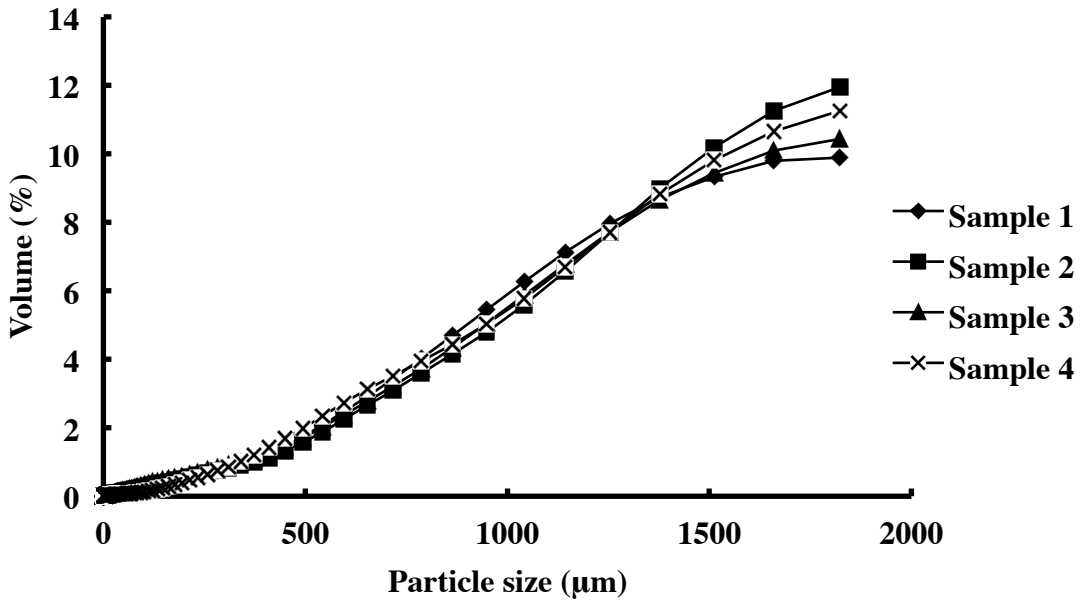

Figure 2.17 Particle size of four randomly picked orange pulp samples.

CHAPTER 3

DETERMINATION OF PRESSURE DROP AND PUMP POWER REQUIREMENT FOR FRESH UNPASTEURIZED VALENCIA ORANGE PULP

Introduction

Orange pulp behaves as a pseudo-plastic fluid and fits the power law before the occurrence of slippage at very low shear rates (0.6-0.9 s^{-1}). Rheological properties determination of orange pulp in Chapter 2 only allowed for the prediction of the friction factor without slippage. However, in the citrus processing industry, the practical shear rates at which pulp flows in conventional pipes and tubular heat exchangers are much higher than the shear rates at which slippage occurs. The vane spindle rheological data of orange pulp at high shear rates measured using a rotational rheometer was unreliable. When a rotational rheometer spins very fast, pulp is gradually displaced and rotates along with the geometry as if carving a hole. Loss of contact between orange pulp and cup wall gave invalid friction factor at high shear rates. Therefore, the rheological properties determination using a rotational rheometer in Chapter 2 cannot be used to calculate the friction factor in the presence of slippage, which is needed to calculate pumping energy requirements under industrial conditions. Payne (2011) described slippage effects on the pressure drop in a flow system. The effect of slippage is usually determined using capillary viscometry with different pipe diameters. To accurately account for the energy loss in a flow system with the presence of slippage, the rheological data of pulp and slip condition needs to be characterized.

Because active PME is present in unpasteurized orange pulp, we hypothesized that the pressure drop increase during storage is due to the gel formation caused by PME reaction with pectin in pulp. The objective of this study was to characterize the effect of storage time on the pressure drop and pump power requirement as a function of flow rate for unpasteurized orange pulp stored for 0 to 72 h at 22 °C using capillary viscometry. Based on the measurements, a mathematical model was developed to predict pump power requirement as a function of storage time for the ~ 650 $g \cdot L^{-1}$ fresh 'Valencia' orange pulp stored at 22 °C.

Materials and Methods

Materials

Frozen unpasteurized 'Valencia' orange pulp (~800 $g \cdot L^{-1}$) and orange juice were provided by JBT Company (Lakeland, FL). The frozen unpasteurized 'Valencia' orange pulp was extracted on April 29, 2015. Moisture content of orange pulp was determined using a HR 73 Halogen Moisture Analyzer from Mettler Toledo (Columbus, OH). Each determination required approximately 0.1 g pulp. The soluble solids content (SSC) of orange pulp was determined from a drop of juice recovered from pulp using an Extech RF 12 Portable Brix Refractometer (0-18%) (Melville, NY). High methoxyl pectin from citrus peel was purchased from Sigma-Aldrich (St. Louis, MO) and 1 N standardized NaOH solution purchased from Fisher Scientific (Pittsburgh, PA) were used for PME activity assay. Sodium benzoate was purchased from Fisher Scientific (Pittsburgh, PA).

Flow system equipment and instruments

Figure 3.1 shows a picture of the home-made pilot scale experimental flow system set up used for capillary viscometry measurements. A progressive cavity pump model B0104 from Orbit Pumps Ltd. (Edenglen, South Africa) with a 60 W motor (Huddersfield, UK) was used to

pump pulp through the system. The flow rate was controlled by adjusting the rotational speed of the pump using an ACS 800 ABB controller (Fort Worth, Texas). The total length of the pipe was 8.69 m. The diameter of the pipe was 0.020 m. A Yokogawa AE 105 magnetic flow meter (Freeport, TX) was mounted at the entrance of the flow system to measure the flow rate. Two pressure transducers PX43E0-500GI and PX43E0-100GI from Omega (Stamford, CT) were mounted at the entrance and the exit of the system to measure the pressure drop. Two 1-mm diameter type T thermocouples from Omega (Stamford, CT) were placed at the entrance and the exit to measure the temperatures at both locations. Flow rate, pressure and temperature data were collected every 2 seconds using a data acquisition board Model N 9219 from National Instruments (Austin, TX), and connected to a laptop computer with program written in LabVIEW 2013, also from National Instruments (Austin, TX).

Methods

Pulp sample preparation

Frozen unpasteurized 'Valencia' orange pulp samples (~800 $g \cdot L^{-1}$) were thawed at 4 °C two days. About 5 kg of ~650 $g \cdot L^{-1}$pulp were prepared for each of three replicates by adding 1 L of orange juice to 4 kg of ~800 $g \cdot L^{-1}$ pulp. Sodium benzoate was added to a concentration of 0.05% to pulp samples as a preservative.

Pressure drop determination as a function of flow rate

Prior to the test, the ~5 kg of orange pulp was loaded into the feed tank of the flow system (See Figure 3.1). Orange pulp samples were then left in the flow system at room temperature (22 °C) for 0, 2, 4, 8, 12, 16, 20, 24, 36, 48, 60, or 72 h. After storage, pressure drop was measured at flow rates of 0.1, 0.2, 0.3, 0.4, 0.5, 0.6, 0.7, or 0.8 GPM (6.31×10^{-6}, 1.26×10^{-5}, 1.89×10^{-5}, 2.52×10^{-5}, 3.15×10^{-5}, 3.79×10^{-5}, 4.42×10^{-5}, or 5.05×10^{-5} $m^3 \cdot s^{-1}$). During each pressure

drop determination, the pulp was re-circulated in the pipe until steady-state (constant flow rate) was obtained. A computer program written in LabVIEW was then executed to collect pressure and flow rate data. Each pressure drop determination was run for 2 min. Pressure drop was then calculated as the average of all 60 data points. Specific pump energy requirements were calculated using Bernoulli's equation. A logarithmic model was built to predict pump power requirement as a function of storage time. Extrapolated data of the friction factor without slippage and Reynolds number without slippage, slip coefficient and slip velocity for unpasteurized orange pulp samples stored for 0 and 48 h were also calculated to characterize the effect of slippage on the flow behavior of unpasteurized orange pulp in flow system as a function of flow rate. Different effects of slippage on the flow behavior of unpasteurized orange pulp stored for 0 and 48 h were caused by PME activity.

Determination of PME activity, moisture content, SSC, particle size and calcium content

The measurement methods of PME activity, moisture content, SSC, and particle size were described in Chapter 2. Determination of calcium content was conducted by the Soil, Plant and Water Laboratory at 2400 College Station Road, Athens GA 30602.

Calculation and data analysis

Pump power requirement calculation

As mentioned by Singh and Heldman (2001), the energy loss associated with friction E_f is given by:

$$E_f = E_{f,major} + E_{f,minor} \tag{3-1}$$

The major friction loss is caused by the viscous fluid flow in the straight portion of a pipe is given by Fanning's equation.

$$E_{f,major} = \frac{2f\bar{v}^2 L}{g_c D} \tag{3-2}$$

So, the major pressure drop due to friction can be calculated as

$$\Delta p_{f,major} = E_{f,major} \times \varrho = \frac{2f\bar{v}^2 L\varrho}{g_c D} \quad (3\text{-}3)$$

Where ϱ is the density of orange pulp, which is 1040 $kg \cdot m^{-3}$.

The density of orange pulp was measured using a graduated cylinder. 5 g of orange pulp was added to 1 L of deionized water in graduated cylinder. The total volume of orange pulp and deionized water was recorded as V. The density of orange pulp was calculated as $\varrho = \frac{0.005\ kg}{(V\text{-}1)\ L}$.

The minor friction loss is caused by sudden contractions, sudden expansions and pipefittings.

$$E_{f,minor} = E_{f,contraction} + E_{f,expansion} + E_{f,fittings} = K_{fe}\left(\frac{\bar{v}_a^2}{2g_c}\right) + K_{fc}\left(\frac{\bar{v}_b^2}{2g_c}\right) + K_{ff}\left(\frac{\bar{v}_a^2}{2g_c}\right) \quad (3\text{-}4)$$

The pressure drop due to minor friction loss can be calculated as

$$\Delta p_{f,minor} = \Delta p_{f,concentration} + \Delta p_{f,expansion} + \Delta p_{f,fittings} = \frac{\varrho v^2}{2g_c}(K_{fe} + K_{fc} + K_{ff}) \quad (3\text{-}5)$$

The energy requirements for pumping liquid from one location to another may be expressed as the energy loss associated with friction force, model rearranged:

$$E_p = \frac{\Delta p_{total}}{\varrho} = \frac{\Delta p}{\varrho} + \frac{g(z_2 - z_1)}{g_c} + \frac{(v_2^2 - v_1^2)}{2g_c} + \frac{2f\bar{v}^2 L}{g_c D} + K_{fe}\left(\frac{\bar{v}_a^2}{2g_c}\right) + K_{fc}\left(\frac{\bar{v}_b^2}{2g_c}\right) + K_{ff}\left(\frac{\bar{v}_a^2}{2g_c}\right) \quad (3\text{-}6)$$

Where Δp_{total} was the pressure drop measured in the flow system; Δp is the difference of pressure between the entrance and the exit, which was consider as zero; z_2,-z_1 is the elevation difference between the entrance and the exit of the pulp, which was 0.762 m in this flow system; since the pipe diameter was constant, the velocity term was null; *f* was the friction factor; L was the pipe length, which was 8.69 m in this flow system; D was the pipe diameter, which was 0.02 m in this flow system; K_{fe} was the coefficient for expansion, $\bar{v}_a$ was the velocity after expansion, K_{fc} was the coefficient for contraction, $\bar{v}_b$ was the velocity before contraction, g_c in Newton's gravitational proportionality factor and K_{ff} was the coefficient for valves and fittings. K_{ff} for

each of two 90° elbow is 0.3. For the contraction and expansion terms, $K_{fe}=2\left(1-\frac{A_1}{A_2}\right)$ and $K_{fc}=0.4[1.25-\left(\frac{A_2}{A_1}\right)]$, where A_1 is the area after expansion, A_2 is the area after contraction. In this flow system, there were two sudden expansions and two sudden contractions at the "tees" where the pressure transducers were mounted. K_{fe} was 0.38 and K_{fc} was 0.55. A diagram of the flow system described above can be found in Figure 3.1.

Pump power requirement in the flow system was calculated as:

$$\text{Power}=\Phi=E_p*W \tag{3-7}$$

Where E_p was the work and W was the mass flow rate.

Friction factor with slippage calculation

As described in equation 3-1, 3-3 and 3-5, pressure drop due to major friction was calculated as

$$\Delta p_{f,major}=\Delta p_{total}-\Delta p_{f,minor} \tag{3-8}$$

So,

$$\Delta p_{f,major}=\Delta p_{total}-\frac{\varrho v^2}{2g_c}(K_{fe}+K_{fc}+K_{ff}) \tag{3-9}$$

Combined with equation 3-3, the friction factor with slippage was then derived as

$$f=\frac{\Delta p_{f,major}g_cD}{2\varrho\bar{v}^2L}=\frac{\Delta p_{total}-\frac{\rho v^2}{2g_c}(K_{fe}+K_{fc}+K_{ff})g_cD}{2\rho\bar{v}^2L} \tag{3-10}$$

Slip coefficient calculation

Equation 3-6 can be rewritten as

$$Q_{ws}=v_{ws}\pi r^2=\pi r^2\sqrt{\frac{\frac{\Delta p_{total}}{\rho}-\frac{g(z_2-z_1)}{g_c}}{\frac{2f_{ws}L}{g_cD}+(K_{fe}+K_{fc}+K_{ff})\frac{1}{2g_c}}} \tag{3-11}$$

In this case, Q_{ws} was flow rate without slippage. Q_{ws} was calculated under the assumption that there was no slippage at the shear rates where slippage occurred in reality. In equation 3-11, Q_{ws} was an extrapolation of flow rate of orange pulp at the same pressure drop as measured flow rate with slippage in the flow system. f_{ws} was the friction factor without slippage, which can be calculated as 16 divided by Reynolds number for power law fluid under laminar flow. f_{ws} was calculated from the K and n value of flow curves of orange pulp before slippage occurred.

Reynolds number (Re_n) is a dimensionless quantity that is used to predict the flow patterns. For power law fluid, Re_n is calculated as

$$Re_n=2^{3-n}\left(\frac{n}{3n+1}\right)^n\left(\frac{D^n\varrho v^{2-n}}{K}\right) \tag{3-12}$$

Where D is diameter (m), ϱ is density ($kg\cdot m^{-3}$), v is the velocity ($m\cdot s^{-1}$) and power law parameters K and n.

Friction factor without slippage can be calculated as

$$f_{ws}=\frac{16}{Re_n} \tag{3-13}$$

Corrected slip coefficient is calculated as

$$\beta_c=\frac{Q_m-Q_{ws}}{\sigma_w r\pi} \tag{3-14}$$

Where Q_m was the measured flow rate with slippage that produces the same pressure drop that was calculated without slippage, r was radius of the pipe and σ_w was wall shear stress.

$$\sigma_w=\frac{\Delta p_m r}{2L} \tag{3-15}$$

Results and discussion

Determination of pressure drop and pump power requirement

Pressure drop due to major friction increased non-linearly with flow rate for all pulp samples stored for all selected storage times, which means the orange pulp still behaved as Non-Newtonian fluid at high shear rates as shown in Figure 3.2. For orange pulp sample stored for 0 h, the pressure drop due to major friction increased 93.4% as flow rates increased from 0.1 to 0.8 GPM. For orange pulp sample stored for 36 h, the pressure drop due to major friction increased 104.8% as flow rates increased from 0.1 to 0.8 GPM. For orange pulp sample stored for 72 h, the pressure drop due to major friction increased 104.9% as flow rates increased from 0.1 to 0.8 GPM. The increase percentage in pressure drop for different storage time samples did not vary a lot (93.35-104.89%). In our flow system, because of slippage, it was difficult to determine Re_n because there were two different velocities need to be considered: the juice layer's velocity near the wall and the other was the velocity of the pulp bulk. However, since the flow velocity was very slow (0.02 to 0.18 $m \cdot s^{-1}$) and orange pulp was very viscous , it is reasonable to assume that the flow was laminar flow. The flow behavior of laminar flow fits to equation 3-13.

Since K, n, D and ϱ were all constants and $v=\frac{Q}{A}$, Re_n can be rewriten as

$$Re_n=C_1Q^{2-n} \tag{3-16}$$

C_1 is defined as the result from calculation of K, n, D, r and ϱ. C_1 can be described as

$$C_1=2^{3-n}\left(\frac{n}{3n+1}\right)^n\left(\frac{D^n\varrho}{K(\pi r^2)^{2-n}}\right) \tag{3-17}$$

Because K, n, D and ϱ are constants, C_1 is therefore, also a constant.

Combining equation 3-13 and 3-16,

$$f=\frac{16}{C_1Q^{2-n}} \tag{3-18}$$

Therefore,

$$f=C_2\frac{1}{Q^{2-n}} \tag{3-19}$$

Where C_2 is a constant equal to 16 divided by C_1.

Since the flow behavior index "n" value was between 0-2, the friction factor value was between $\frac{1}{C_2}$ and $\frac{C_2}{Q^2}$. Combined with equation 3-10, the pressure drop due to major friction can be then calculated as

$$\Delta p_{f,major} = \frac{f2\varrho\bar{v}^2 L}{g_c D} = C_3 Q^n \qquad (3\text{-}20)$$

g_c, D, ϱ and L were all constants and C_3 was a constant resulted from all these constants' calculation.

According to equation 3-20, if the fluid was Newtonian fluid (n=1), the pressure drop due to major friction increases linearly with flow rate, which is not the case as shwon in Figure 3.2. If it was dilatant fluid (n>1), at any selected flow rate, the slope of a straight line drawn from the selected point on the curve to the origin increase as flow rate increases, which was not observed either. If it was pseudo-plastic fluid (n<1), at any selected flow rate, the slope of a straight line drawn from the selected point on the curve to the origin decreases as flow rate increases. The flow curves of pressure drop as a function of flow rate for different n-value ranges shown in Figure 3.3 where suggest that orange pulp behaved as pesudo-plastic fluid at shear rates after slippage occurred.

Similarly, as shown in Figure 3.4, at all flow rates studied, as the storage time increased, the pressure drop due to major friction increased non-linearly. The increase in pressure drop leveled off after approximately 36 h storage at 22 °C probably because all the methoxyl groups in pectin had already been deesterified under the catalytic action of PME. Therefore, the rate of increase in apparent viscosity and hence, the rate of increase in pressure drop decreased. At 0.1 GPM, the pressure drop due to major friction for pulp sample stored for 72 h increased 43.2% compared to pulp stored for 0 h, from 310.13 to 444.10 kPa. At 0.8 GPM, the pressure drop due

to major friction for orange pulp sample stored for 72 h was 909.92 kPa, increasing 51.7% compared to pulp sample stored for 0 h when pumped at the same flow rate.

Like pressure drop due to major friction, the pump power requirement due to major friction increased non-linearly with the studied flow rate as well (Figure 3.5). This can also be explained with

$$\text{Power}=\Phi=E_p*W \tag{3-21}$$

Since pump's work $E_p=\frac{\Delta p_{f,major}}{\varrho}$ and mass flow rate $W=\varrho Q$

$$\text{Power}=\Phi=\frac{\Delta p_{f,major}}{\varrho}\times\varrho Q=Q\Delta p_{f,major} \tag{3-22}$$

Combined with equation 3-20,

$$\text{Power}=\Phi=C_3Q^{n+1} \tag{3-23}$$

Therefore, there was an exponential correlation between pump power requirement and flow rate.

For orange pulp stored for 0 h at 22 °C, power requirement increased from 1.96 to 30.27 W as flow rate increased from 0.1 to 0.8 GPM. For pulp sample stored for 72 h, the pump power requirement increased from 2.80 to 45.93 W as flow rate increased from 0.1 to 0.8 GPM. At 0.8 GPM, pulp stored for 72 h in pipe with length 8.69 m and diameter 0.02 m required 45.93 W pump power. The reason we chose 6/8 inch (0.02 m) pipe diameter instead of 1 inch was that a large amount of orange pulp was required for 1 inch pipe. Smaller pipe diameter helped reducing sample amount for each run.

Figure 3.6 shows the effect of storage time on the pump power requirement for orange pulp flow at 0.1 to 0.8 GPM. At 0.1 GPM, the pump power requirement between pulp samples stored with different storage times did not increase a lot, from 1.96 to 2.8 W as storage time increased from 0 to 72 h. As flow rate increased, the difference of pump power requirement

between pulp samples stored with different storage times increased. At 0.4 GPM, the difference of power requirement between pulp samples stored for 0 and 72 h was 6.07 W. At 0.8 GPM, the difference of power requirement between pulp samples stored for 0 and 72 h increased to 15.66 W. This increase was caused by the increase of pulp consistency strength upon storage. As storage time increased, pump power requirement due to major friction increased and leveled off after 36 h at all studied flow rates (Figure 3.6). Like for the effect of storage time in pressure drop, this can be explained by the completion of the deesterification reaction.

Determination of the friction factor with slippage and Reynolds number

When slippage occurs, different velocities exist between a thin-layer of liquid near the wall and the bulk material that does not interact or only weakly interacted with the wall. In orange pulp flow, the juice orange juice formed the thin liquid layer also called slip layer, which works as lubricant that makes orange pulp flow in the pipe easier. A diagram describing slippage of orange pulp is shown in Figure 3.7. Because of the lubrication effect, slippage affected both friction factor and Reynolds number of orange pulp in the flow system. Friction factors with slippage for all pulp samples were calculated using equation 3-10 and listed in Table 3.1.

Effects of flow rate on the friction factor with slippage as calculated from equation 3-10 were shown in Figures 3.8, 3.9. In Figure 3.8, the friction factor with slippage increased as storage time increased. At 0 h, the friction factor with slippage decreased 97.10% as flow rate increased from 0.1 to 0.8 GPM. At 72 h, the friction factor with slippage decreased 96.97% as flow rate increased from 0.1 to 0.8 GPM. The friction factors decreased non-linearly with flow rate, which can be in part explained with equation 3-18. The non-linear decrease of f versus Q shown in Figure 3.8 can be explained by the fact that the apparent flow behavior index of orange pulp was less than one and my be also due to increased slippage. Therefore, an apparent flow

behavior index cannot be calculated directly from equation 3-18, but it could be approximated for the range of flow rates covered in this research.

In contrast, the plot of the logarithm of the friction factor versus the logarithm of the flow rate was linear, as shown in Figure 3.9. The slopes of lines in Figure 3.9 increased as the storage time increased. This linear behavior indicated that pulp behaves as a pseudo-plastic fluid also when slippage occurs. Linear regressions for all the lines were listed in Table 3.2.

In Figure 3.10, the effect of storage time on the friction factor with slippage was characterized. At 0.1 GPM, after 72 h, the friction factor with slippage of orange pulp increased from 0.69 to 0.99 compared to orange pulp stored for 0 h. The greatest friction factor 0.99 was observed at 0.1 GPM for pulp stored for 72 h.

As mentioned before, a priori, it is not possible to determine Reynolds number due to unknown velocity because of slippage. Literature regarding calculation of Reynolds number with the occurrence of slippage is non-existent to the best of our knowledge. However, as discussed before, and in view of the very large values of the friction factor (> 0.01) it is reasonable to assume that the orange pulp flow was laminar flow. Therefore, the Reynolds number can be calculated as

$$Re_n = \frac{16}{f} \tag{3-24}$$

Reynolds numbers for orange pulp stored with all selected storage times at 22 °C were listed in Table 3.3.

Corrected slippage coefficient and slip velocity determination

Slippage coefficient and slip velocity were calculted for orange pulp stored for 0 and 48 h at 22 °C using equation 3-14. The relationship between flow rate and corrected slip coefficient for orange pulp stored for 0 and 48 h were shown in Figure 3.11. The corrected slip coefficient

increased linearly with flow rate of orange pulp stored for both 0 and 48 h, with both R-square 1.00. As flow rate increased from 6.31×10^{-6} to 5.05×10^{-5} $m^3\cdot s^{-1}$ (0.1 to 0.8 GPM), the slippage coefficient of orange pulp stored for 0 h increased from 2.75×10^{-7} to 1.12×10^{-6} $m\cdot(Pa\cdot s)^{-1}$. For orange pulp stored for 48 h, the slippage coefficient increased from 3.22×10^{-7} to 1.66×10^{-6} $m\cdot(Pa\cdot s)^{-1}$ as flow rate increased from 6.31×10^{-6} to 5.05×10^{-5} $m^3\cdot s^{-1}$ (0.1 to 0.8 GPM). Even though the shear stress increases with flow rate, slippage is exacelated, resulting in an overall increase of the lippage coefficient.

Payne (2011) determined corrected slip coefficient of ~658 $g\cdot L^{-1}$ pasteurized orange pulp at 21°C. Slip coefficient is a function of wall shear stress which is correlated to the flow rate. Since the pipe diameters used in Payne's research was different from ours, velocities of flow were calculated from flow rate and compared to our extrapolated data. In our research, corrected slip coefficient linearly increased from 2.75×10^{-7} to 1.12×10^{-6} $m\cdot(Pa\cdot s)^{-1}$ as velocity increased from 0.02 to 0.18 $m\cdot s^{-1}$ for orange pulp stored for 0 h. Payne concluded that in her research, as velocity increased from 1.36 to 2.02 $m\cdot s^{-1}$, the corrected slip coefficient linearly increased from 7.30×10^{-5} to 9.40×10^{-5} $m\cdot(Pa\cdot s)^{-1}$. Extrapolated corrected coefficients for the same velocities mentioned in Payne's research were calculated for orange pulp stored for 0 h based on the linear regression model developed from our data:

$$\beta_c=6\times10^{-6}\times v+1\times10^{-7} \tag{3-25}$$

where v was the velocity of the flow.

Based on equation 3-25, when the velocities comes to 0.02 to 0.18 $m\cdot s^{-1}$, the extrapolated corrected slip coefficients will be 8.28×10^{-6} to 1.22×10^{-5} $m\cdot(Pa\cdot s)^{-1}$, which is still much smaller compared to data from Payne's research. There might be two reasons. First, the pulp we used was unpasteurized and was shipped to our laboratory as frozen product. Before we did the test,

pulp thawed in the refrigerator for two days. Therefore, active PME might reacted with pectin and formed gel, which induced to more resistance to separate juice and pulp, thus thinner slip layer and smaller slip coefficient.

The effect of flow rate on slip velocity of orange pulp stored for 0 and 48 h was shown in Figure 3.12. Similar with the corrected slip coefficient, the slip velocity of orange pulp stored for 0 and 48 h increased linearly with the flow rate in flow system. For orange pulp stored for 0 h, as flow rate increased from 6.31×10^{-6} to 5.05×10^{-5} $m^3\cdot s^{-1}$ (0.1 to 0.8 GPM), the slip velocity increased from 1.43×10^{-6} to 1.12×10^{-5} $m^3\cdot s^{-1}$. For orange pulp stored for 48 h, the slip velocity increased from 2.29×10^{-6} to 2.40×10^{-5} $m^3\cdot s^{-1}$. This can also be explained by larger wall shear stress as a function of flow rate.

Mathematical model for pump power requirement prediction

Linear, logarithmic, polynomial and exponential models were attempted using Microsoft Excel to fit the curves describing the relationship between pump power requirement and storage time. The logarithm of pump power requirement versus logarithmic storage time best fitted a linear regression model ($Ln(\Phi)=Aln(t) + B$) (Figure 3.13). All the linear regression models describing pump power requirement as a function of storage time for selected flow rates were listed in Table 3.4. For different flow rates, the slope and intercept of the model were different. Figure 3.14 shows the curve and the empirical equation that predicts slope as a function of flow rate. The model used to predict slope is $Slope = -0.2193Q^2 + 0.237Q + 0.0446$, with $R^2= 0.98$. Figure 3.15 was the curve to predict intercept as a function of flow rate. The model used to predict intercept was $Intercept = 1.2815\ln(Q) - 3.2565$, with $R^2= 0.99$. Therefore, given the flow rate, slope and intercept of the pump power requirement can be calculated. These results suggest that it is possible to predict the power requirement for our pilot plant flow system.

Determination of PME activity, moisture content, °Brix, particle size and calcium content

The PME activity of four randomly picked sub-orange pulp samples from different batches was meausred and shown in Table 3.5. The average PME activity of orange pulp used in study was 0.030 ± 0.002 unit/g.

A summary of SSC and MC for three replications are shown in Table 3.4. The SSC of orange pulp in this study was 14.0 ± 0.23 °Brix and the mositure content was 82.24 ± 0.78%, which were similar with the SSC and mositure content of orange pulp in Chapter 2.

Particle sizes of the triplicate orange pulp samples from different batches were shown in Figure 3.16. Particle size distributions of all the orange pulp samples were all similar for particle size before 2000 μm. Particle size more than 2000 μm was undetectable due to the limitation of the particle size analyzer. Since particle size affects the rheological properties of orange pulp, the purpose to measure particle size was to confirm the pasticle size of all the pulp samples were similar.

Calcium content of three randomly picked orange pulp samples from different batches were shown in Table 3.5. The calcium contents of all the samples were 334, 366 and 428.9 ppm. Calcium content also affects the PME activity of orange pulp, the purpose to measure calcium content was also to confirm the calcium content of all the pulp samples were similar. Though in the study, the calcium content varies in triplicate samples, PME activity of these samples was similar. Therefore, the variation of calcium content can be ignored.

Summary

1. Orange pulp behaved as a pesudo-plastic fluid even when slippage occurred.
2. Under our experimental conditions, flow was larminar, as indicated by very high friction factor. Under laminar flow, it was possible to calculate Reynolds' number

at all flow rates and storage conditions of this study. This in turn, allows calculating the apparent Power Law parameters.

3. Slippage coefficients were determined by confining results from rotational and capillary rheology.

Table 3.1 Average values of flow rate, mass flow rate, pressure drop due to major friction, pressure drop due to minor friction, pressure drop due to elevation, total pressure drop, wall shear stress, friction factor and pump power requirement due to major friction for orange pulp stored for 0-72 h at 22 °C (n=3).

T (storage hours) h	Q (flow rate) GPM	m (mass flow rate) kg/s	Δp (major friction) kPa	Δp (minor friction) kPa	Δp (due to elevation) kPa	Δp (total) kPa	σ (wall shear stress) Pa·s	*f* (friction factor)	Φ (pump power requirement due to major friction) W
0	0.1	6.31E-03	310.13	0.38	7.47	317.60	174.04	0.69	1.96
	0.2	1.26E-02	425.00	1.50	7.47	432.47	236.99	0.24	5.36
	0.3	1.89E-02	472.82	3.38	7.47	480.30	263.20	0.12	8.95
	0.4	2.52E-02	498.65	6.00	7.47	506.12	277.35	0.07	12.58
	0.5	3.15E-02	525.64	9.38	7.47	533.11	292.15	0.05	16.58
	0.6	3.79E-02	549.93	13.51	7.47	557.42	305.46	0.03	20.82
	0.7	4.42E-02	574.63	18.38	7.47	582.11	319.00	0.03	25.38
	0.8	5.05E-02	599.65	24.01	7.47	607.15	332.72	0.02	30.27
2	0.1	6.31E-03	346.27	0.38	7.47	353.74	193.85	0.78	2.18
	0.2	1.26E-02	441.08	1.50	7.47	448.55	245.81	0.25	5.57
	0.3	1.89E-02	483.16	3.38	7.47	490.64	268.87	0.12	9.14
	0.4	2.52E-02	513.00	6.00	7.47	520.47	285.22	0.07	12.95
	0.5	3.15E-02	547.64	9.38	7.47	555.11	304.20	0.05	17.28
	0.6	3.79E-02	579.18	13.51	7.47	586.66	321.49	0.04	21.92
	0.7	4.42E-02	613.07	18.38	7.47	620.56	340.07	0.03	27.08
	0.8	5.05E-02	647.11	24.01	7.47	654.60	358.72	0.02	32.66
4	0.1	6.31E-03	356.71	0.38	7.47	364.18	199.57	0.80	2.25
	0.2	1.26E-02	446.97	1.50	7.47	454.44	249.03	0.25	5.64
	0.3	1.89E-02	491.82	3.38	7.47	499.29	273.61	0.12	9.31
	0.4	2.52E-02	531.20	6.00	7.47	538.67	295.19	0.07	13.41
	0.5	3.15E-02	572.64	9.38	7.47	580.11	317.90	0.05	18.06
	0.6	3.79E-02	609.54	13.51	7.47	617.02	338.13	0.04	23.07
	0.7	4.42E-02	646.81	18.38	7.47	654.30	358.55	0.03	28.57
	0.8	5.05E-02	683.91	24.01	7.47	691.40	378.89	0.02	34.52
8	0.1	6.31E-03	369.59	0.38	7.47	377.06	206.63	0.83	2.33
	0.2	1.26E-02	453.56	1.50	7.47	461.03	252.65	0.25	5.72
	0.3	1.89E-02	507.58	3.38	7.47	515.05	282.25	0.13	9.61
	0.4	2.52E-02	557.51	6.00	7.47	564.98	309.61	0.08	14.07
	0.5	3.15E-02	599.60	9.38	7.47	607.07	332.68	0.05	18.91
	0.6	3.79E-02	638.83	13.51	7.47	646.31	354.18	0.04	24.18
	0.7	4.42E-02	677.15	18.38	7.47	684.63	375.18	0.03	29.90
	0.8	5.05E-02	714.56	24.01	7.47	722.05	395.68	0.03	36.07
12	0.1	6.31E-03	369.55	0.38	7.47	377.02	206.61	0.83	2.33
	0.2	1.26E-02	470.07	1.50	7.47	477.54	261.69	0.26	5.93
	0.3	1.89E-02	528.43	3.38	7.47	535.90	293.67	0.13	10.00
	0.4	2.52E-02	580.53	6.00	7.47	588.00	322.23	0.08	14.65
	0.5	3.15E-02	625.04	9.38	7.47	632.52	346.62	0.06	19.72
	0.6	3.79E-02	665.53	13.51	7.47	673.01	368.81	0.04	25.19

	0.7	4.42E-02	704.88	18.38	7.47	712.36	390.37	0.03	31.13
	0.8	5.05E-02	740.00	24.01	7.47	747.49	409.62	0.03	37.35
16	0.1	6.31E-03	377.73	0.38	7.47	385.20	211.09	0.85	2.38
	0.2	1.26E-02	486.82	1.50	7.47	494.29	270.87	0.27	6.14
	0.3	1.89E-02	551.19	3.38	7.47	558.66	306.15	0.14	10.43
	0.4	2.52E-02	607.42	6.00	7.47	614.90	336.96	0.09	15.33
	0.5	3.15E-02	652.82	9.38	7.47	660.30	361.84	0.06	20.59
	0.6	3.79E-02	694.33	13.51	7.47	701.81	384.59	0.04	26.28
	0.7	4.42E-02	731.14	18.38	7.47	738.63	404.77	0.03	32.29
	0.8	5.05E-02	768.09	24.01	7.47	775.58	425.02	0.03	38.77
20	0.1	6.31E-03	379.10	0.38	7.47	386.57	211.84	0.85	2.39
	0.2	1.26E-02	490.79	1.50	7.47	498.26	273.05	0.27	6.19
	0.3	1.89E-02	565.03	3.38	7.47	572.51	313.73	0.14	10.69
	0.4	2.52E-02	620.34	6.00	7.47	627.81	344.04	0.09	15.65
	0.5	3.15E-02	667.01	9.38	7.47	674.48	369.62	0.06	21.04
	0.6	3.79E-02	709.94	13.51	7.47	717.42	393.15	0.04	26.87
	0.7	4.42E-02	748.79	18.38	7.47	756.27	414.44	0.03	33.07
	0.8	5.05E-02	785.47	24.01	7.47	792.96	434.54	0.03	39.64
24	0.1	6.31E-03	386.49	0.38	7.47	393.96	215.89	0.87	2.44
	0.2	1.26E-02	510.83	1.50	7.47	518.30	284.03	0.29	6.45
	0.3	1.89E-02	581.58	3.38	7.47	589.05	322.80	0.14	11.01
	0.4	2.52E-02	639.14	6.00	7.47	646.62	354.35	0.09	16.13
	0.5	3.15E-02	685.00	9.38	7.47	692.47	379.47	0.06	21.61
	0.6	3.79E-02	728.85	13.51	7.47	736.33	403.51	0.05	27.59
	0.7	4.42E-02	768.59	18.38	7.47	776.07	425.29	0.04	33.94
	0.8	5.05E-02	805.21	24.01	7.47	812.70	445.36	0.03	40.64
36	0.1	6.31E-03	407.87	0.38	7.47	415.34	227.60	0.91	2.57
	0.2	1.26E-02	538.85	1.50	7.47	546.32	299.38	0.30	6.80
	0.3	1.89E-02	618.71	3.38	7.47	626.18	343.14	0.15	11.71
	0.4	2.52E-02	674.24	6.00	7.47	681.72	373.58	0.09	17.02
	0.5	3.15E-02	720.93	9.38	7.47	728.41	399.17	0.06	22.74
	0.6	3.79E-02	763.75	13.51	7.47	771.23	422.64	0.05	28.91
	0.7	4.42E-02	802.84	18.38	7.47	810.33	444.06	0.04	35.46
	0.8	5.05E-02	838.94	24.01	7.47	846.43	463.85	0.03	42.34
48	0.1	6.31E-03	426.80	0.38	7.47	434.26	237.98	0.96	2.69
	0.2	1.26E-02	561.76	1.50	7.47	569.22	311.94	0.31	7.09
	0.3	1.89E-02	648.68	3.38	7.47	656.15	359.57	0.16	12.28
	0.4	2.52E-02	706.23	6.00	7.47	713.70	391.11	0.10	17.82
	0.5	3.15E-02	757.07	9.38	7.47	764.55	418.97	0.07	23.88
	0.6	3.79E-02	798.47	13.51	7.47	805.95	441.66	0.05	30.23
	0.7	4.42E-02	835.41	18.38	7.47	842.89	461.91	0.04	36.89
	0.8	5.05E-02	874.27	24.01	7.47	881.76	483.20	0.03	44.13
60	0.1	6.31E-03	420.16	0.38	7.47	427.63	234.34	0.94	2.65
	0.2	1.26E-02	559.65	1.50	7.47	567.11	310.78	0.31	7.06
	0.3	1.89E-02	646.34	3.38	7.47	653.81	358.29	0.16	12.23
	0.4	2.52E-02	714.46	6.00	7.47	721.93	395.62	0.10	18.03
	0.5	3.15E-02	772.21	9.38	7.47	779.69	427.27	0.07	24.36
	0.6	3.79E-02	812.04	13.51	7.47	819.52	449.10	0.05	30.74
	0.7	4.42E-02	847.27	18.38	7.47	854.75	468.41	0.04	37.42
	0.8	5.05E-02	878.28	24.01	7.47	885.78	485.41	0.03	44.33
72	0.1	6.31E-03	444.10	0.38	7.47	451.57	247.46	0.99	2.80

0.2	1.26E-02	568.77	1.50	7.47	576.24	315.78	0.32	7.18
0.3	1.89E-02	664.12	3.38	7.47	671.59	368.03	0.17	12.57
0.4	2.52E-02	738.96	6.00	7.47	746.43	409.04	0.10	18.65
0.5	3.15E-02	790.28	9.38	7.47	797.75	437.17	0.07	24.93
0.6	3.79E-02	838.75	13.51	7.47	846.23	463.73	0.05	31.75
0.7	4.42E-02	874.88	18.38	7.47	882.36	483.54	0.04	38.64
0.8	5.05E-02	909.92	24.01	7.47	917.42	502.74	0.03	45.93

Table 3.2 Linear regressions for all the lines describing correlation between logarithm of friction Ln(*f*) factor with slippage and logarithm of flow rate Ln(Q).

Storage time (h)	Mathematical model	R^2
0	Ln(*f*)=-1.70Ln(Q)-4.23	1.00
2	Ln(*f*)=-1.71Ln(Q)-4.19	1.00
4	Ln(*f*)=-1.70Ln(Q)-4.13	1.00
8	Ln(*f*)=-1.69Ln(Q)-4.08	1.00
12	Ln(*f*)=-1.67Ln(Q)-4.03	1.00
16	Ln(*f*)=-1.66 Ln(Q)-3.99	1.00
20	Ln(*f*)=-1.65Ln(Q)-3.96	1.00
24	Ln(*f*)=-1.65Ln(Q)-3.93	1.00
36	Ln(*f*)=-1.66Ln(Q)-3.89	1.00
48	Ln(*f*)=-1.66Ln(Q)-3.85	1.00
60	Ln(*f*)=-1.65Ln(Q)-3.83	1.00
72	Ln(*f*)=-1.65Ln(Q)-3.80	1.00

Table 3.3 Reynolds number of orange pulp stored for 0-72 h at 22 °C at flow rate from 0.1-0.8 GPM. Reynolds numbers were calculated with equation 3-24.

Storage Time (h)	Flow rate (GPM) 0.1	0.2	0.3	0.4	0.5	0.6	0.7	0.8
0	23.03	67.23	135.96	229.19	339.72	467.59	609.09	762.34
2	20.63	64.78	133.05	222.78	326.08	443.98	570.90	706.44
4	20.02	63.92	130.71	215.15	311.84	421.87	541.12	668.42
8	19.33	62.99	126.65	204.99	297.82	402.52	516.87	639.76
12	19.33	60.78	121.65	196.86	285.69	386.37	496.54	617.76
16	18.91	58.69	116.63	188.15	273.54	370.35	478.70	595.17
20	18.84	58.22	113.77	184.23	267.72	362.20	467.42	582.00
24	18.48	55.93	110.54	178.81	260.69	352.81	455.38	567.73
36	17.51	53.02	103.90	169.50	247.70	336.68	435.95	544.90
48	16.74	50.86	99.10	161.83	235.87	322.04	418.96	522.89
60	17.00	51.05	99.46	159.96	231.25	316.66	413.09	520.50
72	16.08	50.23	96.80	154.66	225.96	306.58	400.06	502.40

Table 3.4 Mathematical models to predict pump power requirement as a function of storage time for selected flow rates.

Flow rate (GPM)	Mathematical model	R^2
0.1	Ln (Φ)=0.07ln(t) + 0.71	0.90
0.2	Ln (Φ)=0.08ln(t) + 1.61	0.91
0.3	Ln (Φ)=0.10ln(t) + 2.09	0.94
0.4	Ln (Φ)=0.11ln(t) + 2.45	0.97
0.5	Ln (Φ)=0.11ln(t) + 2.74	0.98
0.6	Ln (Φ)=0.11ln(t) + 2.99	0.98
0.7	Ln (Φ)=0.10ln(t) + 3.21	0.99
0.8	Ln (Φ)=0.10ln(t) + 3.40	0.99

Table 3.5 PME activity, moisture content, soluble solid content and calcium content of the triplicate orange pulp samples.

Sample	PME activity (Unit/mL)	Moisture content (%)	Soluble solid content (°Brix)	Calcium content (ppm)
Rep 1	0.028	81.34	14.1	334
Rep 2	0.031	82.67	13.7	366
Rep 3	0.030	82.70	14.1	428.9
Mean	0.030	82.24	14.0	376.3
SD	0.002	0.78	0.23	48.2

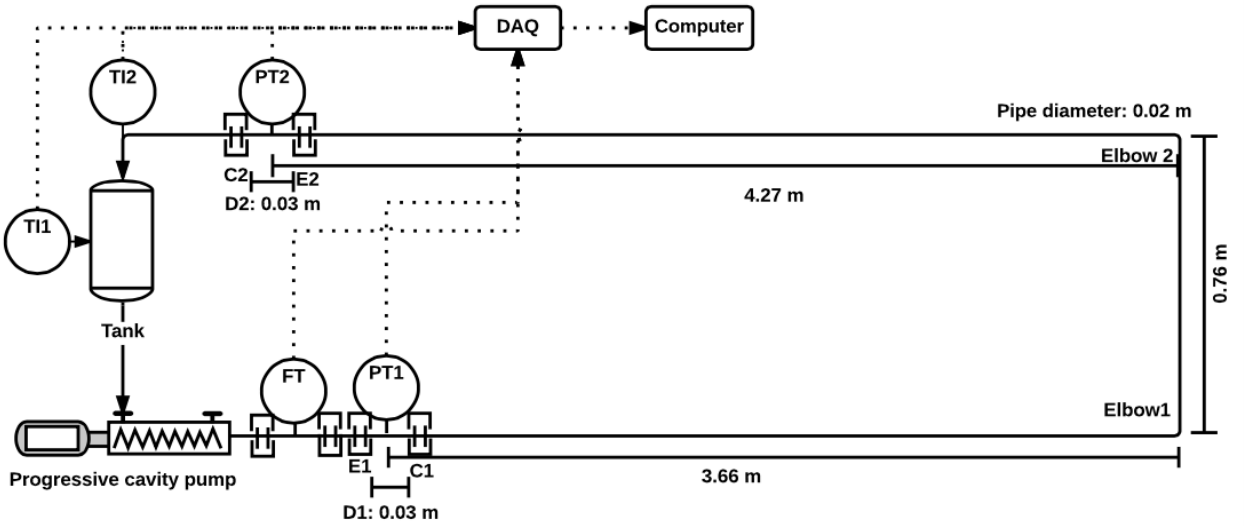

Figure 3.1 Diagram of the pilot scale experimental set up of the flow system. E1 and E2 were two expansion spots; C1 and C2 were two contraction spots; D1 and D2 were diameters of tubes between E1 and C1, E2 and C2; Elbow 1 and Elbow 2 were two 90° elbow-shaped areas.

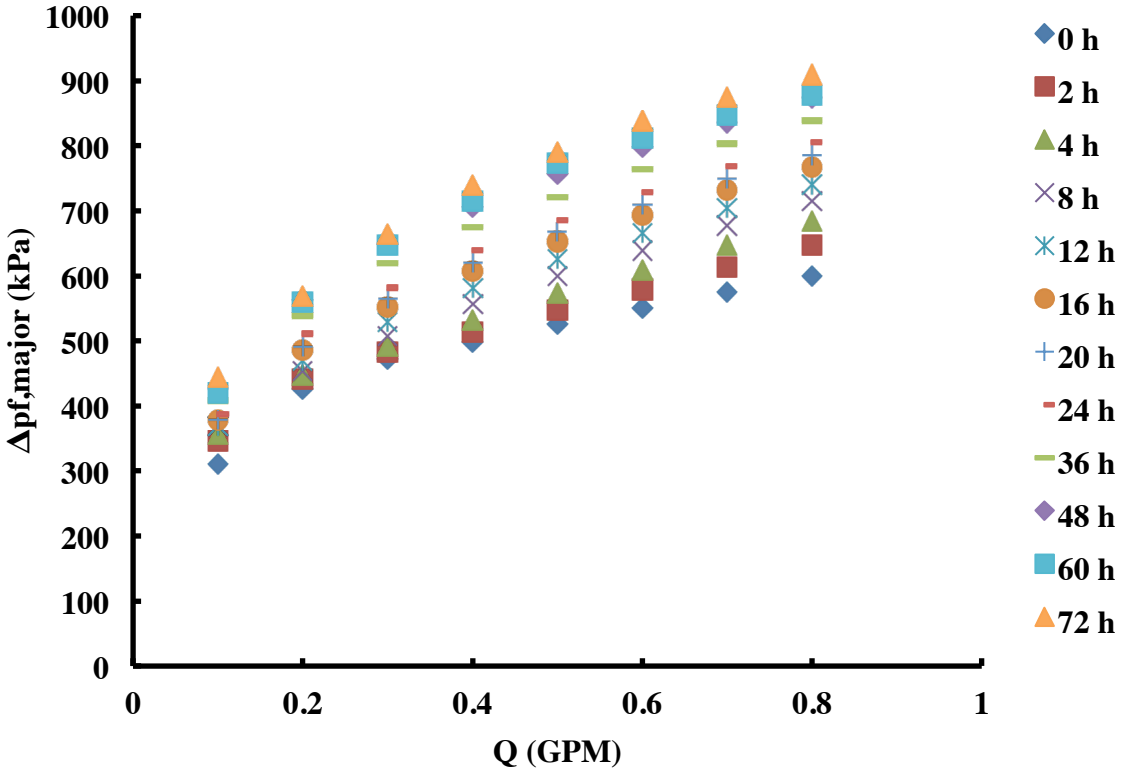

Figure 3.2 Effect of the flow rate on the pressure drop due to major friction for orange pulp stored for 0-72 h at 22 °C.

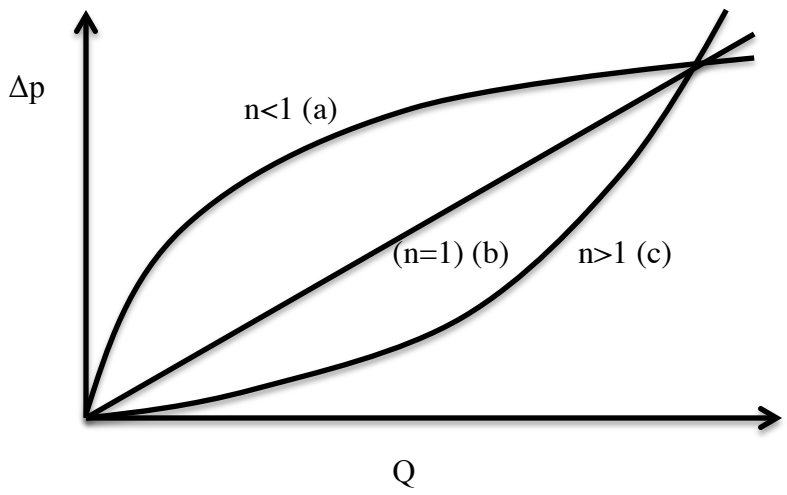

Figure 3.3 Pressure drop as a function of flow rate for different flow properties fluids (0<n<2). (a) pseudo-plastic fluid, (b) Newtonian fluid, (c) dilatant fluid.

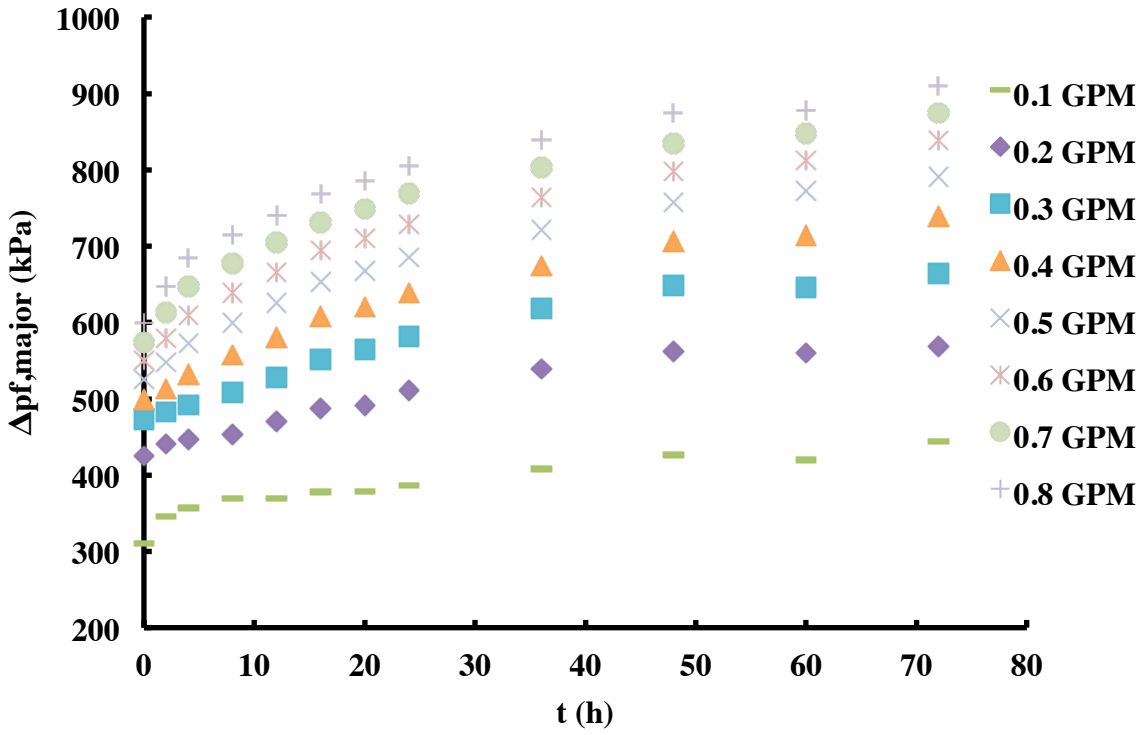

Figure 3.4 Effect of the storage time on pressure drop due to major friction for orange pulp stored at 22 °C at flow rates 0.1-0.8 GPM.

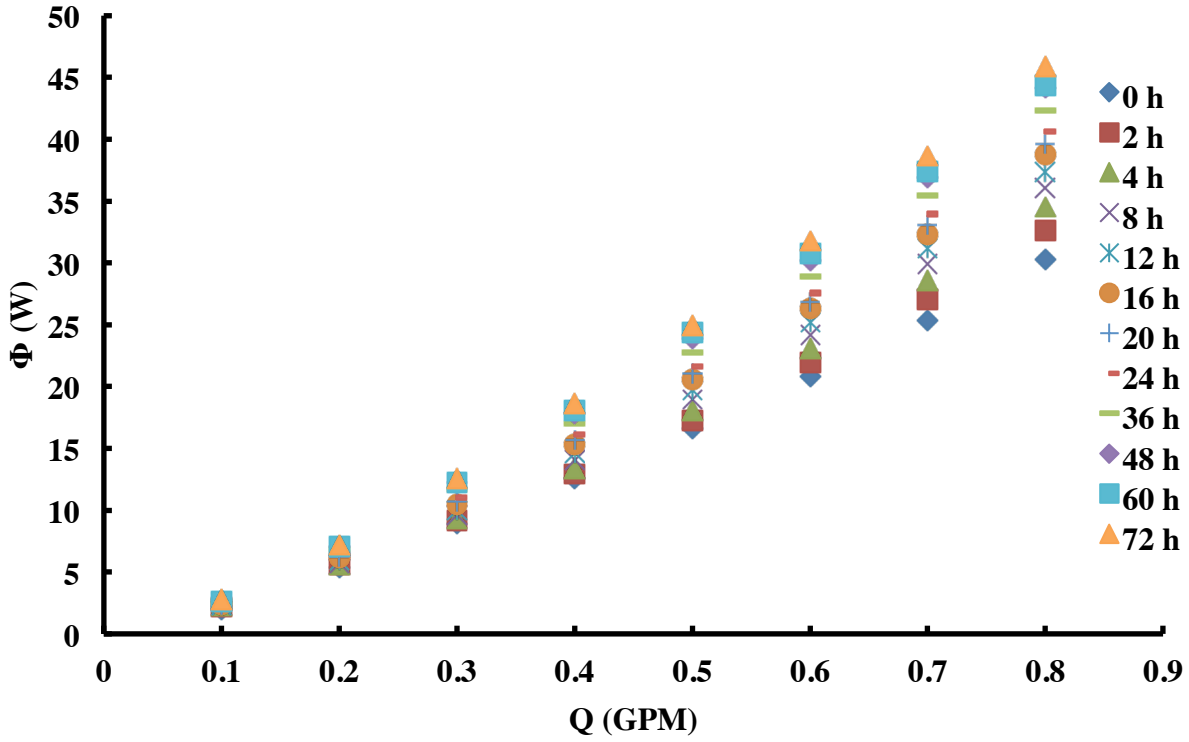

Figure 3.5 Effect of the flow rate on pump power requirement for orange pulp stored for 0-72 h at 22 °C.

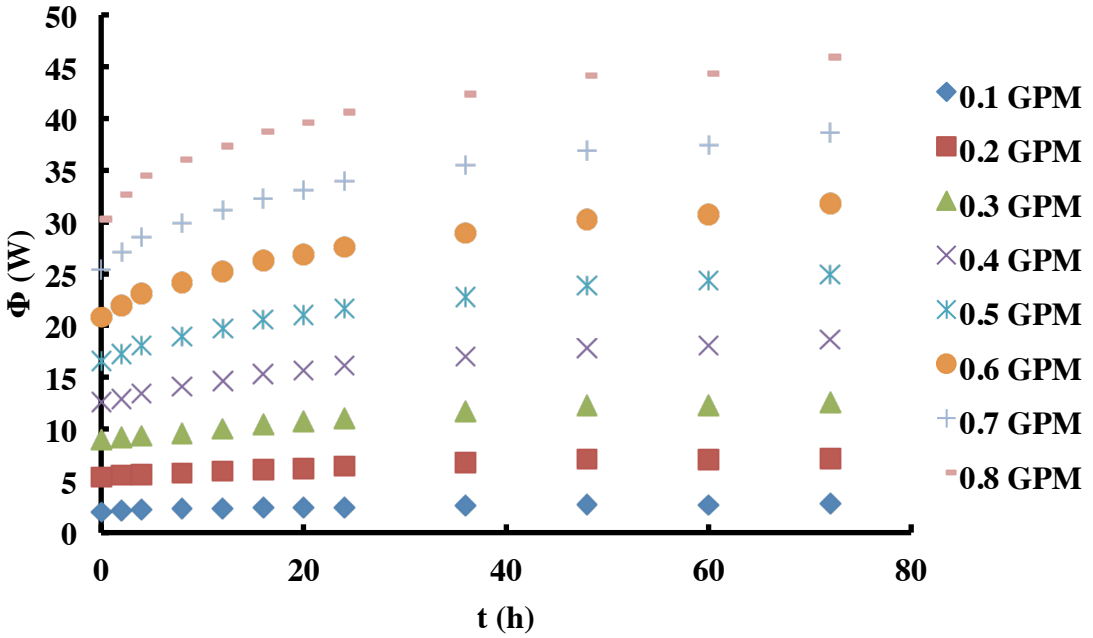

Figure 3.6 Effect of the storage time on pump power requirement for orange pulp stored for 0-72 h at 22 °C at flow rates 0.1-0.8 GPM.

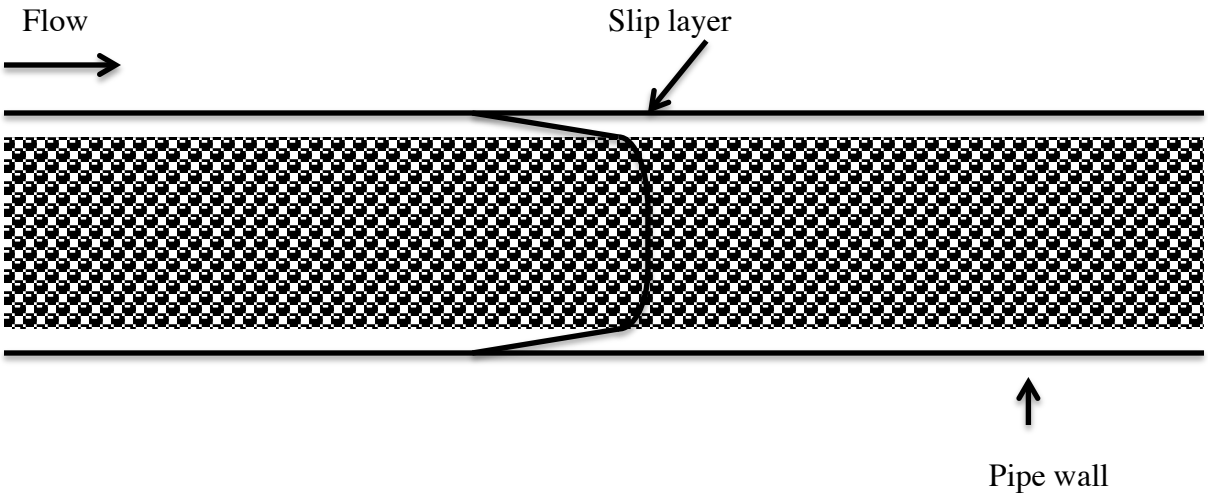

Figure 3.7 Schematic of slip flow of fresh orange pulp in pipeline.

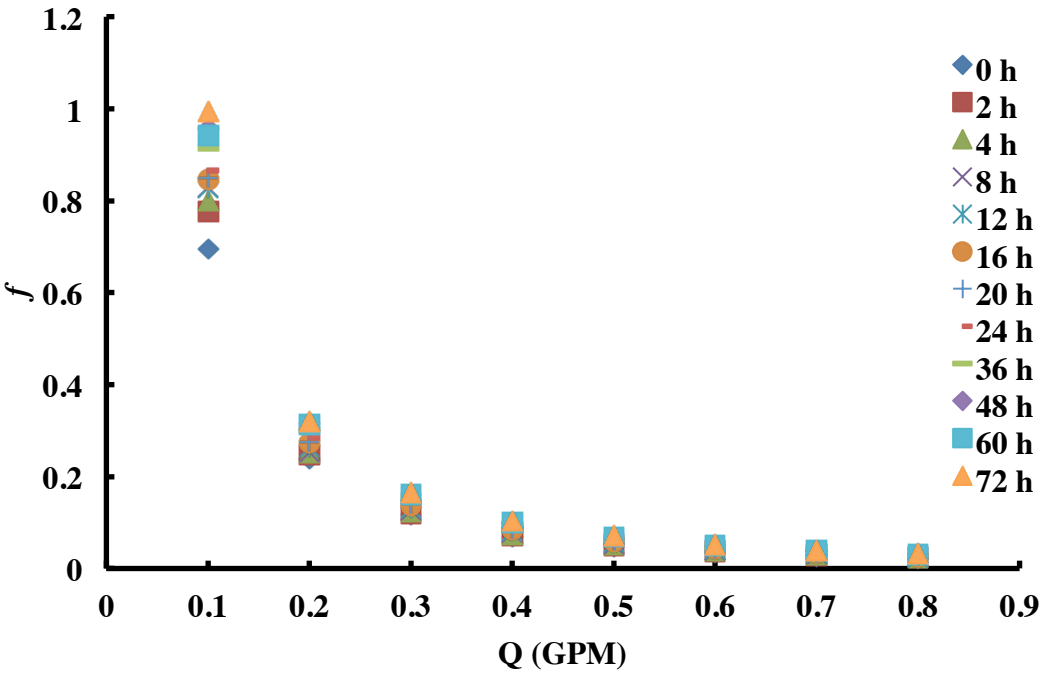

Figure 3.8 Effect of the flow rate on friction factor with slippage for orange pulp samples stored for 0-72 h at 22 °C.

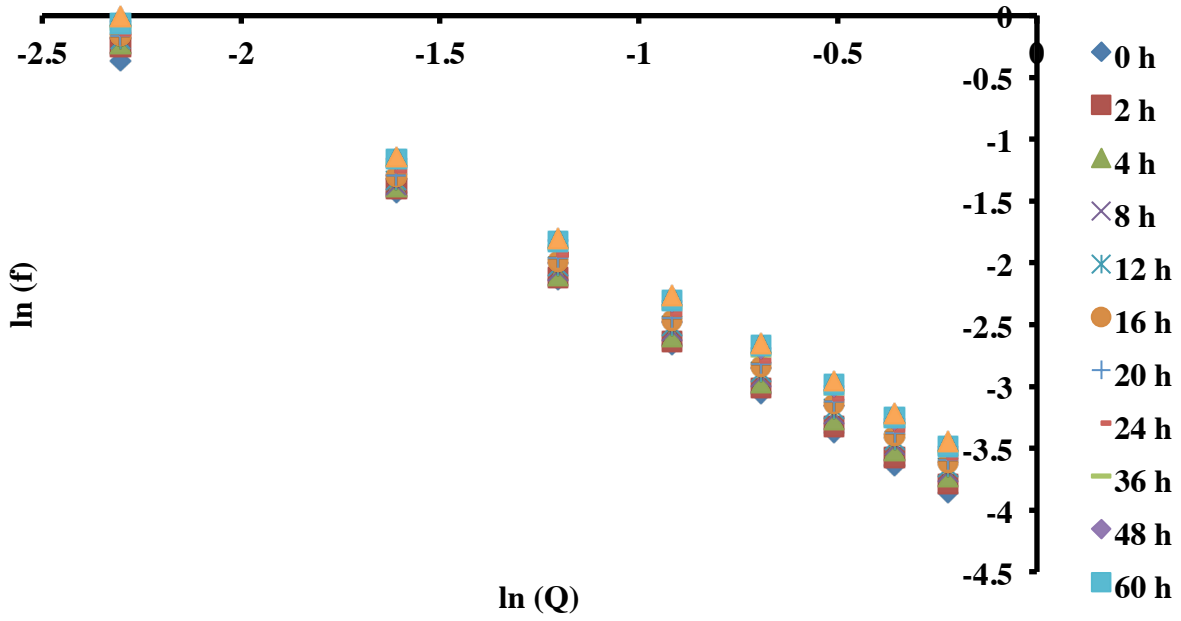

Figure 3.9 Effect of the logarithm of flow rate on the logarithm of friction factor with slippage for orange pulp stored for 0-72 h.

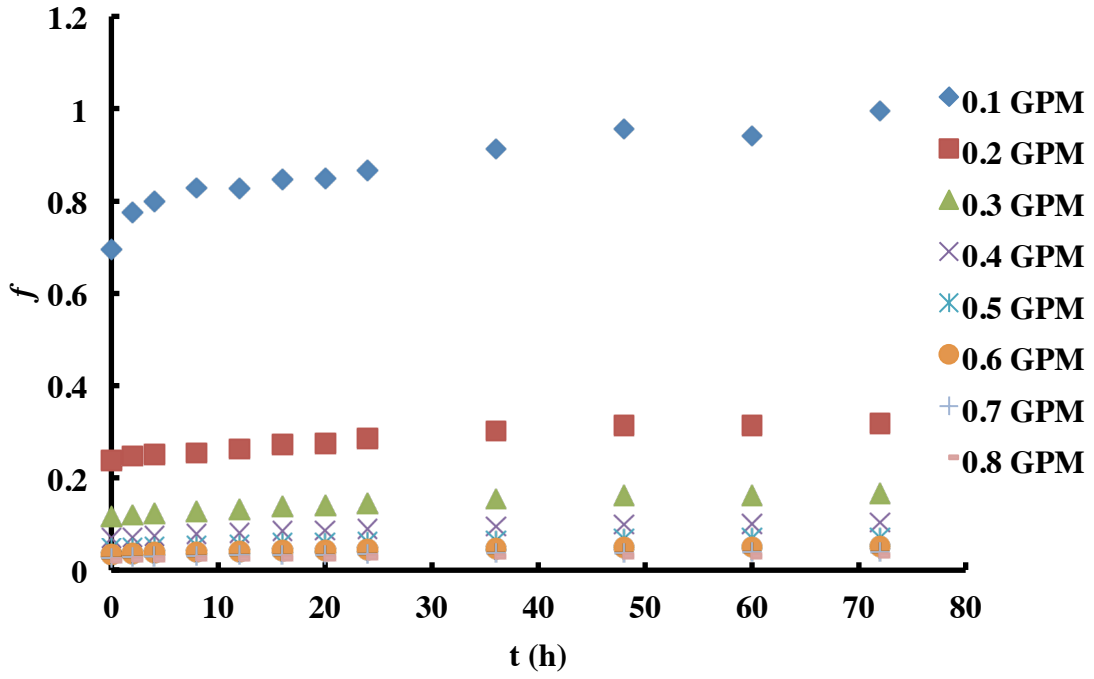

Figure 3.10 Effect of the storage time on friction factor with slippage for orange pulp at flow rates 0.1-0.8 GPM at 22 °C.

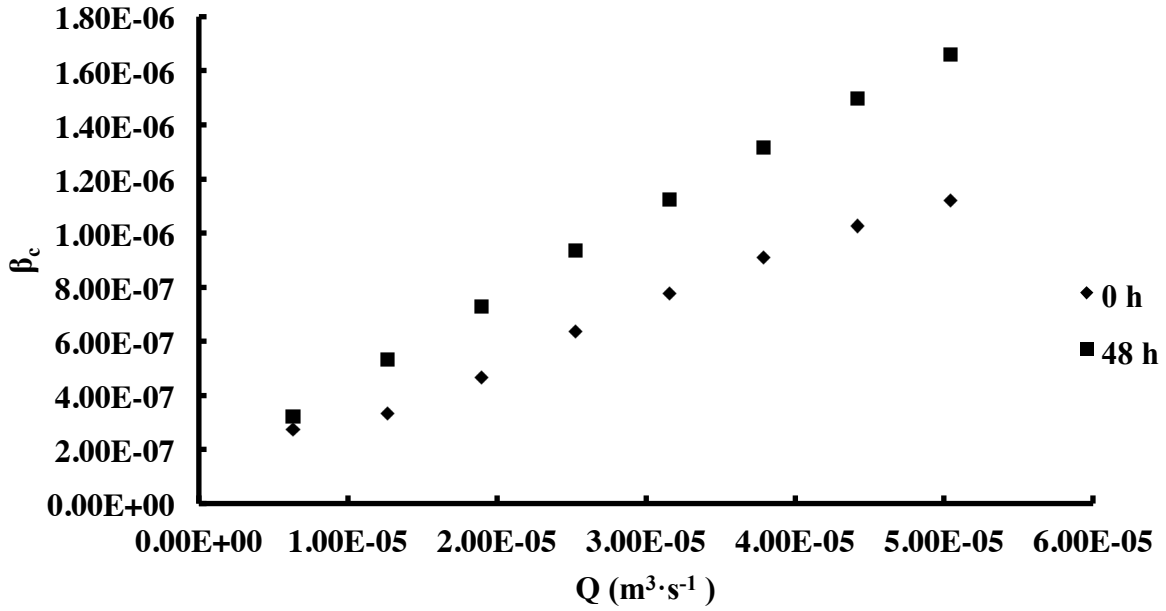

Figure 3.11 Effect of the flow rate on the corrected slip coefficient for orange pulp samples stored for 0 and 48 h at 22 °C.

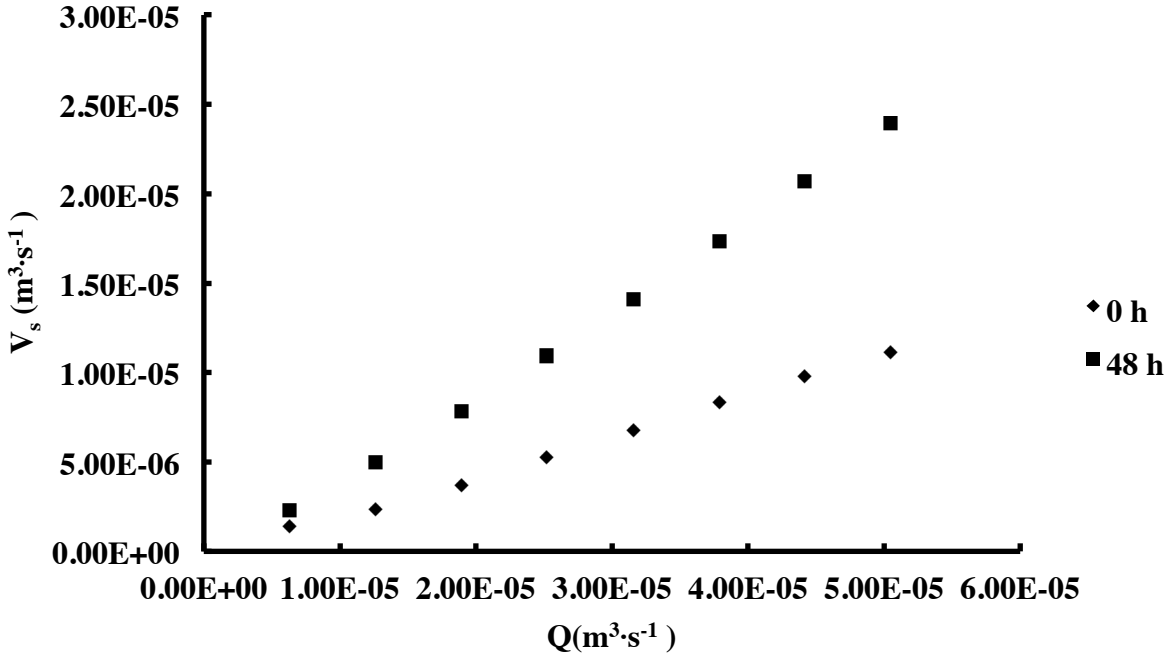

Figure 3.12 Effect of the flow rate on slip velocity of orange pulp stored for 0 and 48 h at 22 °C.

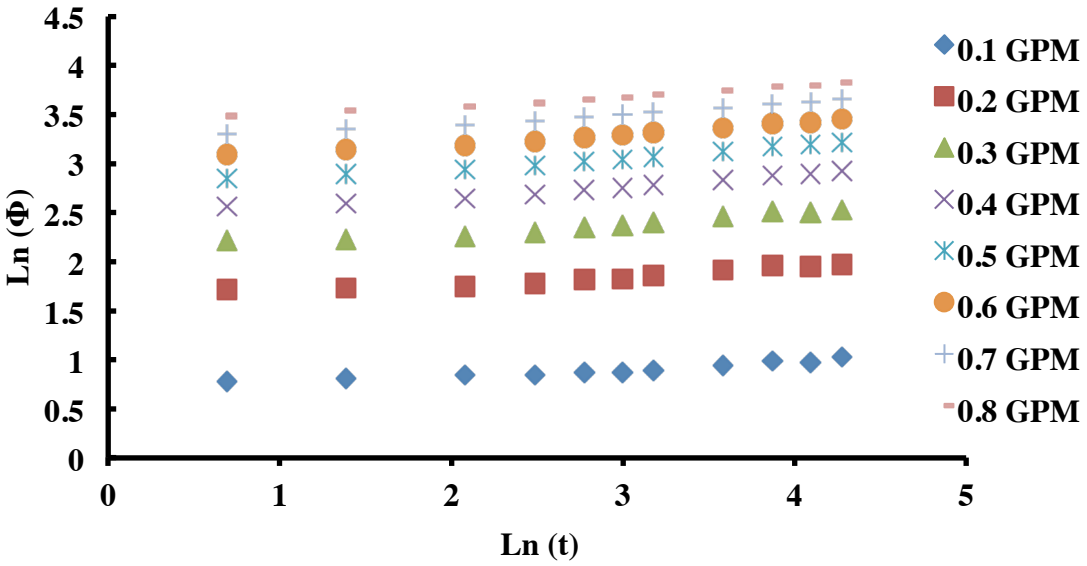

Figure 3.13 Logarithm of pump power requirement versus the logarithm of storage time at flow rates 0.1-0.8 GPM. **ln(Φ)=Aln(t) + B**

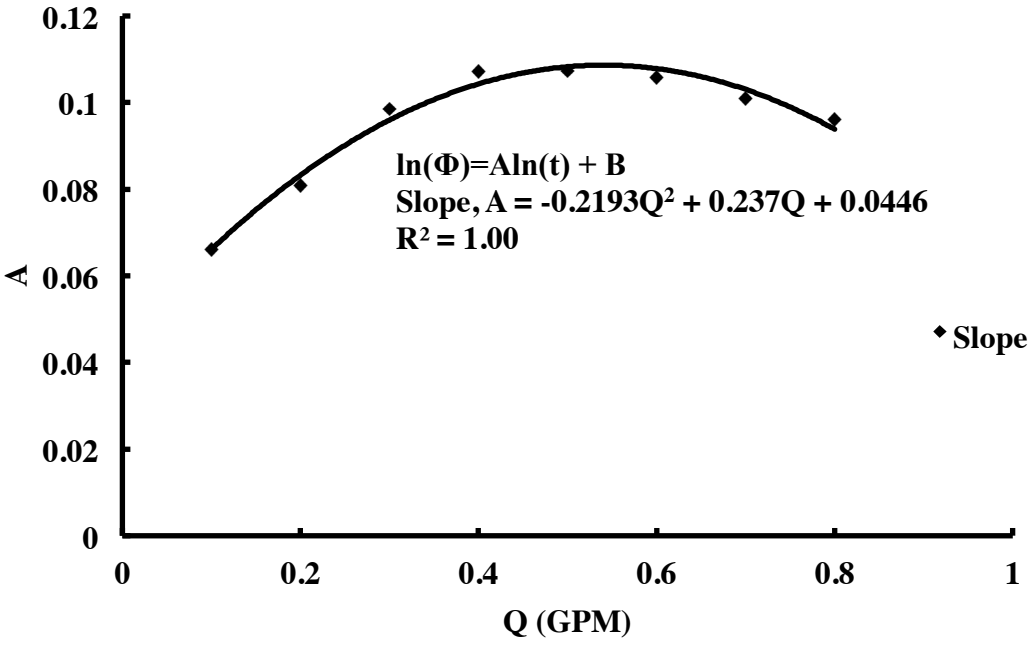

Figure 3.14 Effect of the flow rate on slope for the mathematical model to describe pump power requirement.

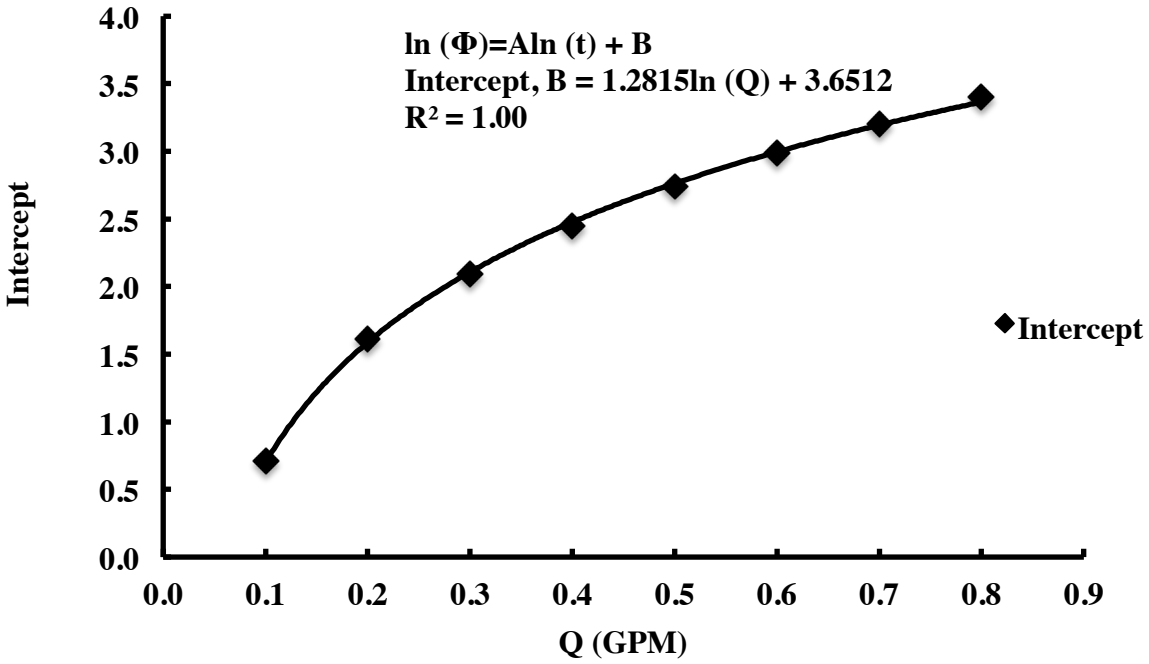

Figure 3.15 Effect of the flow rate on intercept for the mathematical model to describe pump power requirement.

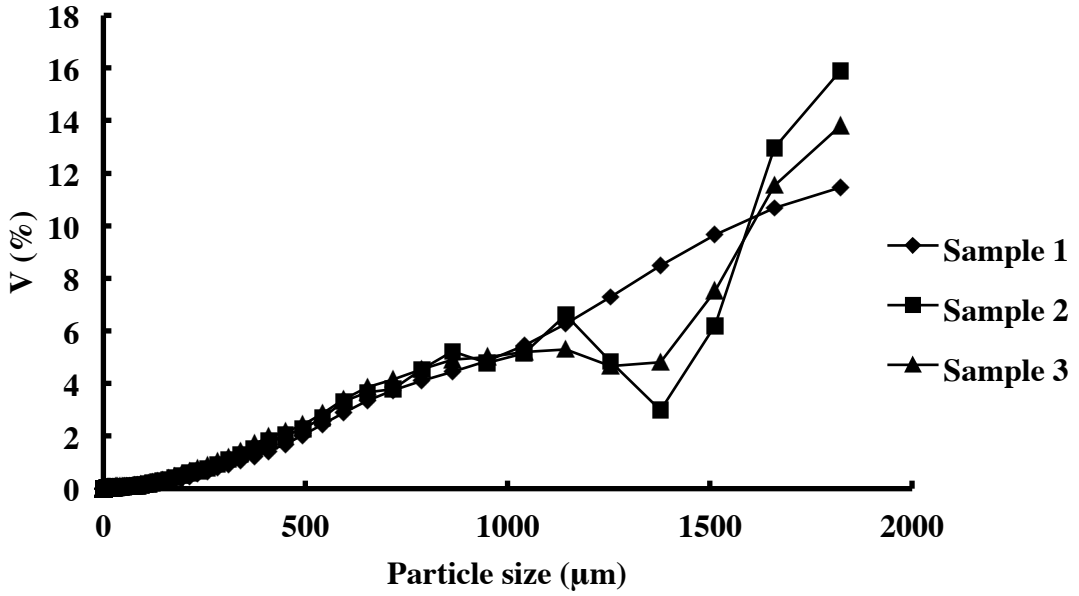

Figure 3.16 Particle size of the triplicate orange pulp samples.

CHAPTER 4

OVERALL CONCLUSIONS AND FUTURE WORK

Overall conclusions

Orange pulp has a complex flow behavior with slippage at very low shear rates, about 0.6-0.9 s^{-1}. We confirmed that, orange pulp behaved as pseudoplastic fluid ($n<1$) and can be modeled with the power law before slippage occurred. For fresh Valencia orange pulp, as storage time increased, K-value increased. In shear stress-controlled rotational rheometry measurements, K-value increased 65.5% for pulp sample stored for 48 h at 4 °C compared to fresh pulp without storage, from 119.7 to 198.1 $Pa \cdot s^n$. The flow behavior of orange pulp ~650 g • L^{-1} stored for 0-72 h at 22 °C was determined in the capillary viscometry. The pressure drop due to major friction increased as the flow rate or storage time increased, from 310.03-909.92 kPa at 22 °C. The pump power requirement also increased as the flow rate or storage time increased, from 1.96-45.93 W. The friction factor decreased from 0.99 to 0.02 as the flow rate increased from 6.39×10^{-5} to 5.04×10^{-4} $m^3 \cdot s^{-1}$ (0.1-0.8 GPM). At 0.8 GPM, the corrected slip coefficient increased from 1.12×10^{-6} to 1.66×10^{-6} $m \cdot (Pa \cdot s)^{-1}$ as storage time of orange pulp increased to 48 h. Therefore, we concluded that for the citrus processing industry, pasteurizing pulp as soon as possible helps reducing pump power requirement and costs. Based on our findings, unpasteurized orange pulp stored for 24 h required 40.64 W energy requirement at 0.8 GPM, increased 34.26% compared to pulp without storage at the same flow rate. For the scientific community, we found that there was a negative linear correlation between logarithm of friction factor and logarithm of flow rate.

Accounting accurately the energy loss in flow system is only possible if both the rheological properties of orange pulp and the effect of slippage on the flow behavior of pulp are available.

Future work

First, the pulp we used in research came from various sources. Different harvest seasons, handling methods and cultivar might affect the rheological properties of orange pulp. For example, the pulp we used in study #1 was extracted using a kitchen style citrus juicer but pulp in study #2 was extracted using industrial extractor and finisher from JBT Company. Pulp in study #1 was extracted late September 2014 but pulp provided by JBT Company was extracted early May 2015. The first part of the future work is to characterize the effect of variety of orange pulp source on the pulp's rheology.

Second, results of K and n values in study #1 cannot corellate to study #2 due to pulp's different storage temperature. Orange pulp in study #1 was stored at 4 °C while the orange pulp was stored at 22°C in study #2. The shear rates in study #2 were much higher than in study #1. The second part of future work will be characterzing K and n value for orange pulp stored for 0-72 h at 22 °C with rotational rheometry.

The power law parameters in capillary viscometry have not been determined in present work. K and n value in capillary viscometry can be determined using modified Mooney's method with various diameters pipes. The third part of future work will be changing 3/8 inch pipe to 1 inch pipe and measure pressure drop as a function of flow rate for orange pulp stored for 0-72 h at 22 °C. Then, the effect of slippage on K and n in flow system can be determined.

REFERENCES

Allal, A., Vergnes, B., (2007). Molecular design to eliminate sharkskin defect for linear polymers. Journal of Non-newtonian fluid mechanics 146(1), 45-50.

Alonso, J., Rodríguez, M.T., Canet, W., (1996). Purification and characterization of four pectinesterases from sweet cherry (Prunus avium L.). Journal of agricultural and food chemistry 44(11), 3416-3422.

Arslan, E., Yener, M., Esin, A., (2005). Rheological characterization of tahin/pekmez (sesame paste/concentrated grape juice) blends. Journal of food engineering 69(2), 167-172.

Baker, R.A., Cameron, R.G., (1999). Clouds of citrus juices and juice drinks. Food technology 53(1), 63-69.

Belibağli, K.B., Dalgic, A.C., (2007). Rheological properties of sour-cherry juice and concentrate. International journal of food science & technology 42(6), 773-776.

Bosch, M.H., P.K., (2005). Pectin methylesterases and pectin dynamics in pollen tubes. The plant cell 17, 3219-3226.

Braddock, R.J., (1999). Handbook of citrus by-products processing technology. John Wiley & Sons, Inc. pp 98-99.

Cameron, R.G., Baker, R.A., Grohmann, K., (1998). Multiple forms of pectinmethylesterase from citrus peel and their effects on juice cloud stability. Journal of food science 63(2), 253-256.

Cameron, R.G., Grohmaa, K., (1995). Partial purification and thermal characterization of pectinmethylesterase from red grapefruit finisher pulp. Journal of food science 60(4), 821-825.

Cameron, R.G., Niedz, R.P., Grohmann, K., (1994). Variable heat stability for multiple forms of pectin methylesterase from citrus tissue culture cells. Journal of agriculture and food chemistry 42(4), 903-908.

Chakrabandhu, K., Singh, R.K., (2005). Wall slip determination for coarse food suspensions in tube flow at high temperatures. Journal of food engineering 70(1), 73-81.

Chen, L., Duan, Y., Zhao, C., Yang, L., (2009). Rheological behavior and wall slip of concentrated coal water slurry in pipe flows. Chemical engineering and processing: process intensification 48(7), 1241-1248.

Corredig, M., Kerr, W., Wicker, L., (2000). Separation of thermostable pectinmethylesterase from marsh grapefruit pulp. Journal of agricultural and food chemistry 48(10), 4918-4923.

Corredig, M., Wicker, L., (2001). Changes in the molecular weight distribution of three commercial pectins after valve homogenization. Food hydrocolloids 15(1), 17-23.

Crawford, B., Watterson, J., Spedding, P., Raghunathan, S., Herron, W., Proctor, M., (2005). Wall slippage with siloxane gum and silicon rubbers. Journal of Non-newtonian fluid mechanics 129(1), 38-45.

Falguera, V., Ibarz, A., (2010). A new model to describe flow behaviour of concentrated orange juice. Food biophysics 5(2), 114-119.

Gomez, J.A., Tarrega, A., Bayarri, S., Carbonell, J.V., (2011). Clarification and gelation of a minimally heated orange juice concentrate during its refrigerated storage. Journal of Food Process Engineering 34(4), 1187-1198.

Halliday, P., Smith, A., (1995). Estimation of the wall slip velocity in the capillary flow of potato granule pastes. Journal of rheology 39(1), 139-149.

Hatzikiriakos, S., Dealy, J., (1991). Wall slip of molten high density polyethylene. I. Sliding plate rheometer studies. Journal of rheology 35(4), 497-523.

Hatzikiriakos, S.G., (1995). A multimode interfacial constitutive equation for molten polymers. Journal of rheology 39(1), 61-71.

Hatzikiriakos, S.G., (2012). Wall slip of molten polymers. Progress in polymer science 37(4), 624-643.

Hernandez, E., Chen, C., Johnson, J., Carter, R., (1995). Viscosity changes in orange juice after ultrafiltration and evaporation. Journal of food engineering 25(3), 387-396.

Jacon, S., Rao, M., Cooley, H., Walter, R., (1993). The isolation and characterization of a water extract of konjac flour gum. Carbohydrate polymers 20(1), 35-41.

Jana, S., Kapoor, B., Acrivos, A., (1995). Apparent wall slip velocity coefficients in concentrated suspensions of noncolloidal particles. Journal of rheology 39(6), 1123-1132.

Jastrzebski, Z., (1967). Entrance effects and wall effects in an extrusion rheometer during flow of concentrated suspensions. Industrial & Engineering chemistry fundamentals 6(3), 445-454.

Jayani, R.S., Saxena, S., Gupta, R., (2005). Microbial pectinolytic enzymes: a review. Process biochemistry 40(9), 2931-2944.

Joel Gaffe, D.M.T., Avtar K. Handa, (1994). Pectin methylesterase isoforms in tomato. Plant physiology 105, 199-203.

Jolie, R.P., Duvetter, T., Van Loey, A.M., Hendrickx, M.E., (2010). Pectin methylesterase and its proteinaceous inhibitor: a review. Carbohydrate research 345(18), 2583-2595.

Kar, F., Arslan, N., (1999). Effect of temperature and concentration on viscosity of orange peel pectin solutions and intrinsic viscosity–molecular weight relationship. Carbohydrate polymers 40(4), 277-284.

Kim, Y., (2004). Valencia pectinmethylesterase isozymes result in pectins of unique charge domain and functionality. The University of Georgia, dissertation, pp.5-7.

Kimball, D., (2012). Citrus processing: a complete guide. Springer science and business media. pp 257-262.

Kok, P.H., Kazarian, S., Lawrence, C., Briscoe, B., (2002). Near-wall particle depletion in a flowing colloidal suspension. Journal of rheology 46(2), 481-493.

Lam, Y., Wang, Z., Chen, X., Joshi, S., (2007). Wall slip of concentrated suspension melts in capillary flows. Powder technology 177(3), 162-169.

Larrea, M.A., Chang, Y.K., Bustos, F.M.n., (2005). Effect of some operational extrusion parameters on the constituents of orange pulp. Food chemistry 89(2), 301-308.

Lee, J.W., Feng, H., Kushad, M., (2005). Effect of manothermosonication (MTS) on quality of orange juice, Proceedings of AIChE 2005 annual meeting. http://www.nt.ntnu.no/users/skoge/prost/proceedings/aiche2005/topical/pdffiles/T9/papers/444d.pdf. Accessed on 10/8/2015.

Lee, J.Y., Lin, Y.S., Chang, H.M., Chen, W., Wu, M.C., (2003). Temperature–time relationships for thermal inactivation of pectinesterases in orange juice. Journal of the science of food and agriculture 83(7), 681-684.

Löfgren, C., Walkenström, P., Hermansson, A.-M., (2002). Microstructure and rheological behavior of pure and mixed pectin gels. Biomacromolecules 3(6), 1144-1153.

Maria, T.P, Pedro.L., Fernando R. and Fe1ix R., (1997). Pectic enzymes in fresh fruit processing: optimization of enzymic peeling of oranges. Process biochemistry 32(1), 43-49.

Matthew, J.A., Howson, S.J., Keenan, M.H.J., Belton, P.S., (1990). Improvement of the gelation properties of sugarbeet pectin following treatment with an enzyme preparation derived from Aspergillus niger — Comparison with a chemical modification. Carbohydrate polymers 12(3), 295-306.

Mierczyńska, J., Cybulska, J., Pieczywek, P.M., Zdunek, A., (2015). Effect of storage on rheology of water-soluble, chelate-soluble and diluted alkali-soluble pectin in carrot cell walls. Food and bioprocess technology 8(1), 171-180.

Mooney, M., (1931). Explicit formulas for slip and fluidity. Journal of rheology (1929-1932) 2(2), 210-222.

Mourniac, P., Agassant, J., Vergnes, B., (1992). Determination of the wall slip velocity in the flow of a SBR compound. Rheologica acta 31(6), 565-574.

Munoz, J.F., (2012). Determination of the thermal properties and heat transfercharacteristics of high concentration orange pulp. The University of Florida, thesis for master of science.

Naidu, G., Panda, T., (1998). Production of pectolytic enzymes–a review. Bioprocess engineering 19(5), 355-361.

Payne, E.M., (2011). Rheological properties of high and low concentrated orange pulp. Thesis from University of Florida. The University of Florida, thesis for master of science.

Pelloux, J., Rusterucci, C., Mellerowicz, E.J., (2007). New insights into pectin methylesterase structure and function. Trends in plant science 12(6), 267-277.

Ramamurthy, A., (1986). Wall slip in viscous fluids and influence of materials of construction. Journal of rheology 30(2), 337-357.

Rao, D., (1993). Studies on viscosity-molecular weight relationship of chitosan solutions. Journal of food science and technology (India) 30(1), 66-67.

Rao, M.A., (2010). Rheology of fluid and semisolid foods: Principles and applications: Principles and applications. Springer, pp.276-323.

Rao, M.A., (2014). Flow and functional models for rheological properties of fluid foods, Rheology of fluid, semisolid, and solid foods. Springer, pp. 27-61.

Rinaudo, M., (1996). Physicochemical properties of pectins in solution and gel states, in: Visser, J., Voragen, A.G.J. (Eds.), Progress in biotechnology. Elsevier, pp. 21-33.

Rodriguez-Nogales, J.M., Ortega, N., Perez-Mateos, M., Busto, M.D., (2008). Pectin hydrolysis in a free enzyme membrane reactor: An approach to the wine and juice clarification. Food chemistry 107(1), 112-119.

Rolin, C., Vries, J., (1990). Pectin, in: Harris, P. (Ed.), Food Gels. Springer Netherlands, pp. 401-434.

Saak, A.W., Jennings, H.M., Shah, S.P., (2001). The influence of wall slip on yield stress and viscoelastic measurements of cement paste. Cement and concrete research 31(2), 205-212.

Schmelter, T., Wientjes, R., Vreeker, R., Klaffke, W., (2002). Enzymatic modifications of pectins and the impact on their rheological properties. Carbohydrate polymers 47(2), 99-108.

Seymour, G.B., Taylor, J.E., Tucker, G.A., (2012). Biochemistry of fruit ripening. Springer Science & Business Media, pp 311-320.

Silva, J.L., Gonçalves, M., Rao, M., (1992). Rheological properties of high‐methoxyl pectin and locust bean gum solutions in steady shear. Journal of food science 57(2), 443-448.

Singh, R.P., Heldman, D.R., (2001). Introduction to food engineering. Gulf Professional Publishing, fourth edition, pp 84-115.

Soltani, F., Yilmazer, Ü., (1998). Slip velocity and slip layer thickness in flow of concentrated suspensions. Journal of applied polymer science 70(3), 515-522.

Thakur, B.R., Singh, R.K., Handa, A.K., Rao, M., (1997). Chemistry and uses of pectin—a review. Critical reviews in food science & nutrition 37(1), 47-73.

Thibault, J.-F., Rombouts, F.M., (1986). Effects of some oxidising agents, especially ammonium peroxysulfate, on sugar-beet pectins. Carbohydrate research 154(1), 205-215.

USDA, (2014). Citrus Fruits 2014 Summary. National agricultural statistics service. http://usda.mannlib.cornell.edu/usda/nass/CitrFrui//2010s/2014/CitrFrui-09-18-2014.pdf. Accessed on 10/8/2015.

Van Buggenhout, S., Sila, D., Duvetter, T., Van Loey, A., Hendrickx, M., (2009). Pectins in processed fruits and vegetables: Part III—Texture engineering. Comprehensive reviews in food science and food safety 8(2), 105-117.

Vélez-Ruiz, J.F., Barbosa-Cánovas, G.V., (1998). Rheological properties of concentrated milk as a function of concentration, temperature and storage time. Journal of food engineering 35(2), 177-190.

Vinogradov, G., Ivanova, L., (1968). Wall slippage and elastic turbulence of polymers in the rubbery state. Rheologica acta 7(3), 243-254.

Vitali, A., Rao, M., (1984). Flow properties of low‐pulp concentrated orange juice: Effect of temperature and concentration. Journal of food science 49(3), 882-888.

Voragen, A., Pilnik, W., Thibault, J., Axelos, M., Renard, C., (1995). Pectins. Food polysaccharides and their applications pp 287− 339. Marcel Dekker Inc., New York.

Walls, H., Caines, S.B., Sanchez, A.M., Khan, S.A., (2003). Yield stress and wall slip phenomena in colloidal silica gels. Journal of rheology 47(4), 847-868.

Wicker, L., (1992). Selective extraction of thermostable pectinesterase. Journal of food science 57(2), 534-535.

Wicker, L., Ackerley, J., Corredig, M., (2002). Clarification of juice by thermolabile Valencia pectinmethylesterase is accelerated by cations. Journal of agricultural and food chemistry 50(14), 4091-4095.

Willats, W.G.T., Knox, P., Mikkelsen, J.D., (2006). Pectin: new insights into an old polymer are starting to gel. Trends in Food science & technology 17(3), 97-104.

Yadav, S., Yadav, P.K., Yadav, D., Yadav, K.D.S., (2009). Pectin lyase: a review. Process biochemistry 44(1), 1-10.

Yoo, B., Rao, M., Steffe, J., (1995). Yield stress of food dispersions with the vane method at controlled shear rate and shear stress. Journal of texture studies 26(1), 1-10.